Correlated Electrons in Chemical Systems: Theory and Practice

by

David Scott Hollman

(Under the direction of Professor Henry F. Schaefer)

Abstract

Efficient and accurate determination of the effects of electron correlation on chemical systems is the principal task of modern computational quantum chemistry. Experience has shown that *ab inito* wavefunction methods provide the most reliable means of computating properties of chemical systems. The exponential scaling of the exact electron correlation problem demands the development of approximate solutions that minimize error with respect to computational effort. Herein we discuss the development and utilization of methods for computing the effects of electron correlation on chemical systems. Case studies demonstrating the importance of wavefunction methods and their applicability to experimental results are presented, and new formulas useful for the computation of spectroscopic values are derived. Finally, a new method for the efficient computation of electron correlation in large molecular systems is derived, which represents an archetype for efficient electron correlation computation in the future.

Index words: electron structure theory, computational quantum chemistry, electron correlation, R12 methods, F12 methods, explicitly correlated methods, Møller–Plesset perturbation theory, atomic orbital basis methods, AO-MP2-F12, quartic force fields

Correlated Electrons in Chemical Systems: Theory and Practice

by

David Scott Hollman

B.S., Wheaton College, 2009

A Dissertation Submitted to the Graduate Faculty
of The University of Georgia in Partial Fulfillment
of the
Requirements for the Degree

Doctor of Philosophy

Athens, Georgia

2013

Correlated Electrons in Chemical Systems:

Theory and Practice

by

David Scott Hollman

Major Professors: Henry F. Schaefer

Committee: Paul von Rague Schleyer
Henning Meyer

Electronic Version Approved:

Dr. Maureen Grasso
Dean of the Graduate School
The University of Georgia
May 2013

Acknowledgments

Wow, where do I start? It's hard to believe it has been four years already. I know I'm going to look back on this later and wonder why I didn't thank someone or say something more about someone else, but I have to try anyway.

To Professor Schaefer, my advisor, thank you for giving me the opportunity to work for you. Thank you for the constant freedom you gave me to pursue my own ideas during my time at CCQC, even if a lot of them turned out to be duds.

To my wife, Mandy, thanks for everything you do for me. Thanks for putting up with the late nights, my grouchiness when things aren't working, my excited yammering when things are working, my general negligence of chores around the house, and everything else. In short — thanks for putting up with me and loving me. I look forward to spending the rest of my life with you; if it's as good as these past four years have been, then I truly did hit the "wife jackpot" when I married you. Anything else I say here will be insufficient to fully express my gratitude, so I'll just leave it at this: I couldn't have done this without you.

To my parents and family, thank you for raising me the way you did. Thank you for teaching me to work hard (even if I didn't want to learn sometimes), and thank you for instilling in me a love of learning, science, computers, and (most importantly) God from a young age. To my parents, thank you especially for sending me to (and paying for) Wheaton. To my brother Peter, thanks for always being my counter and teaching me to argue well. To my brother James, thank you for always reminding me of what's important in life. Thanks

also to my parents-in-law, Jeff and Darlene, for being so supportive of both Mandy and myself throughout this whole experience.

To all of the people who helped me along in my scientific journey, I wouldn't be where I am today without you. Thanks particularly to Jeremy for believing I could take on the AO-MP2-F12 project, for guiding my introduction to the world of theoretical chemistry research, and for answering all of my myriad questions. Thanks to Andy for his help with my first paper, for the introduction to to world of computational quantum chemistry, and for answering all of my crazy questions. To Jet, Alex Sokolov, Jay, Stefan, Francesco, and all of the other people I bounced ideas off of in my time at CCQC, thanks for listening and not calling me crazy right away. Thanks to Dr. Schleyer and Dr. Meyer for serving on my committee (Thanks also to Henning for such a fantastic intro to quantum course and for letting us call you "Henning"). Thanks to Ed Valeev and Christian Ochsenfeld for pushing me to pursue my AO-MP2-F12 paper further. To Linda, Amy, Karen, and Rebecca, the people who hold this place together, thanks for making the CCQC such a great place to do science.

To my college professors, thanks for getting me to where I am today and inspiring me to pursue academia. Dr. Eggimann, thank you for introducing me to the world of computational chemistry. I would probably be a very bewildered math graduate student right now if it weren't for you (and Daniel Crawford, whose talk at an undergraduate research conference showed me that there *is* interesting math in quantum chemistry). To Dr. Walhout, my P-chem professor, thank you for introducing me to quantum mechanics and for teaching me that even the best get lost in the middle of a derivation on the board sometimes. To Dr. Perciante and Doc Hayward, thank you for letting me pursue majors in math and computer science without giving up chemistry. Finally, to my high school chemistry teacher, Mr. Liner, thanks for instilling a love of chemistry in me so early. Just about everyone I've met in chemistry says they're here because they had a fantastic high school chemistry teacher,

and I'm no exception.

I'm sure there are a bunch of people I'm forgetting. My best friends, John and Chris, I wouldn't be who I am without you two. Anyone else who I've forgotten, please accept my apologies for leaving you out, and thank you for your contribution to my life that I will inevitably remember as soon as this manuscript goes to print.

To my God, I owe you my life. *Soli Deo gloria.*

Contents

Chapter 1

Introduction and Literature Review

1.1 Electron Correlation

The study of many-body problems constitutes a large portion of modern computational physics and chemistry. Of particular importance to the chemical sciences are the many-body problems arising from the interactions between electrons in molecules. Specifically, electron-electron correlation constitutes the bulk of modern research in theoretical quantum chemistry. Indeed, one recent review[1] referred to electron correlation as "the many-body problem at the heart of chemistry."

The central difficulty with many-body problems in physics and chemistry is the concept of correlation. Indeed, the determination of how much of correlation between dependent events needs to be included in the analysis of results in order to obtain the qualitatively correct understanding is crucial to all areas of science. Two events A and B are considered statistically uncorrelated if

$$P_{AB} = P_A P_B \tag{1.1}$$

In practice, events of research interest are rarely completely uncorrelated, and the task of the researcher is to determine which correlated events can be ignored without compromising the qualitative correctness of the result. Thus practice we have

$$|P_{AB} - P_A P_B| < \epsilon \tag{1.2}$$

and the job of the scientist is to determine an acceptable ϵ for the matter at hand and, in most cases, to determine some function $f(A, B)$ that correlates events A and B with sufficient accuracy such that when added to the left-hand side of equation (1.2), the equation holds for this minimum acceptable ϵ.

In many-body systems, the events in question are the presence or absence of a particle at a given point in space. It is thus convenient to think in terms of a function ρ that represents the density of positive outcomes ("events" in which the particle is found to be present) at a given point in space. Two particles are uncorrelated if the pair probability density is equal to the product of one-particle densities. That is,[2]

$$\Gamma_2(\mathbf{x}_1, \mathbf{x}_2) = \rho_1(\mathbf{x}_1)\rho_2(\mathbf{x}_2) \tag{1.3}$$

where $\mathbf{x}_i$ is a composite coordinate describing the ith particle (perhaps including spin, color, etc. if relevant for the given particle). For indistinguishable particles, $\rho_1 = \rho_2$, and thus the subscripts can be dropped. From basic quantum mechanics, these probability densities can be obtained for an n particle system by integrating the square of the wavefunction over the other electrons:[3,4]*

$$\rho(\mathbf{x}_1) = \int \Psi^*(\mathbf{x}_1, \mathbf{x}_2, \ldots, \mathbf{x}_n)\Psi(\mathbf{x}_1, \mathbf{x}_2, \ldots, \mathbf{x}_n)d\mathbf{x}_2 d\mathbf{x}_3 \ldots d\mathbf{x}_n \tag{1.4}$$

$$\Gamma_2(\mathbf{x}_1, \mathbf{x}_2) = \int \Psi^*(\mathbf{x}_1, \mathbf{x}_2, \ldots, \mathbf{x}_n)\Psi(\mathbf{x}_1, \mathbf{x}_2, \ldots, \mathbf{x}_n)d\mathbf{x}_3 \ldots d\mathbf{x}_n \tag{1.5}$$

Typically in electron structure theory, the wavefunction Ψ is taken to be the solution to the time independent Schrödinger equation

$$\hat{H}\Psi = E\Psi \tag{1.6}$$

The Born–Openheimer approximation[6] is typically assumed, thus allowing us to compute the electronic energy separately from the vibrational and rotational energies of a molecule,

*When these probability densities are used to represent the probability of finding *any* particle in the n particle system at a given point, these formulas are multiplied by n and $n(n-1)$, respectively. This is why the formulas given here differ from those of other authors, for instance ref. 5.

and the electronic Hamiltonian can be written simply as

$$\hat{H} = \hat{T}_e + \hat{V}_{en} + \hat{V}_{ee} \tag{1.7}$$

where $\hat{T}_e$ is the electronic kinetic energy, $\hat{V}_{en}$ is the electron-nuclear potential, and $\hat{V}_{ee}$ is the electron-electron potential.

This perspective leads immediately to two possible approaches to the determination of electron correlation: either one can attempt to obtain the various densities as a function of position directly, or one can attempt to obtain the wavefunction itself, thus indirectly obtaining the densities and quantifying the electron correlation of the system. In this work, we will focus on the latter approach.

1.2 Solving for the Wavefunction

The first solution to the non-relativistic hydrogen atom[7] appeared around the same time as the development of the famous Schrödinger equation and the emergence of the wave mechanics approach quantum theory.[8] For hydrogen-like systems, a closed-form, analytic solution can be derived, and thus the problem is not of particular further interest to the study of many-body quantum mechanics. Perhaps the simplest chemical system for which no such closed-form, analytic solution exists is the helium atom. Wavefunction-based study of helium atom and helium-like two-electron systems dates back to at least the 1927 work of J.C. Slater[9] and the 1929 work of Hylleraas.[10,11] Even at this early date, it was known that an exact (though not closed-form) wavefunction for helium-like systems existed in an infinite-dimensional, separable Hilbert space† and thus could be expressed as a linear combination

†A Hilbert space is separable if and only if a countable orthonormal basis for it can be constructed. Many early sources[12] required all Hilbert spaces to be separable. Under this definition, all infinite-dimensional Hilbert spaces would be isomorphic to each other, and thus this particular Hilbert space is sometimes referred to as "the Hilbert space" or simply "Hilbert space." Despite the nomenclatural sloppiness, this convention will be used occasionally throughout the remainder of this work.

of the basis vectors for that Hilbert space. Mathematically speaking, the same wavefunction is obtained regardless of the basis used, so long as that basis spans the entire Hilbert space. Practically speaking, however, this infinite basis must be truncated at some point to yield a finite form usable for chemical applications. The efficient trade-off between accuracy and computational cost in the making of this truncation is the principle focus of modern electron structure research.

1.2.1 Forming Wavefunctions

To obtain a wavefunction as a linear combination of basis vectors in a Hilbert space, one must first construct such an orthonormal basis which spans the Hilbert space to which the exact wavefunction belongs. The typical approach to this sort of problem is to combine or modify solutions to a similar, simpler problem with a known solution. In this case, the obvious choice is the set of hydrogen-like atom wavefunctions[13,14]

$$\psi_{nlm}(\mathbf{r}) = \phi_{nlm}(r,\theta,\varphi) = R_{nl}(r)Y_{lm}(\theta,\varphi) \tag{1.8}$$

$$R_{nl}(r) = \left(\frac{2Z}{n}\right)^{3/2}\sqrt{\frac{(n-l-1)!}{2n(n+l)!}}\left(\frac{2Zr}{n}\right)^{l} L_{n-l-1}^{2l+1}\left(\frac{2Zr}{n}\right)\exp\left(-\frac{Zr}{n}\right) \tag{1.9}$$

where L_n^α are the associated Laguerre polynomials, Y_{lm} are spherical harmonics, Z is the charge of the nucleus, and n, l, and m are the usual quantum numbers of a given hydrogenic eigenstate. These functions can be easily shown to span an infinite Hilbert space.[‡] In practice, a Gaussian function $\exp(-\zeta r^2)$ is used in place of the exact radial portion of the hydrogenic eigenstates when forming a basis. Using this basis of the one-electron Hilbert

[‡]Even though an isomorphism exists between the one-electron and n-electron Hilbert spaces, their bases can be expressed as functions of different numbers of electrons. Though most mathematicians would refer to these spaces as the same thing, we will distinguish them for the sake of discussing their physical manifestations

space, an arbitrary one-electron basis function (often called an *orbital*) can be written:

$$\chi_\mu(\mathbf{r}) = \chi_\mu(r,\theta,\varphi) = \sum_{\alpha}^{N_\mu} C_\alpha \exp(-\zeta_\alpha r^2) Y_{l_\alpha m_\alpha}(\theta,\varphi) \tag{1.10}$$

For systems of more than one fermion, a spin function must be appended to the basic hydrogen atom wavefunctions, leading to one-electron functions $\phi_\mu(\mathbf{x}) = \chi(\mathbf{r})\sigma(s)$ called *spin orbitals*. The simplest way to form n-electron basis functions from a set of one-electron spin orbitals is to utilize the direct product basis. In the case of fermionic systems, however, the exact wavefunction must be antisymmetric with respect to exchange of electrons. It is therefore useful to take an antisymmetrized product of spin orbitals as our basis, which leads to the ubiquitous Slater determinant:[15]

$$\Phi(\mathbf{x}_1,\mathbf{x}_2,\ldots,\mathbf{x}_n) = |\phi_1(\mathbf{x}_1)\phi_2(\mathbf{x}_2)\cdots\phi_n(\mathbf{x}_n)| \tag{1.11}$$

$$= \hat{\mathcal{A}}_n[\phi_1(\mathbf{x}_1)\phi_2(\mathbf{x}_2)\cdots\phi_n(\mathbf{x}_n)] \tag{1.12}$$

$$= \phi_1(\mathbf{x}_1)\phi_2(\mathbf{x}_2)\cdots\phi_n(\mathbf{x}_n) - \phi_1(\mathbf{x}_2)\phi_2(\mathbf{x}_1)\cdots\phi_n(\mathbf{x}_n) + \ldots \tag{1.13}$$

where the antisymmetrization operator $\hat{\mathcal{A}}_n$ takes a sum over all permutations of electrons with the odd permutations taking a negative sign and the even permutations taking a positive sign. These determinants are often called configuration state functions (CSFs).

Example: Helium Atom

In the simple case of helium atom, the exact wavefunction can be written as

$$\Psi_{\text{exact}} = \sum_{\mu,\nu} C_{\mu\nu}\hat{\mathcal{A}}_2\left[\phi_\mu(\mathbf{x}_1)\phi_\nu(\mathbf{x}_2)\right] \tag{1.14}$$

where μ and ν run over all (infinitely many) hydrogenic spin-orbitals and the $C_{\mu\nu}$ are variationally optimized.[16] If we assume this expansion is very rapidly convergent and take only the first (largest coefficient) term to be approximately the exact wavefunction, then for the ground ^1S ($1s^2$) electronic state we have

$$\Psi_{1^1S}(\mathbf{x}_1, \mathbf{x}_2) = \chi_{1s}(\mathbf{r}_1)\chi_{1s}(\mathbf{r}_2)\left[\alpha(s_1)\beta(s_2) - \beta(s_1)\alpha(s_2)\right] \tag{1.15}$$

where s_i is the spin coordinate of the ith electron (note that $\mathbf{x}_i = \{\mathbf{r}_i, s_i\}$). Computing the one- and two-electron density matrices directly using equations (1.5), we see that

$$\rho(\mathbf{x}) = |\chi_{1s}(\mathbf{r})|^2 \tag{1.16}$$

$$\Gamma_2(\mathbf{x}_1, \mathbf{x}_2) = |\chi_{1s}(\mathbf{r}_1)|^2|\chi_{1s}(\mathbf{r}_2)|^2 \tag{1.17}$$

$$= \rho(\mathbf{x}_1)\rho(\mathbf{x}_2) \tag{1.18}$$

where we have used the orthogonality of the spin functions α and β. Thus, in this simple case, taking only the CSF with the largest coefficient leads to the inclusion of *no* electron correlation in the approximate wavefunction.

Repeating this same procedure for the second ^1S state ($1s_\alpha 2s_\beta$), we get[§]

$$\Psi_{2^1S}(\mathbf{x}_1, \mathbf{x}_2) = \left[\chi_{1s}(\mathbf{r}_1)\chi_{2s}(\mathbf{r}_2) + \chi_{2s}(\mathbf{r}_1)\chi_{1s}(\mathbf{r}_2)\right] 2^{-1/2}\left[\alpha(s_1)\beta(s_2) - \beta(s_1)\alpha(s_2)\right] \tag{1.19}$$

$$= |\phi_{1s}^{\alpha}\phi_{2s}^{\beta}\rangle - |\phi_{1s}^{\beta}\phi_{2s}^{\alpha}\rangle \tag{1.20}$$

where Dirac bra–ket notation[17] has been used to indicate Slater determinants. Computing

[§]The normalization for these wavefunctions is a bit abnormal. This is the result of the normalization used in equation (1.5). See the footnote preceding that equation for an explanation

the one- and two-electron density matrices as before, we get

$$\rho(\mathbf{x}) = |\chi_{1s}(\mathbf{r})|^2 + |\chi_{2s}(\mathbf{r})|^2 \tag{1.21}$$

$$\Gamma_2(\mathbf{x}_1, \mathbf{x}_2) = |\chi_{1s}(\mathbf{r}_1)|^2|\chi_{2s}(\mathbf{r}_2)|^2 + |\chi_{2s}(\mathbf{r}_1)|^2|\chi_{1s}(\mathbf{r}_2)|^2 + 2\chi^*_{1s}(\mathbf{r}_1)\chi^*_{2s}(\mathbf{r}_2)\chi_{2s}(\mathbf{r}_1)\chi_{1s}(\mathbf{r}_2) \tag{1.22}$$

$$\begin{aligned} &= \rho(\mathbf{x}_1)\rho(\mathbf{x}_2) - |\chi_{1s}(\mathbf{r}_1)|^2|\chi_{1s}(\mathbf{r}_2)|^2 - |\chi_{2s}(\mathbf{r}_1)|^2|\chi_{2s}(\mathbf{r}_2)|^2 \\ &\qquad + 2\chi^*_{1s}(\mathbf{r}_1)\chi^*_{2s}(\mathbf{r}_2)\chi_{2s}(\mathbf{r}_1)\chi_{1s}(\mathbf{r}_2) \end{aligned} \tag{1.23}$$

and thus even with only one CSF, statistical electron correlation is present. This phenomenon is known as *Fermi correlation*, since it arises purely from the fermionic exchange of electrons in the reference CSF. Notice that if the fermionic antisymmetrization requirement is ignored (known as a *Hartree product* wavefunction), equations (1.19), (1.21), and (1.23) become

$$\Psi^{\text{Hartree}}_{2^1S}(\mathbf{x}_1, \mathbf{x}_2) = \chi_{1s}(\mathbf{r}_1)\alpha(s_1)\chi_{2s}(\mathbf{r}_2)\beta(s_2) \tag{1.24}$$

$$\rho_1(\mathbf{x}_1) = \chi_{1s}(\mathbf{r}_1) \tag{1.25}$$

$$\rho_2(\mathbf{x}_2) = \chi_{2s}(\mathbf{r}_2) \tag{1.26}$$

$$\Gamma_2(\mathbf{x}_1, \mathbf{x}_2) = \rho_1(\mathbf{x}_1)\rho_2(\mathbf{x}_2) \tag{1.27}$$

Thus, the statistical correlation in equation (1.23) is entirely the result of the fermionic nature of electrons and brings us no closer to solving the spacial aspect of the many-body correlation problem.

1.2.2 Hartree–Fock Theory and Configuration Interaction

Clearly, then, to incorporate spacial electron correlation — called *Coulomb correlation* because it arises from the coulomb potential — into the wavefunction, the contributions of more than one CSF must be considered. A molecular generalization of the single determi-

nantal approach used in section 1.2.1 is known as the Hartree–Fock (HF) method.[18] HF theory typically recovers more than 99% of the total electronic energy,[19] but the remaining 1% that constitutes Coulomb correlation is still significant, given that the total electronic energy of hydrogen molecule is already 600 kcal mol^{-1}. (For perspective, errors of 3 kcal mol^{-1} have been shown to lead to an order of magnitude error[20] in computed reaction rate constants, and 13 kcal mol^{-1} error can lead to up to 5 orders of magnitude difference[21]). When relative energies of similar systems are computed, much of the correlation error may cancel. If bonds are formed or broken over the course of the reaction, however, this error cancellation is diminished and accurate computation of electron correlation becomes much more important for quantitative (and often even qualitative) study of chemical systems. Indeed, in chapter 3, a case is presented in which correlated treatment is critical even for relative energies of very similar systems (specifically, finite difference displacements along a potential energy surface) because the quantitative accuracy demanded by the experiment to which the computations are being compared is so high.

Nonetheless, it is usually reasonable to assume that the exact wavefunction differs by a small perturbation from the HF wavefunction, often called the *reference* wavefunction. Noting the invariance of (1.14) to unitary rotations of the orbitals in Hilbert space, the n-electron generalization of equation (1.14) can be rewritten in terms of successively more modified versions of the reference determinant:

$$|\Psi\rangle = C_0\Phi_{\mathrm{HF}} + \sum_{ia} C_a^i\,|\Phi_i^a\rangle + \sum_{ijab} C_{ab}^{ij}\,|\Phi_{ij}^{ab}\rangle + \sum_{ijkabc} C_{abc}^{ijk}\,|\Phi_{ijk}^{abc}\rangle + \ldots \tag{1.28}$$

where $|\Phi_{ij\ldots}^{ab\cdots}\rangle$ is the reference determinant with the ith orbital replaced by orbital a, the jth orbital replaced by orbital b, and so on. The orbitals used to form these determinants are

typically taken to be the solutions to the eigenvalue equations

$$\hat{f}\,|\phi_p\rangle = \epsilon_p\,|\phi_p\rangle \tag{1.29}$$

where $\hat{f}$ is the Fock operator which includes kinetic energy, electron-nuclear attraction, and mean-field electron repulsion terms.[22] These orbitals are often called canonical molecular orbitals (MOs). In practice, they are formed from a unitary transformation of a basis of atomic orbitals (AOs), which are of the form given in equation (1.10). Because the CSFs in equation (1.28) can be conceptually thought of as constructed by the placement of one or more electrons into orbitals not occupied by electrons in the reference, they are often referred to as *excitations*, with $|\Phi_i^a\rangle$ referred to as single excitations, $|\Phi_{ij}^{ab}\rangle$ referred to as double excitations, and so on.

1.2.3 Truncations and Convergence

For practical use with all but the smallest molecular systems, the expansion in equation (1.28) must be truncated in two different ways. First, the expansion must be truncated at a given excitation order smaller than the total number of electrons in this system. Mathematically, it can be shown that truncating this expansion after double excitations leads to a wavefunction that essentially only correlates two electrons at a time. Inclusion of triple excitations correlates at most three electrons at a time, and so on. The obvious downside is that the number of variationally optimized coefficients increases exponentially with the excitation rank. Indeed, inclusion of only double excitations leads to a method requiring $\mathcal{O}(N_{\text{basis}}^6)$ computational effort, and inclusion of triple excitations requires $\mathcal{O}(N_{\text{basis}}^8)$ effort.[¶‖]

[¶]Note that the number of basis functions for a given basis set such as 6-31G*[23,24] or cc-pVTZ[25] the total number of basis functions N_{basis} for a given system is directly proportional to the number of electrons in that system.

[‖]Note that perturbative inclusion of two-body and three-body effects can be accomplished with only $\mathcal{O}(N_{\text{basis}}^5)$ and $\mathcal{O}(N_{\text{basis}}^7)$ effort, respectively.

Numerous chemically relevant systems have been shown to have contributions from triple excitations on the order of 10 kcal mol^{-1}, even for relative energies (see, for instance, refs.[26], 27, and 28). This relatively slow convergence of the expansion in equation (1.28) leads to the well-known problem of the "exponential wall" of computational effort discussed in Walter Kohn's 1998 Nobel prize lecture.[29] A plethora of approaches to the truncation of excitation rank and the determination of coefficients have been developed,[4,30] and the details of these methods will not be belabored here. The direct implementation of the method suggested by equation (1.28) is referred to as configuration interaction (CI) theory; though the details of other so-called "post-Hartree–Fock" methods differ from CI theory, this simple approach is sufficient to illustrate the issues relevant to the current discussion.

Even utilizing the full expansion of equation (1.28), leading to a method known as full configuration interaction (FCI), the expansion of the wavefunction must be truncated to use a finite subset of the basis vectors of the Hilbert space. In other words, the number of singly and doubly excited configurations must be finite for practical implementation, leading to truncation error even for a two-electron system. Fortunately, the error due to truncation of the basis set, known as basis set incompleteness error (BSIE), is relatively well separated from the excitation rank truncation error. This separation has led to a number of computational approaches which use a systematic series of basis sets and extrapolation of results to estimate the complete basis set (CBS) limit wavefunction. One such method — the focal point method[31] — is employed in chapter 2 to benchmark the accuracy of less expensive computational methods. Even when extrapolation techniques are utilized, unphysically large basis sets must be used to obtain sufficiently accurate results. For instance, the computations in chapter 2 use a basis set with h functions ($\ell = 5$) on hydrogen! Analysis of atoms using partial wave expansions[32] has shown that the convergence of the BSIE for HF theory is exponential with respect to basis set size, while the BSIE in the correlated part of the expansion only falls off as ℓ_{max}^{-3}, where ℓ_{max} is the maximum angular momentum in the

basis set. To maintain consistency with regard to the subset of the Hilbert space chosen as a basis, experience has shown that on the order of $\ell_{\max}^3$ total basis functions are needed.[25] This means that correlation BSIE only falls off at the painfully slow rate of $\mathcal{O}(N_{\text{basis}}^{-1})$. The slow convergence of the correlation BSIE is attributed to the poor representation of the cusp in the wavefunction resulting from the coalescence of two electrons.[5,32–35] In 1957, Tosio Kato showed that, to first order for an atom, the wave function near the coalescence point of two electrons with opposite spin must satisfy

$$\lim_{r_{12}\to 0} \frac{\partial \widetilde{\Psi}}{\partial r_{12}} = \frac{1}{2}\Psi_{r_{12}=0} \tag{1.30}$$

where the tilde indicates spherical averaging. This difficulty associated with expressing the interelectronic cusp in terms of one-particle basis functions has long been known. When first trying to describe the helium atom in the late 1920s, E. A. Hylleraas originally tried to carry out a simple CI expansion using only one electron basis functions, but he found the convergence to be too slow.[36] When he included explicit functions of the interelectronic distance r_{12} in the wavefunction expansion, the convergence improved dramatically: using only a six term expansion, Hylleraas was able to obtain an estimate for the non-relativistic, Born–Oppenheimer electronic energy of helium atom that differs from the modern day value by only 0.17 kcal mol^{-1}— less than 0.01%![5,10,37] This was a phenomenal achievement for a time more than a quarter century before the dawn of the computing age.

1.3 R12 and F12 Methods

Unfortunately, when Hylleraas' method is applied directly to larger systems, untenable three- and four-electron integrals arise, making the method only suitable for systems of very few electrons. To date, Hylleraas-style CI computations have been performed only on systems of

at most three or four electrons.[38–40] In the 1980s, Kutzelnigg and Klopper realized that the many-electron integrals could be approximated using a resolution of the identity (RI).[41–45] The resulting methods were referred to as R12 methods, since they included terms that depend explicitly on the interelectronic distance r_{12}. Later improvements[46–49] to this approach led to the use of arbitrary functions of r_{12} in the wavefunction ansatz (rather than just linear terms), and these methods were termed F12 methods. In general, theoretical techniques that use the R12/F12 approach are known as *explicitly correlated* methods. The explicitly correlated methodology has been applied to a wide variety of theoretical methods, including second-order Møller–Plesset theory,[49–65] coupled cluster singles and doubles (CCSD),[66–76] CCSD with perturbative triples,[77–84] multireference perturbation theory,[61] and multireference configuration interaction.[85,86] The success of R12/F12 methods for chemical applications can be seen in the fact that they are now used in a wide variety of quantum chemical computations.[87–95] Explicitly correlated methods are discussed in greater depth in chapters 3 and 5.

1.4 AO Basis Methods

The orthonormality requirement imposed on canonical molecular orbitals, a result of equation (1.29), leads to a further complication with respect to scaling of computational effort. As the size of a system increases, there comes a point where the interactions between electrons localized to opposite sides of the system is numerically negligible. However, since canonical MOs are delocalized across the entire molecular system, there is no single term in the wavefunction corresponding to specific interaction between electrons on distant centers which may be neglected. The inability to neglect distant interactions leads to unphysical scaling in computational effort. For instance, the computational cost of computing the energy of a system of two benzene molecules separated by 5000 Å to 10 significant digits of precision

should require exactly twice the computational effort required for computing one benzene molecule, since the interaction of two benzene fragments at 5000 Å contributes negligibly to total energy of the system. However, with second order Møller–Plesset theory in the canonical MO basis for instance, which scales as $\mathcal{O}(N_{\text{basis}}^5)$, the computation of the distant pair would cost 32 times as much as the monomer. At least as early as the 1980s,[96] researchers realized that if correlated wavefunction methods are to be applied to large molecular systems, a means of localizing the orbital basis must be devised. A number of different schemes for doing so have been devised over the years, beginning with localized molecular orbital (LMO) methods.[96–100] The basic idea behind LMO methods is that the set of virtual orbitals which contribute most to the correlation of electrons in a given pair of localized occupied orbitals should different for different orbital pairs. The LMO basis is constructed using one of a variety of localization schemes,[101–104] and for each pair of occupied LMOs, a separate set of nonorthogonal, local virtual orbitals is constructed. These sets of virtual orbitals are then truncated to only include those virtual orbitals which make a significant contribution to the correlation of the corresponding occupied pair. This sort of procedure has been implemented for a variety of methods in the literature, including configuration interaction,[97] second- and fourth-order Møller–Plesset theory (MP2 and MP4),[98,100] explicitly correlated MP2 theory (MP2-F12),[53,58,63,64] coupled-cluster (CC) theories,[105–107] and explicitly correlated CC theories.[72,76] AO basis methods go one step further, using nonorthogonal atomic orbitals for the occupied space as well. As a result, no orbital localization scheme need be applied; instead, contributions to the electronic energy can be screened based on some mathematically rigorous criterion. For instance, since the two-electron integrals over the electron repulsion

operator $\frac{1}{r_{12}}$ form an inner product space, the Cauchy–Schwarz inequality can be utilized:

$$\langle \mu\nu|\varrho\sigma\rangle^2 \leq \langle \mu\nu|\mu\nu\rangle \langle \varrho\sigma|\varrho\sigma\rangle \tag{1.31}$$

$$\langle \mu\nu|\varrho\sigma\rangle \equiv \int \chi_\mu(\mathbf{r}_1)\chi_\nu(\mathbf{r}_2)\frac{1}{r_{12}}\chi_\varrho(\mathbf{r}_1)\chi_\sigma(\mathbf{r}_2)d\mathbf{r}_1 d\mathbf{r}_2 \tag{1.32}$$

Far more sophisticated integral screening criteria have been developed over the past decade by Ochsenfeld and co-workers,[108–113] who have performed AO basis MP2 computations on systems of more than 1000 atoms, demonstrating the efficacy of this approach. AO basis methods are discussed in further detail in chapter 5.

1.5 Prospectus

Herein, the use of wavefunction methods to study electron correlation is examined in more detail. In chapter 2, a case study demonstrating the importance of wavefunction-based *ab initio* methods is presented. The potential energy surface of the interaction between benzene and hydroxyl radical is studied using the focal point approach[31] and a variety of density functional theory (DFT) methods. It is shown that the potential energy surfaces obtained using DFT are insufficiently accurate for many quantitative uses in atmospheric modeling and combustion. An example of the benefits of using explicitly correlated wavefunction methods for the prediction of spectroscopic properties is presented in chapter 3, in which explicitly correlated coupled cluster methods are employed in the construction of quartic force fields for several hydrogen polyoxides and there isotopologues. The success of the technique is demonstrated in the fact that most of the fundamental vibrational frequencies predicted in the paper agree with experiment to better than 5 cm^{-1} or about 1% error. This across-the-board consistency allows us to make a couple of reassignments of previously published experimental spectra. Rigorous electron structure treatment of potential energy

surfaces can only go so far, however, in predicting experimental results if only quartic potential energy terms are considered, so chapter 4 presents new formulas for the conversion of internal coordinate force fields of arbitrary order to Cartesian and normal coordinates useful for comparison with spectroscopic data. Chapter 4 also serves as a case study into the discrepancies between that which is easily implemented with modern computer programming languages and that which is easily expressed in familiar mathematical notation. With the importance of wavefunction methods and explicit correlation of electrons demonstrated concretely in chapters 2 and 3, in chapter 5 we explore a new technique for the application of explicitly correlated wavefunction methods to large systems. Equations for explicitly correlated second-order Møller–Plesset theory in the atomic orbital basis (AO-MP2-F12) are presented, implemented and discussed. The successful implementation of AO-MP2-F12 theory presented in chapter 5 paves the way for future study of methods that address the unphysical scaling of electron structure computations in both the number of basis functions per atom and the number of atoms in a system. Finally, chapter 6 presents some concluding remarks and briefly discusses the prospects for future extensions of the research presented herein.

Chapter 2

The Benzene+OH Potential Energy Surface: Intermediates and Transition States*

*David S. Hollman, Andrew C. Simmonett, and H. F. Schaefer, Phys. Chem. Chem. Phys. **13**, 2214 (2011). Reproduced by permission of the PCCP Owner Societies.

2.1 Abstract

The potential energy surface for the interaction between benzene and hydroxyl radical is studied in detail using quantum mechanical methods, with a particular focus on the hydrogen abstraction pathway. Geometric parameters are optimized using a variety of density functional methods as well as perturbation theory. Energies are refined using coupled cluster singles and doubles with perturbative triples [CCSD(T)] extrapolated to the complete basis set limit. At our most reliable level of theory, complexation energies are found to be (with zero-point corrected energies in parentheses) 3.7 (2.8) kcal mol^{-1} for the benzene–hydroxyl radical complex and 2.9 (-1.7) kcal mol^{-1} for the phenyl radical–water complex. The barrier to H abstraction lies 6.5 (4.2) kcal mol^{-1} above the infinitely separated benzene and hydroxyl radical monomers.

2.2 Introduction

The importance of hydroxyl radical ($HO^{\bullet}$) for combustion,[114–118] biological systems,[119–124] atmospheric studies,[125–132] and environmental sciences[133–135] is well documented. Consequently, hydroxyl radical interactions have been the subject of numerous experimental[136–139] and theoretical[140–144] studies. Specifically, hydroxyl interactions with organic substrates are important for the study of DNA damage[145–147] and carcinogenesis[148–150] because the radical can easily be generated by the heterolytic cleavage of water.

Polycyclic aromatic hydrocarbons (PAHs) are known to play a significant role in both combustion chemistry[151–153] and atmospheric pollution,[130,154] as well as their deleterious role in biology. In combustion chemistry, the formation of an initial six-membered ring is considered to be the rate determining step, beyond which rapid ring growth results in soot formation.[155–157] Benzene, in particular, is known to contribute significantly to the pollution

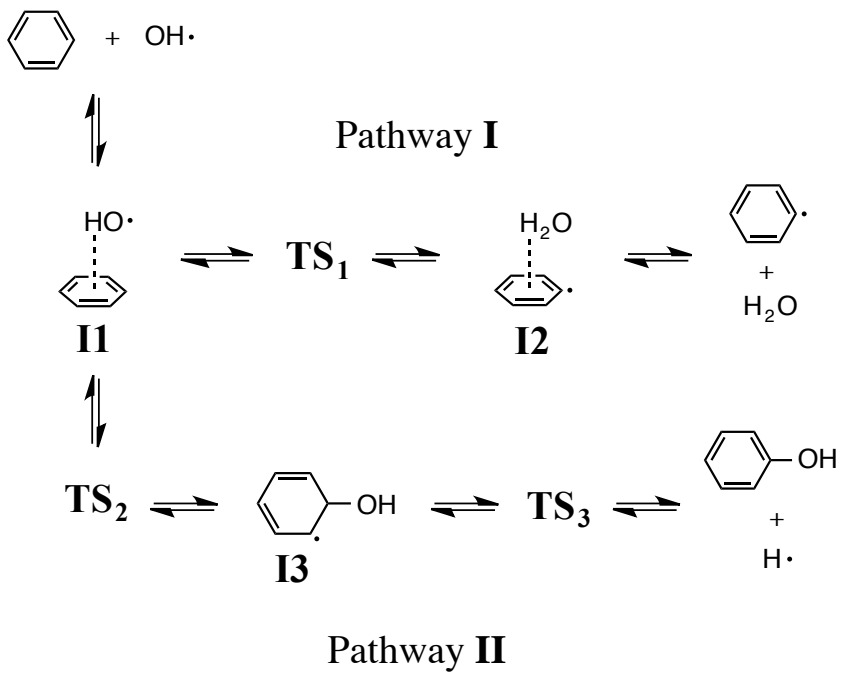

Figure 2.1: The two reaction pathways studied in detail in this research

of the troposphere.[158] Currently, the primary mechanism for removal of benzene from the troposphere is thought to start with the interaction of benzene and hydroxyl radical.[159]

Accurate relative energetics for PAH–radical systems are crucial for atmospheric simulation and macroscale kinetic modeling of hydrocarbon combustion. Consequently, many theoretical studies have been performed on these types of systems in the past. The benzene–OH potential energy surface (PES) was first studied using the MINDO/3 semiempirical method by Lobanov, *et al.*[160] in 1986. Later semiempirical studies include a PM3 study conducted by Lay, *et al.*[132] and an AM1 study of Cheney.[161] The most thorough *ab initio* study of the potential surface to date was carried out by Tokmakov and Lin,[162] who used the G3 method for single point energies assuming B3LYP/6-311++G(d,p) geometry optimizations. Other *ab initio* studies have been carried out by Barkholtz, *et al.*,[163] Chen,

et al.,[164] DeMatteo, *et al.*,[165] Seta, *et al.*,[166] and most recently by Mardyukov, *et al.*[159] Figure 2.1 shows the two lowest energy reaction pathways along the benzene + OH potential energy surface, which have been the focus of most past studies. Pathway **II** dominates at lower temperatures, but the hydroxycyclohexadienyl radical (**I3**) is not stable above about 500 K,[162,167] and so pathway **I** dominates at higher temperatures.[157,166]

Despite the difficulty associated with conducting experiments involving radical complexes, a significant amount of experimental work has also been done on the benzene + OH potential energy surface. A large number of temperature dependent studies[157,167–178] have been performed on the H-abstraction and OH-addition pathways (Pathways **I** and **II**, respectively, in Figure 2.1). However, the first experiment to accomplish the significantly harder task of detecting Intermediates **I1** and **I2** was performed by Mardyukov, Sanchez-Garcia, Crespo-Otero, and Sander (MSCS)[159] in 2009. MSCS performed flash vacuum pyrolyses of azobenzene and trapped the products in a argon matrix at 10 K. Upon doping the matrix to the extent of 1% water, **I2** was observed in the IR spectrum. Exposure to 350 nm radiation for several minutes yielded a subsidence in the IR signal assigned to **I2** and the appearance of the IR signal corresponding to **I1**.

Previous computational studies have characterized **I1** in some detail. Tokmakov and Lin (TL)[162] studied the C_{6v} Intermediate **I1a**, which they say has "virtually the same energy" as the C_s **I1b** (both structures are shown in Figure 2.2) that is immediately connected to $\mathbf{TS_1}$. TL also performed a reaction path computation along the C_{6v} separation pathway, which they say serves as an "upper bound to the minimum-energy path," and found that "even at separations greater than 5 Å substantial attraction still exists." A molecular orbital analysis was also performed on **I1a**, with the short-range MO interactions' contribution to the overall stabilization found to be "very weak." For Intermediate **I1b**, however, TL found a fairly significant contribution to the stabilization from the frontier MOs, even though the overall complexation energy is roughly the same.

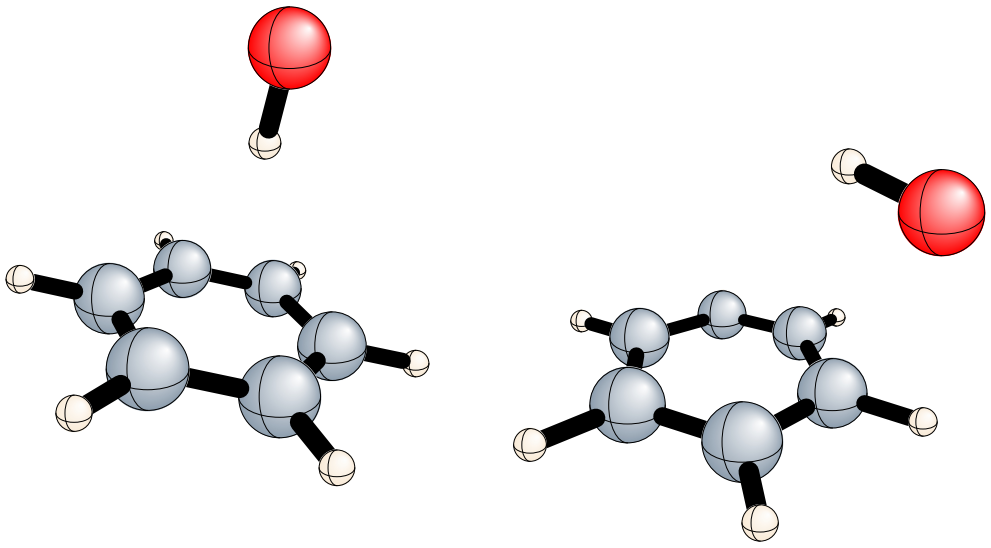

(a) The C_{6v} structure

(b) The C_s structure

Figure 2.2: Two of the previously proposed theoretical equilibrium structures for Intermediate **I1**, the loose complex between benzene and OH radical. The full Cartesian geometries are provided in the supplementary material.

TL, however, did not study the phenyl radical–water [$C_6H_5 \cdots H_2O$] complex (**I2**); this was first done by DeMatteo, et. al.[165], though their identification is tangential to the main point of their paper. Their complex, however, is the result of a side-on interaction similar to **I2b**, rather than the over-ring interaction similar to **I2a** found from a combination of experiment and theoretical computations by MSCS. These two complexes are connected by a very flat potential, so there is probably little chemical significance to this difference except at very low temperatures.

In the present work, we study the potential energy surface of the benzene + hydroxyl radical interaction along the two pathways given in Figure 2.1. Our primary focus is on the two complexes, **I1** and **I2**, formed along pathway **I**, with the intent to provide further analysis and interpretation of the recent experimental results from MSCS.[159] Given the inability of many popular DFT functionals to describe non-bonded interactions and barrier heights, we provide reliable *ab initio* predictions to quantitatively describe this important chemical system.

2.3 Computational Methods

We investigated the benzene + OH PES using a range of DFT methods for geometry optimizations and harmonic vibrational frequency computations. However, higher level theoretical methods are usually necessary to reliably predict barrier heights for abstraction reactions.[179] Further geometry optimizations were thus performed with the more robust RI-MP2 method[180–182] using the Ahlrichs def2–TZVPP basis.[183] We then obtained complete basis set (CBS) limit coupled cluster with single, double, and perturbative triple excitations [CCSD(T)][184–187] relative energies using the RI-MP2 geometries within the focal point scheme of Allen, *et al.*[31,188]

A variety of density functionals and basis sets were examined for the species with exper-

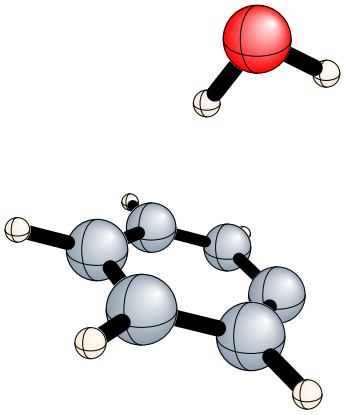

I2a

(a) The "over-ring" structure

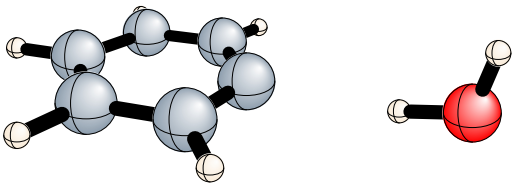

I2b

(b) The "side-on" structure

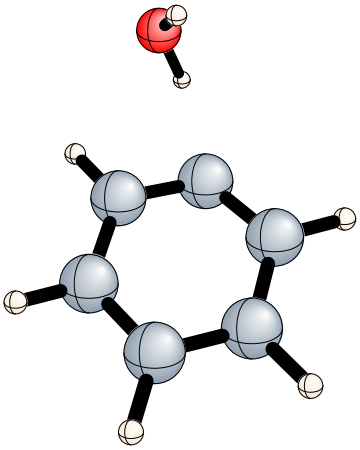

I2c

(c) The C_1 "side-on" structure, resulting from our theoretical computations

Figure 2.3: Two of the previously proposed theoretical equilibrium structures for Intermediate I2, as well as one that is a result of our computations.

imentally known fragment structures to help determine the best computational method for geometry optimizations. After some preliminary investigation into a larger number of methods, we selected six density functionals, B3LYP,[189] ωB97, ωB97X,[190,191] ωB97X–D,[192] M06, and M062X,[193] with two different basis sets, 6-31G*[194] and def2–TZVPP.[183] For all DFT computations, an ultrafine integration grid was used with 70 radial points and 590 angular points. All of the optimizations were subject to tightened convergence criteria due to the relative flatness of the potential above the benzene ring. For a refinement of our DFT geometries, resolution-of-the-identity second-order Møller–Plesset perturbation theory (RI-MP2)[195] was used with the def2–TZVPP basis set. IRC computations were performed at several levels of theory to confirm the connectedness of the PES. For all of the methods/basis set pairs investigated, we computed harmonic vibrational frequencies to make sure that all of the transition state geometries had only one imaginary frequency and that the other stationary points did not have imaginary frequencies. For methods without available analytic second derivatives, Hessians were computed via finite differences of analytic gradients.

Using the focal point method of Allen, *et al.*, we examined the basis set and level-of-theory dependence of the nine distinct stationary points along the potential energy surface, sketched in Figure 2.1. Def2–TZVPP RI-MP2 geometries were used for these computations unless otherwise stated. The focal point method allows us to extrapolate to the complete basis set (CBS) limit while monitoring the importance of higher-order excitations. For each of the nine stationary points, energy computations were performed at the cc-pVXZ (X = D, T, Q, 5, 6)[196] restricted open-shell Hartree–Fock (ROHF)[197] level of theory, as well as cc-pVXZ (X = D, T, Q, 5, 6) second-order Z-averaged perturbation theory (ZAPT2),[198] cc-pVXZ (X = D, T, Q) coupled cluster with single and double excitations (CCSD),[199–202] and cc-pVXZ (X = D, T) CCSD(T). The difference between the cc-pVQZ ZAPT2 and cc-pVQZ CCSD energies is added to the CBS-extrapolated correlation energy at the ZAPT2 level, and the difference between the cc-pVTZ CCSD and cc-pVTZ CCSD(T) energies is further added

to give an estimate of the total correlation energy. The CBS correlation energy is added to the CBS extrapolated Hartree–Fock energy to get the focal point energy of the system. CBS energies for ROHF (E_{HF}) and ZAPT2 correlation (E_{corr}) theories are computed by extrapolating functions of the forms[203,204]

$$E_{HF}(X) = A + Be^{-CX}$$

and

$$E_{corr}(X) = A + BX^{-3},$$

where X is the number of zetas in the basis set (two for cc-pVDZ, three for cc-pVTZ, etc.). Core correlation corrections (Δ_{core}) were computed at the cc-pCVTZ[196] ZAPT2 level of theory using

$$\Delta_{\text{core}} = E_{\text{ae}} - E_{\text{fc}},$$

where E_{ae} and E_{fc} are the all-electron and frozen core energies, respectively.

The Q-Chem 3.2 computational package[205] was used for all geometry, frequency, and IRC computations, including DFT and RI-MP2 computations. The Molpro 2006[206] computational package was used to calculate single-point coupled cluster energies, and MPQC 2.3[207] was used to compute large-basis ZAPT2 single point energies. MPQC computations were performed at the National Energy Research Scientific Computing center (NERSC); the superb MPQC parallel scaling made it possible to run the largest of our computations, which used 1617 basis functions, in less than 6 hours.

	6-31G*			TZVPP					
Parameter*	B3LYP	M06	M062X	B3LYP	ωB97X–D	M06	M062X	RI-MP2	Expt.‡
·OH									
r(O–H)	0.983	0.978	0.979	0.974	0.969	0.969	0.971	0.966	0.970
H_2O									
r(O–H)	0.969	0.964	0.966	0.961	0.956		0.959	0.957	0.958
∠(H–O–H)	103.6	104.1	104.3	104.9	105.0	104.8	105.0	104.0	104.5
C_6H_6									
r(C–C)	1.397	1.392	1.393	1.391	1.387	1.385	1.388	1.390	1.397
r(C–H)	1.087	1.089	1.086	1.082	1.082	1.083	1.082	1.079	1.084

∗ Bond lengths are in angstroms, angles are in degrees.
‡The experimental structures were obtained from ref. 209 for OH, ref. 210 for water, and ref. 211 for benzene.

Table 2.1: A comparison of selected geometry optimization methods with experiment for three immediately relevant covalently bonded systems.

2.4 Results and Discussion

2.4.1 Geometry Optimizations

A comparison of some of the geometry optimization methods for OH, H_2O, and C_6H_6 is shown in Table 2.1, though it is well known that all of the methods we used perform reasonably well for most simple, covalently-bonded systems. These data show that the experimental values are reproduced well enough by def2–TZVPP RI-MP2 for the covalently bonded systems relevant to this study. Since RI-MP2 with the def2–TZVPP basis set has specifically been shown to accurately reproduce geometries for non-covalent interactions as well,[208] we decided to use these geometries in our higher-level computations.

The geometries of both of the pathway **I** intermediate complexes, **I1** and **I2**, present some particular issues that merit further discussion. Many previous studies[159,162,165] come to qualitatively different conclusions about the geometries of these intermediates. For instance,

there is a noticeable difference between the structures of DeMatteo, *et al.*[165], similar to **I1b** and **I2b** in Figures 2.2 and 2.3, and those of MSCS,[159] whose geometries are similar to **I1a** and **I2a**. Intrinsic reaction coordinate (IRC) computations at the 6-31+G* B3LYP level of theory performed by DeMatteo, et. al.[165] show that **I1b** and **I2b** are directly connected by $\mathbf{TS_1}$; **I1a** and **I2a** are not directly connected by $\mathbf{TS_1}$. We confirmed this connection (or some reasonable approximation of it) at several other levels of theory, including 6-31G* B3LYP and def2–TZVPP with B3LYP, M062X and RI-MP2. As noted earlier, however, the potential surface connecting the two proposed structures for each intermediate is extremely flat. The flatness of this potential means that the intermediates' geometries will be highly fluxional except at very low temperatures. To support this conclusion, we performed focal point computations on several possible intermediate geometries, which we obtained as follows. The def2–TZVPP RI-MP2 computations for **I1** converged to **I1a** (Figure 2.2); the same geometry is obtained when **I1b** is used as an initial guess. To obtain the geometry of **I1b**, we had to optimize the geometry of the intermediate at the def2–TZVPP B3LYP level of theory. However, all of the key covalently-bonded geometric parameters (C–C bond length, C–H bond length, O–H bond length, *etc.*) were the same in both optimized geometries of **I1**. Similarly, three structures were obtained for **I2** (def2–TZVPP with RI-MP2, B3LYP, and M062X, corresponding to **I2a**, **I2b**, and **I2c**, respectively, in Figure 2.3). All relevant geometric parameters can be found in the supporting information.

In order to qualitatively compare the structures of **I1** and **I2** to the recent experimental infrared data of MSCS,[159] we computed the shifts in harmonic OH-stretching frequency for each structure relative to its monomers at infinite separation. At the def2–TZVPP B3LYP level of theory, Intermediate **I2a** exhibited a red shift of 14 cm^{-1} relative to isolated water, and **I2b** exhibited a much larger red shift of 118 cm^{-1}. The experimentally observed shift is 21 cm^{-1}, leading us to conclude that the experimentally observed structure is closer to **I2a** than to **I2b**, in agreement with MSCS. At the same level of theory, **I1a** exhibited a

red shift of 17 cm^{-1}, while **I1b** exhibited a *blue* shift of 34 cm^{-1}. The MSCS experiments gave a red shift of 46 cm^{-1}, suggesting that the experimentally observed structure is closer to **I1a** than to **I1b**. Other methods, such as def2–TZVPP M06 and def2–TZVPP RI-MP2, lead us to similar conclusions; a table of these additional results is given in the supporting information. The fairly significant errors in these frequencies compared to experiment can be attributed to anharmonicity and matrix effects, in addition to the intrinsic errors in the method. The anharmonic correction to these results is likely to be similar for both the isolated and complexed species, so this is probably not a very large source of error. Argon matrix shifts for OH stretches have been shown to be as high as 61 cm^{-1} for tethered OH species such as HCOH,[212] but the argon matrix shift for the free hydroxyl radical is known experimentally to be a red shift of only about 20 cm^{-1}.[213–215] Even though the matrix shifts for the complexes are unknown, they are not likely to be more than a factor of two different from that of free hydroxyl radical; however, this may explain the difference from experiment of the frequency we obtained for **I1a**. Even so, we conclude that these predictions lead us to a qualitatively correct understanding about the experimentally observed complexes.

2.4.2 H Abstraction PES

The focal-point-extrapolated potential energy surface for the pathway leading to phenyl radical plus water is given in Figure 2.4. The zero point vibrational energy (ZPVE) corrected predictions are given in parentheses; ZPVE computations were performed at the def2–TZVPP M06 level of theory. The focal point extrapolation tables showing how we arrived at these predictions are given in Tables 2.2 ($\mathbf{TS_1}$), 2.3 (**I1**), and 2.4 (**I2**). In all three of these focal point tables, we can be confident that we have thoroughly represented the basis set dependence, since at the ROHF level of theory, no extrapolated value differs from the best explicitly computed value by more than 0.02 kcal mol^{-1}. The greatest probable source of error for the computation of the forward barrier (and the effective barrier) is the com-

Basis Set	ΔE_e[ROHF]	δ[ZAPT2]	δ[CCSD]	δ[CCSD(T)]	ΔE_e[CCSD(T)]
cc-pVDZ	26.72	-16.31	-0.62	-2.08	[+7.71]
cc-pVTZ	27.78	-18.18	-0.26	-2.87	[+6.48]
cc-pVQZ	28.16	-18.55	-0.27	-3.07	[+6.27]
cc-pV5Z	28.36	-18.57	[-0.27]	[-3.07]	[+6.45]
cc-pV6Z	28.40	-18.58	[-0.27]	[-3.07]	[+6.49]
∞	[28.41]	[-18.59]	[-0.27]	[-3.07]	**[+6.48]**
ΔE_e (final) = ΔE_e[CBS CCSD(T)] + Δ_{core} + Δ_{ZPVE} = 6.46 − 0.05 − 2.28 = **4.16** kcal mol^{-1}					

[a]The symbol δ denotes the increment in the relative energy (ΔE_e) with respect to the preceding level of theory in the hierarchy ROHF→ZAPT2→CCSD→CCSD(T). Square brackets signify results obtained from basis set extrapolations or additivity assumptions. Final predictions are boldfaced.

Table 2.2: Energy (in kcal mol^{-1}) of $\mathbf{TS_1}$ relative to separated benzene and hydroxyl radical.[a]

Basis Set	ΔE_e[ROHF]	δ[ZAPT2]	δ[CCSD]	δ[CCSD(T)]	ΔE_e[CCSD(T)]
cc-pVDZ	-1.74	-2.29	+0.65	-0.32	[-3.70]
cc-pVTZ	-1.32	-3.11	+0.76	-0.46	[-4.12]
cc-pVQZ	-1.03	-3.24	+0.77	[-0.46]	[-3.96]
cc-pV5Z	-0.79	-3.27	[+0.77]	[-0.46]	[-3.74]
cc-pV6Z	-0.73	-3.26	[+0.77]	[-0.46]	[-3.67]
∞	[-0.72]	[-3.24]	[+0.77]	[-0.46]	**[-3.65]**
ΔE_e (final) = ΔE_e[CBS CCSD(T)] + Δ_{core} + Δ_{ZPVE} = −3.65 − 0.03 + 0.89 = **-2.79** kcal mol^{-1}					

Table 2.3: Energy (in kcal mol^{-1}) of **I1a** relative to separated benzene and hydroxyl radical, giving the complexation energy. See footnote *a* in Table 2.2 for more details.

Basis Set	ΔE_e[ROHF]	δ[ZAPT2]	δ[CCSD]	δ[CCSD(T)]	ΔE_e[CCSD(T)]
cc-pVDZ	-1.20	-2.74	+0.78	-0.38	[-3.54]
cc-pVTZ	-0.64	-3.68	+1.01	-0.56	[-3.87]
cc-pVQZ	-0.25	-3.73	+1.00	[-0.56]	[-3.53]
cc-pV5Z	0.07	-3.65	[+1.00]	[-0.56]	[-3.13]
cc-pV6Z	0.15	-3.60	[+1.00]	[-0.56]	[-3.00]
∞	[0.17]	[-3.53]	[+1.00]	[-0.56]	**[-2.91]**
ΔE_e (final) = ΔE_e[CBS CCSD(T)] + Δ_{core} + Δ_{ZPVE} = $-2.91 - 0.03 + 1.22$ = **-1.72** kcal mol^{-1}					

Table 2.4: Energy (in kcal mol^{-1}) of **I2a** relative to separated phenyl radical and water, giving the complexation energy. See footnote *a* in Table 2.2 for more details.

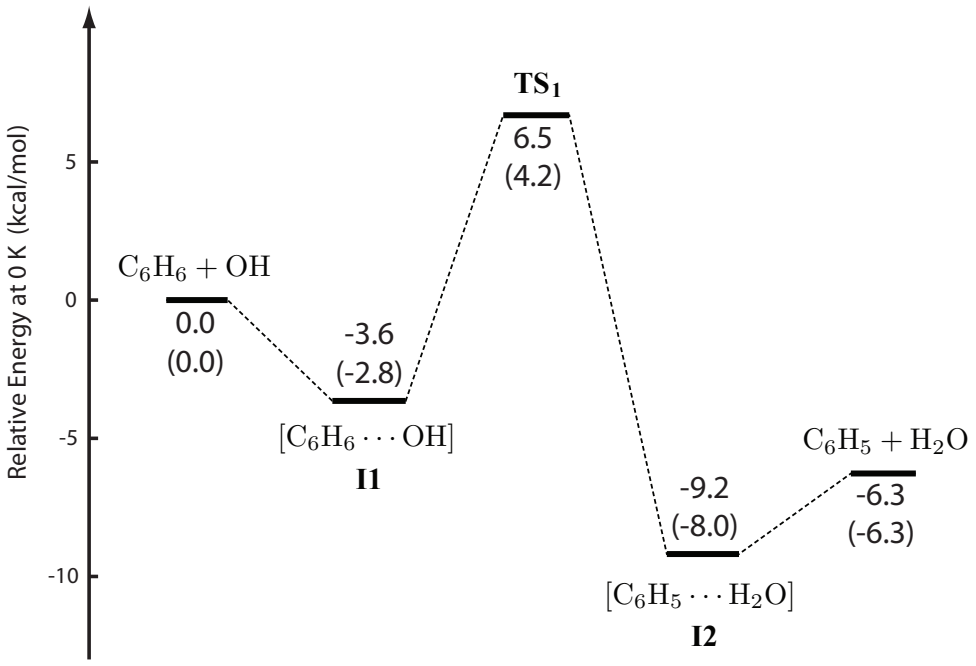

Figure 2.4: Potential energy diagram for the H abstraction reaction pathway. All results are extrapolated focal point energies; the corresponding focal point tables are given in the supporting information. ZPVE-corrected energies are given in parentheses.

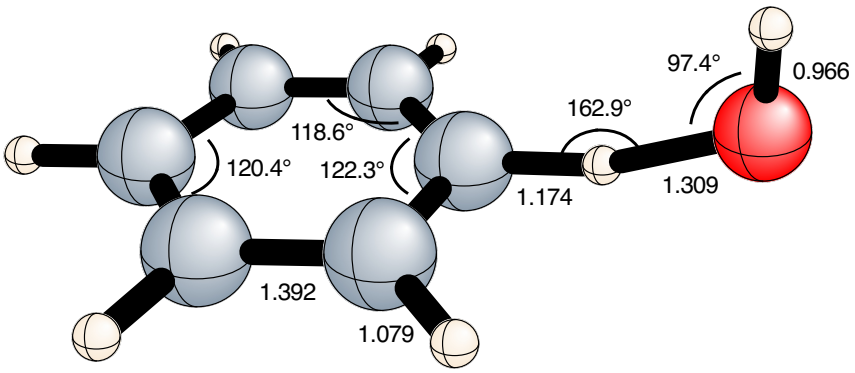

Figure 2.5: The def2–TZVPP RI-MP2 theoretical geometry of $\mathbf{TS_1}$, which has C_s symmetry. All bond lengths are in angstroms. The full Cartesian coordinates of this geometry can be found in the supporting information.

putation of the transition state energy itself, which showed a -3.1 kcal mol^{-1} perturbative triples contribution (Table 2.2) with the cc-pVQZ basis set; clearly, higher-order excitations are essential for a quantitative elucidation of this PES. The transition state, the geometry of which is shown in Figure 2.5, exhibits a lowering in energy at each successive level of theory, suggesting that we have obtained an effective upper bound for the fully correlated energy. When the ZPVE corrections are included, the previously computed range of 3.5 to 5.0 kcal mol^{-1} from TL[162] is consistent with our findings, but we find that the true value is probably in the upper part of this range.

The binding energies of the intermediates, on the other hand, exhibit an oscillating pattern as excitations are added, leading us to conclude that the CCSDT correction will likely be positive, but smaller than the CCSD(T) correction in each case. If the pattern could be carried out to the fully correlated result, it is likely that there would be substantial error cancellation in the successive consideration of higher-order excitations. The complexation energies for both **I1** and **I2** are also not as correlation-dependent as the aforementioned barrier height, with only -0.5 kcal mol^{-1} and -0.6 kcal mol^{-1} triples contributions with the

I2b relative to **I2a**

Basis Set	ΔE_e[ROHF]	δ[ZAPT2]	δ[CCSD]	δ[CCSD(T)]	ΔE_e[CCSD(T)]
cc-pVDZ	1.16	-0.21	-0.47	-0.04	[+0.44]
cc-pVTZ	1.00	+0.57	-0.61	+0.01	[+0.97]
cc-pVQZ	0.85	+0.67	-0.61	[+0.01]	[+0.93]
cc-pV5Z	0.76	+0.72	[-0.61]	[+0.01]	[+0.89]
cc-pV6Z	0.75	+0.71	[-0.61]	[+0.01]	[+0.87]
∞	[0.75]	[+0.70]	[-0.61]	[+0.01]	**[+0.85]**

I2c relative to **I2a**

Basis Set	ΔE_e[ROHF]	δ[ZAPT2]	δ[CCSD]	δ[CCSD(T)]	ΔE_e[CCSD(T)]
cc-pVDZ	-0.83	-0.17	-0.28	+0.02	[-1.25]
cc-pVTZ	0.25	+0.85	-0.54	+0.10	[+0.66]
cc-pVQZ	0.47	+1.09	[-0.54]	[+0.10]	[+1.12]
cc-pV5Z	0.48	+1.23	[-0.54]	[+0.10]	[+1.27]
cc-pV6Z	0.48	+1.23	[-0.54]	[+0.10]	[+1.28]
∞	[0.48]	[+1.24]	[-0.54]	[+0.10]	**[+1.29]**

Table 2.5: Energies (in kcal mol^{-1}) of **I2b** and **I2c** relative to **I2a** (see Figure 2.3), showing that the intermediates more closely connected to the transition state are higher in energy than the structure found by MSCS.[159] See footnote *a* in Table 2.2 for more details.

Basis Set	ΔE_e[ROHF]	δ[ZAPT2]	δ[CCSD]	δ[CCSD(T)]	ΔE_e[CCSD(T)]
cc-pVDZ	4.75	-2.16	-0.72	-0.41	[+1.47]
cc-pVTZ	5.51	-2.29	-0.70	-0.58	[+1.94]
cc-pVQZ	5.54	-2.48	[-0.70]	[-0.58]	[+1.78]
cc-pV5Z	5.48	-2.56	[-0.70]	[-0.58]	[+1.63]
∞	[5.43]	[-2.65]	[-0.70]	[-0.58]	**[+1.50]**

Table 2.6: Energy (in kcal mol^{-1}) of **I1b** relative to **I1a** (see Figure 2.2), showing that the intermediate directly connected to the transition state (**I1b**) is higher in energy than the structure proposed by MSCS (**I1a**). See footnote *a* in Table 2.2 for more details.

cc-pVTZ basis set for **I1** and **I2**, respectively. The larger source of error here comes from the uncertainty in the geometries. For **I2**, the complexation energies for **I2b** and **I2a** differ by 0.9 kcal mol^{-1}, with **I2a** showing the strongest complexation energy. The focal point extrapolation results for **I2b** and **I2c** are given in Table 2.5 relative to the minimum energy structure, **I2a**. Notice that structures **I2b** and **I2c** are higher in energy, even though both appear to be more strongly complexed with a smaller basis set, and the correct relative ordering of all three structures is not obtained until the cc-pVQZ basis set is used, at the Hartree–Fock level of theory. Similarly, the focal-point-extrapolated complexation energy of **I1a** is 1.5 kcal mol^{-1} higher in energy than **I1b**. The focal point table for the **I1b** energy relative to **I1a** is given in Table 2.6. It is possible that these two complexes are nearer to being isoenergetic than the 1.5 kcal mol^{-1} difference in Table 2.5, since the level-of-theory dependence of the differential energy appears to be monotonically decreasing.

Comparison of DFT Results

Table 2.7 gives a comparison of some geometric and energetic parameters of the best density functional methods we tested for **I1** and **I2**. Not surprisingly, the M062X method, which is designed with noncovalent systems like this one in mind, performed the most like the wavefunction method, RI–MP2. Care should be taken in the interpretation of these data; most of the outlier values are not actually indicative of qualitative differences. For instance, the def2–TZVPP M06 C_1XH angle for **I1** differs from the def2–TZVPP RIMP2 value by 13 degrees, but this is mostly because the OH radical is off-center on the benzene ring (see picture in supplementary material). In each case given in the table, the computations converged on geometries similar to **I1a** and **I2a**, rather than the alternatives discussed above.

In general, the best density functional method we investigated for examining the energetics of this potential energy surface is def2–TZVPP M062X, which gives a complexation energies of 4.8 kcal mol^{-1} for **I1**, 4.2 kcal mol^{-1} for **I2**, and a relative energy of 5.7 kcal

	I1					**I2**						
Method	r(XH)	r(XO)	$\angle$(C_1XH)	$\angle$(C_1XO)	E_{complex}	r(XH_1)	r(XH_2)	r(XO)	$\angle$(C_1XH_1)	$\angle$(C_1XH_2)	$\angle$(C_1HO)	E_{complex}
B3LYP	3.430	2.454	90.0	90.0	2.5	3.594	2.742	3.604	85.1	108.2	100.4	1.9
M06	2.391	3.307	103.8	97.1	3.7	3.338	2.524	3.370	81.0	106.3	97.4	3.2
M062X	2.225	3.198	90.3	89.7	4.8	2.944	2.508	3.200	70.6	101.4	87.9	4.2
M06L	2.696	3.003	71.6	53.0	5.2	3.045	2.538	3.267	72.7	102.1	89.7	3.0
RI-MP2	2.240	3.208	90.4	89.8	4.8	3.210	2.410	3.253	76.7	103.2	93.8	4.5

Table 2.7: A comparison of the non-covalently-bonded parameters for several DFT and wavefunction geometries of **I1** and **I2**. All results in this table were carried out using the def2–TZVPP basis set. In the parameter names, X refers to the center of the ring, C_1 refers to the carbon from which the hydrogen is being abstracted, H_1 is the abstracted hydrogen in water, and H_2 is the other hydrogen in water. E_{complex} is the complexation energy, which has a focal-point-extrapolated value of 3.6 for **I1** and 2.9 for **I2**. All distances are given in angstroms, all angles are in degrees, and all energies are in kcal mol^{-1}. ZPVE corrections are *not* included in the values given below.

mol^{-1} for $\mathbf{TS_1}$ (excluding ZPVE corrections). Several other methods performed surprisingly well for certain aspects of the PES. For instance, 6-31G* B3LYP gave complexation energies of 3.3 kcal mol^{-1} and 2.8 kcal mol^{-1} for **I1** and **I2**, respectively, but it underestimates the relative energy of $\mathbf{TS_1}$ as only 4.0 kcal mol^{-1} (see supplementary material). Interestingly, B3LYP with the much larger def2–TZVPP basis actually performs significantly worse for all three of these parameters, predicting complexation energies of 2.5 kcal mol^{-1} and 1.9 kcal mol^{-1} for the **I1** and **I2** stabilization energies, and 2.5 kcal mol^{-1} for the relative energy of $\mathbf{TS_1}$. The small basis set results benefit from partial cancellation of intrinsic functional errors and basis set incompleteness errors; the larger basis result is a more true measure of the intrinsic functional error. All of the DFT energetics and geometries for the methods examined are given in the supporting information.

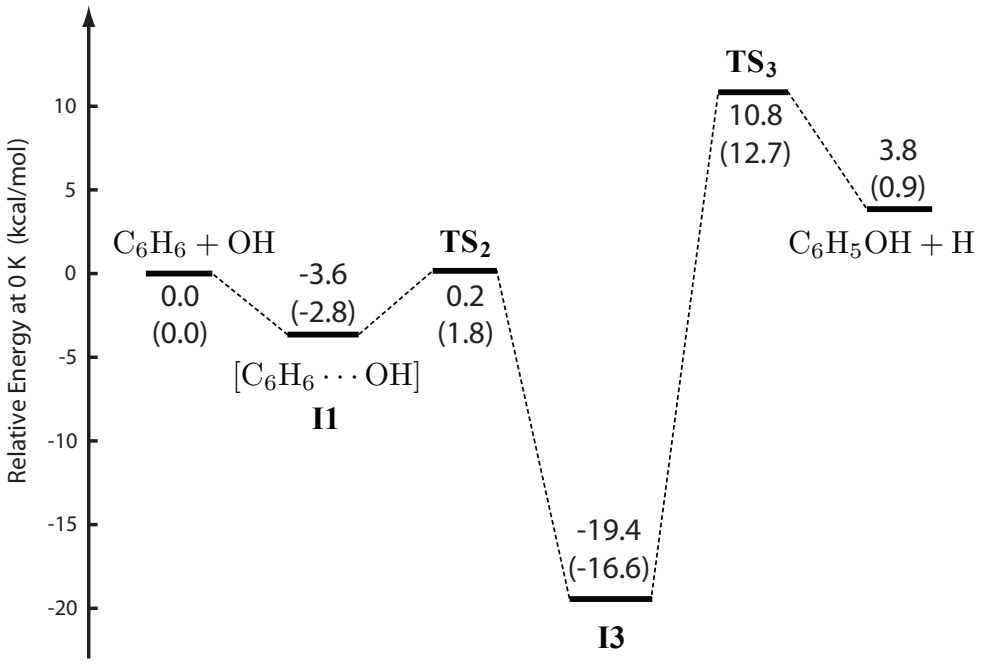

Figure 2.6: Potential energy diagram for the OH addition pathway. All predictions are based on extrapolated focal point energies; the corresponding focal point tables are given in the supporting information. ZPVE-corrected energies are given in parentheses.

2.4.3 OH Addition PES

Figure 2.6 gives a sketch of the potential energy surface for the reaction pathway leading to phenol. The most notable feature is the global minimum, **I3**, which lies 16.6 kcal mol^{-1} below the separated benzene and OH reference. This stabilization energy is surprisingly close to the previous studies' values: 16.2 kcal mol^{-1} [165] and 16.4 kcal mol^{-1}.[162] The value for the $\mathbf{TS_2}$ barrier is puzzling in some respects. Our focal point analysis leads us to conclude that this transition state lies only 1.7 kcal mol^{-1} above separated benzene plus OH (after the ZPVE correction), which puts the barrier with respect to **I1** at only 4.6 kcal mol^{-1} (see Table 2.8). Roughly similar conclusions were reached by previous authors, whose estimated **I1**–$\mathbf{TS_2}$ barriers of 2.7 kcal mol^{-1} [162] and 1.2 kcal mol^{-1} [165] are even lower. Studies of

similar systems have also reached this type of conclusion; the analogous benzene + CCH addition reaction is barrierless,[216] so no analogue for **I1** and $\mathbf{TS_2}$ exists for this system, which is consistent with the low barrier obtained in our study. However, the isoelectronic benzene + CH_3 system has a much larger barrier of 13.9 kcal mol^{-1} relative to isolated reactants, while that of benzene + H is roughly 8.5 kcal mol^{-1} according to G2M(cc,MP2) theory.[217] The low barrier height for $\mathbf{TS_2}$ is interesting, given the recent observation of **I1** by MSCS.[159]

Due to the lengthened covalent-like bonding nature of the $\mathbf{TS_2}$ C–O bond (pictured in Figure 2.7), this transition state has more multireference character than either the complexed **I1b** or the covalently-bound **I3** (the global minimum, pictured in Figure 2.8), making it preferentially stabilized by higher order excitations. This is evident from the focal point analysis in Table 2.8, where the effective barrier height is reduced with increasing excitation treatment. Therefore, our value for the effective barrier height may represent an upper bound to the true value.

Another transition state, $\mathbf{TS_3}$ (shown in Figure 2.9), separates **I3** from isolated phenol plus H radical. The elimination of H allows **I3** to return to an aromatic system (phenol), which is indicated by the shortening of the C1–C6 and C1–C2 bonds in the transition state. Our computations show that $\mathbf{TS_3}$ lies 10.7 kcal mol^{-1} (12.7 kcal mol^{-1} with ZPVE correction) above separated benzene plus OH. TL came to a roughly similar conclusion of 8.3 kcal mol^{-1}.[162] Even at this lower barrier height, however, they conclude that the H-elimination branch makes a small enough contribution the OH addition channel rate constant that it could be safely ignored at temperatures below 400 K. As already noted, **I3** is not viable above about 500 K, so it is not likely that this part of the potential energy surface makes a major contribution to the chemistry of the system.

Basis Set	ΔE_e[ROHF]	δ[ZAPT2]	δ[CCSD]	δ[CCSD(T)]	ΔE_e[CCSD(T)]
cc-pVDZ	26.31	-13.54	-3.08	-2.45	[+7.25]
cc-pVTZ	26.91	-15.89	-2.68	-3.25	[+5.09]
cc-pVQZ	26.99	-16.63	-2.72	[-3.25]	[+4.39]
cc-pV5Z	26.94	-16.93	[-2.72]	[-3.25]	[+4.04]
cc-pV6Z	26.93	-17.02	[-2.72]	[-3.25]	[+3.94]
∞	[26.93]	[-17.15]	[-2.72]	[-3.25]	**[+3.81]**
ΔE_e (final) = ΔE_e[CBS CCSD(T)] + Δ_{core} + Δ_{ZPVE} = 3.81 + 0.01 + 0.72 = **4.55** kcal mol^{-1}					

Table 2.8: Energy (in kcal mol^{-1}) of $\mathbf{TS_2}$ relative to relative to **I1**, giving the effective barrier height. See footnote *a* in Table 2.2 for more details.

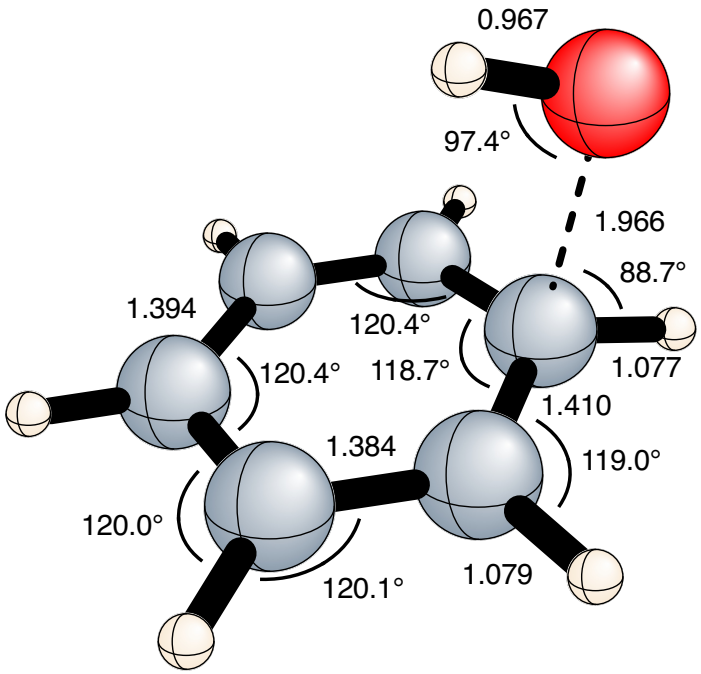

Figure 2.7: The def2–TZVPP RI-MP2 geometry of $\mathbf{TS_2}$, which has C_s symmetry. All bond lengths are in angstroms. For a rough comparison, the IRC-connected def2–TZVPP B3LYP geometry of **I1b** in Figure 2.2 has a C–O distance of 2.465 Å. (Def2–TZVPP RI-MP2 computations of the **I1b** structure converged on **I1a**).

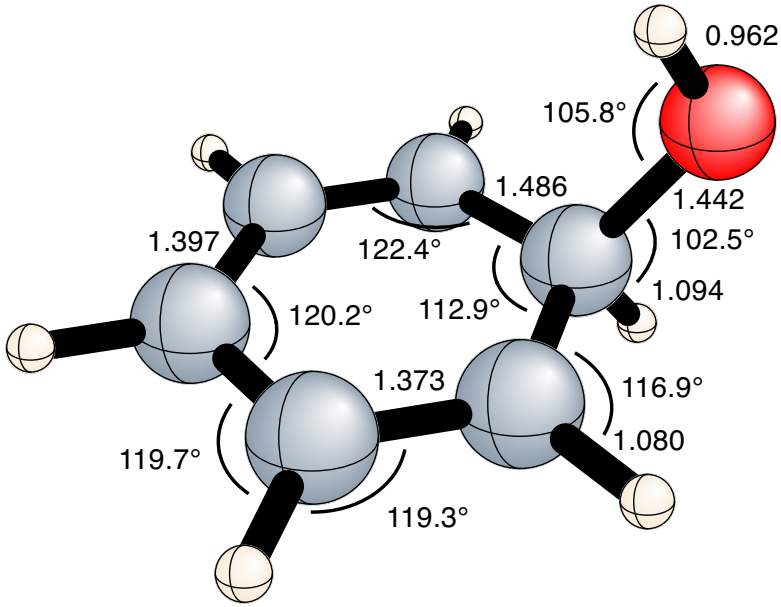

Figure 2.8: The def2–TZVPP RI-MP2 theoretical equilibrium geometry of **I3**, which has C_s symmetry. All bond lengths are in angstroms. The full Cartesian coordinates of this geometry can be found in the supporting information.

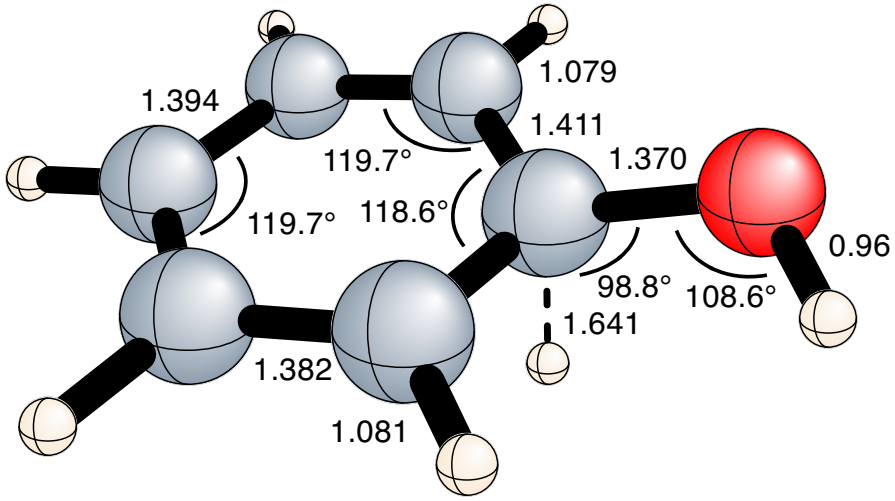

Figure 2.9: The def2–TZVPP RI-MP2 theoretical geometry of $\mathbf{TS_3}$, which has C_1 symmetry. All bond lengths are in angstroms. The full Cartesian coordinates of this geometry can be found in the supporting information.

2.5 Conclusions

The potential energy surface describing the interaction between benzene and hydroxyl radical has been investigated along two different pathways to an unprecedented accuracy. We have shown that DFT methods alone are insufficient to quantitatively characterize this potential energy surface. Refinements of DFT energetics within the G3 composite scheme by previous authors[162] yield results closer to our benchmark, but with less theoretical rigor (G3 employs an empirical correction) and greater statistical uncertainty. The importance of connected triple excitations and basis set size has been examined for each of the nine distinct stationary points along the potential energy surface as well as three additional conjectured intermediate structures. We have shown that a number of different geometries for **I1** and **I2** can be obtained which span a very small energy range; this is a consequence of the flat potential energy surface describing these noncovalent interactions. In summary, we have provided accurate *ab initio* results in an attempt to quantitatively describe the two lowest energy pathways of the benzene plus hydroxyl radical interaction potential energy surface.

2.6 Acknowledgements

This research was supported by the Department of Energy, Office of Basic Energy Sciences, Chemistry Division, Fundamental Interactions Program, Grant No. DE-FG02-97-ER14748, and used resources of the National Energy Research Scientific Computing Center, which is supported by the Office of Science of the U.S. Department of Energy under Contract No. DE-AC02-05CH11231.

2.7 Supplementary Material

Electronic supplementary information (ESI) is available online It contains: full Cartesian geometries, additional focal point tables, comparison of geometry optimization methods, and a comparison of OH frequency shifts for different methods. See DOI: 10.1039/c0cp01607a.

Chapter 3

In Search of the Next Holy Grail of Polyoxide Chemistry: Explicitly Correlated *Ab Initio* Full Quartic Force Fields for HOOH, HOOOH, HOOOOH, and their Isotopologues*

*David S. Hollman and H. F. Schaefer, J. Chem. Phys. **136**, 084302 (2012). Reprinted here with permission of the American Institute of Physics.

3.1 Abstract

Explicitly correlated *ab initio* methods have been used to compute full quartic force fields for the three chain minima for HOOOOH, which are found to lie within 1 kcal mol^{-1}. The CCSD(T)-F12 method with the cc-pVTZ-F12 basis set was used to compute equilibrium structures, anharmonic vibrational frequencies, and rotational constants for HOOH, HOOOH, and three chain isomers of HOOOOH, with the two former force fields being used as benchmarks for the latter three. The full quartic force fields were computed in such a way as to yield fundamental frequencies for all isotopologues at once. The present research confirms the recent experimental identification of HOOOH and provides reliable force fields in support of future experimental work on the enigmatic bonding paradigms involved in the HOOOOH chain.

3.2 Introduction

It has been stated that the most important reaction in combustion chemistry is

$$H + O_2 \rightarrow HO_2.$$

Over the years, this reaction and its applications have been among the most studied topics in physical chemistry.[218–225] The role of higher polyoxides in this reaction as transient intermediates was first suggested in 1940,[226] via the reaction pathway

$$2HO_2 \rightarrow H_2O_4$$

$$H_2O_4 \rightarrow H_2O_2 + O_2.$$

Although this pathway does not directly implicate the chain structure (and recent findings[227] suggest that the role of any chain structure of H_2O_4 in this particular pathway may be minimal), early discussions of this pathway assumed a chain structure.[228] The first widely accepted detection of H_2O_4, by means of infrared and Raman spectroscopy, was reported in 1974,[229] though this study was unable to isolate the species. In 1982, Diem, Tso, and Lee[230] reported the matrix isolation IR spectrum of the ring HO_2 radical dimer, but the chemically bonded HO_4H chain isomer eluded detection.

The notion of higher polyoxides dates all the way back to 1895, when Mendeleev hypothesized the existence of H_2O_4 in the sixth edition of his famous *Osnovy Khimii*,[231] the English translation of which states: "If the sulphur be replaced by oxygen, then instead of H_2SO_3 and SO_2, we have H_2OO_3 and OO_2." This insight is remarkable, given that it had only been shown definitively that hydrogen peroxide is H_2O_2 and not HO or H_3O_3 in 1892. Though the analogy to sulfurous acid is a bit misguided structurally, the surprising discrepancy between the readily isolated hydrogen polysulfide chains and the vexingly elusive hydrogen polyoxide chains has been a driving force behind much research in subsequent years.

The 2002 matrix isolation study of HOOOH by Engdahl and Nelander[232] reignited interest in higher closed-shell polyoxide chains, their complexes, and potential reactions in a wide range of contexts.[222,223,227,233–240] The Engdahl-Nelander experiments were preceded by a number of progressively more rigorous theoretical studies in the late 1990's suggesting the feasibility of HOOOH synthesis.[241–243] An analogous trend in studies during the past decade has led many to speculate that the experimental isolation of the HO_4H chain may not be far in the future.[235,244] In 2005, HOOOH was observed by Suma, Sumiyoshi and Endo[234] in the gas phase using Fourier transform microwave spectroscopy. Endo and coworkers further note that "observations of rotational transitions of species such as H_2O_4 ... are well expected by a similar experimental setup."[234] More recently still, theoretical evidence has suggested the need to include hydrogen polyoxide radicals in atmospheric models,[236–238]

prompting numerous studies of the HOOO radical and its reactions.[245–248] Other evidence suggests that hydrogen polyoxides may be involved in biological processes,[249] and both small and large hydrogen polyoxides are known to contribute to the decomposition of ozone in water.[239,240,244,250] This potential for applications of molecules that are interesting in their own right as paradigms (and anomalies) in bonding theories has further fueled the excitement surrounding the polyoxide series.

A separate but related vein of study has been carried out on the HO_2 dimer potential energy surface,[227,251–253] leading to the theoretical characterization of several HO_4H chains as well as the aforementioned HO_2 ring dimer complex. *Ab initio* calculations in this line of research date back to at least 1984, when Fitzgerald computed properties of the cyclic, double hydrogen bonded structure.[251,252] Even at this early date, this region of the singlet potential energy surface was found to be highly multi-reference in character, making energetic stability comparisons to the chain structures difficult. The most recent research in this respect used CASSCF(14,12) and predicted that the energies of the singlet and triplet ring structures lie only 1.5 kcal mol^{-1} and 1.2 kcal mol^{-1}, respectively, below the lowest energy chain structure.[227]

After the completion of this work, a new experimental study was published by Levanov and coworkers,[254] in which they claim to have detected an HOOOOH chain structure by means of Raman spectroscopy. Their results represent the first steps towards a full experimental isolation and geometric characterization of HOOOOH.

In 2009, Denis and Ornellas[235] used *ab initio* computations to predict fundamental frequencies for HOOH, HOOOH, and HOOOOH. These authors used high-level coupled-cluster computations to predict harmonic frequencies, but they used only density functional theory computations to predict anharmonic corrections. Their work also lacks any mention of the two other HOOOOH isomers, thought from previous work to lie within 1 kcal mol^{-1} of the minimum structure.[227] Given the scientific importance of HOOOOH, we believe this

system merits further investigation. The present research summarizes the preparation and analysis of rigorous *ab initio* full quartic force fields (QFFs) for three energetically comparable isomers of the HO_4H chain structure. The methods used were extensively benchmarked on the smaller polyoxides HOOOH and HOOH, for which reliable experimental results are available. We hope that our results will serve as a guide for future experimental work, particularly for experiments that may seek to isolate and characterize all three of the HO_4H chain isomers.

3.3 Computational Methods

Our methodological approach to the computation of QFFs for the species under study is in several ways unique. To the best of our knowledge, this work presents the largest full QFF computation to date that uses explicitly correlated coupled-cluster methods. The reasonableness of this approach was thoroughly established in a seminal work by Rauhut, Knizia, and Werner (RKW)[87] in 2009, and since then it has been applied to a large number of systems.[88–92,94,95,255–257] The RKW study concluded that the quality of the force field obtained with explicitly-correlated coupled-cluster singles and doubles with single-particle basis perturbative triples[80,84] (more accurately denoted CCSD-F12(T), but often misleadingly referred to in the literature as simply CCSD(T)-F12, which is the convention we will adopt here)† and the cc-pVTZ-F12 basis set of Peterson and co-workers[258,259] yields a QFF of CCSD(T) with an augmented quintuple zeta basis set (aug-cc-pV5Z)[25] quality or better. Even the CCSD(T)-F12/cc-pVDZ-F12 results are "more accurate than CCSD(T) calculations with the aug-cc-pVQZ basis set." In light of this analysis (and further analysis of

†The actual approximation we used is referred to as "CCSD(T)-F12b," and the differences between this method and the sibling "CCSD(T)-F12a" method are discussed in refs.[84] and[80]. In our experience, however, the difference between the two methods is usually less than (or at most, on the order of) 1 cm^{-1}. The RKW study[87] recommends the CCSD(T)-F12b method for use with the basis sets used in our paper, but they note as we do that the difference is very slight and of virtually no consequence.

HOOH and HOOOH, described below), we chose to investigate the QFF of the three HO_4H chain isomers at the CCSD(T)-F12/cc-pVTZ-F12 level of theory with second-order vibrational perturbation theory (VPT2).[260–263] For brevity, we will refer to the cc-pVnZ-F12 basis sets as simply VnZ for the remainder of this work, but the reader is advised to keep in mind that these are a very specific set of bases designed particularly for explicitly correlated methods. Optimizations utilizing the Complete Active Space Self Consistent Field method with a 14 electron, 12 molecular orbital active space [CASSCF(14,12)] method and the aug-cc-pVQZ basis set were also performed on all three HO_4H chain isomers to demonstrate the validity of our single-reference approach in light of the findings of Anglada, et al.[227]

An outline of the basic procedure used to generate full QFFs follows. First, the geometry of the species in question was optimized with the same level of theory to be employed in the forcefield calculation—in this case, CCSD(T)-F12/VTZ—using the `MOLPRO`[206] software package (for a description of the various density fitting approximations and other implementation details, see the RKW study[87] and the literature sources cited therein). Geometries were optimized using extremely tight convergence criteria: energies were converged to 10^{-12} hartrees in all electronic structure computations, geometric gradients were converged to 10^{-6} atomic units, and integrals were retained to machine precision (10^{-16} atomic units). A five-point stencil formula was used in the optimization process in order to ensure beyond all doubt that each geometry represented a local minimum at the given level of theory. We then employed the `GRENDEL++` program[264] to generate enough displacements along a set of curvilinear internal coordinates to allow for the computation of fourth derivatives by finite difference of energy points. The number of displacements required for such a fit grows very rapidly with system size, particularly for low symmetry species, and for the C_1 symmetry HO_4H chain isomer, 3327 separate energy calculations were required after the determination of the equilibrium geometry. These calculations were performed simultaneously on a large number of nodes using the `MOLPRO` package and the computational resources at the

National Energy Supercomputing Research Center (NERSC). The `GRENDEL++` program then used these computed energies to fit second, third, and fourth derivatives with respect to the aforementioned internal coordinates. These internal coordinate derivatives were then transformed directly to normal coordinate force constants using the methodology described by Hoy, Mills, and Strey,[265] and these normal coordinate force constants were used with VPT2 theory to predict fundamental vibrational frequencies and other spectroscopic properties. This procedure computes a *full* QFF, which, unlike more popular procedures that only compute semi-diagonal fourth-order force constants, allows us to compute QFFs for all possible isotopologues simultaneously.

In keeping with the advice of the RKW study, core-correlation corrections were excluded from our calculations, since Ruden and co-workers,[266] among others, have found these corrections to be roughly equal in magnitude and opposite in sign to the corrections introduced by the inclusion of quadruple and pentuple excitations in the coupled-cluster wavefunction (which were, of course, also excluded from our study). Scalar relativistic corrections were also excluded because they are expected to be small (≈ 1 cm^{-1}) compared to other sources of error.

In order to further establish the credibility of our approach, benchmark computations were performed on both HOOH and HOOOH. For HOOH, a QFF was also calculated at the CCSD(T)-F12/VQZ level of theory, which represents an elimination of basis set incompleteness error to beyond numerical machine precision. Again, to our knowledge, our calculations on both of these species represent the most accurate computations of this type to date, particularly if our inclusion of all minor isotopologues is taken into account. The results from these benchmark computations are included here and in the supplementary material in hope that they will be useful for future laboratory and astronomical observations.

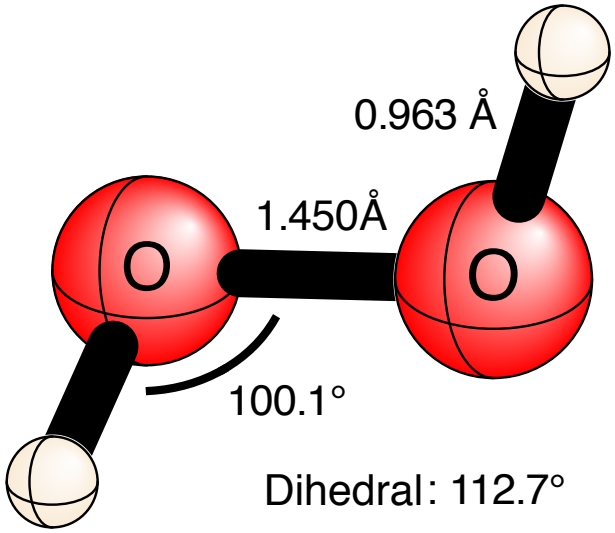

Figure 3.1: The CCSD(T)-F12/cc-pVQZ-F12 optimized equilibrium geometry of HOOH. To the precision given, this is also the CCSD(T)-F12/cc-pVTZ-F12 geometry, with the exception of the OO bond length, which is 1.451 Å at this level of theory.

3.4 Results and Discussion

3.4.1 HOOH benchmark

The CCSD(T)-F12/VQZ geometry for HOOH is shown in Figure 3.1. To within 0.001 Å, these geometric parameters are the same as those for CCSD(T)-F12/VTZ. Selected spectroscopic data derived from the calculated QFFs with CCSD(T)-F12 and the VDZ, VTZ and VQZ basis sets are given in Table 3.1. The first thing to note from these data is the remarkable degree to which the basis set is converged even with the VDZ basis set. The fundamental frequencies differ across the three basis sets by no more than 0.5%. The anharmonic corrections ($\Delta_{anh.}$) in particular are almost constant with increasing basis set size. This confirms the findings of RKW that CCSD(T)-F12/VDZ yields at least the equivalent of quadruple zeta quality for a non-explicitly correlated methods. The similarity of the re-

		Basis	HOOH harm.	$\Delta_{anh.}$	HOOH fund.	HOOH expt.[a]	DOOD $\Delta_{iso.}$	DOOD fund.	DOOD expt.[b]	$H^{18}O^{18}OH$ $\Delta_{iso.}$	$H^{18}O^{18}OH$ fund.
ν_1	HOOH tors.	VDZ	378	-63	315	255	-53	262		0	315
		VTZ	378	-63	315	371	-53	262	251[c]	0	315
		VQZ	380	-64	316		-54	263		0	316
ν_2	OO str.	VDZ	912	-36	877	866	+3	880		-49	828
		VTZ	911	-36	875	878	+3	878	867	-49	826
		VQZ	915	-36	879		+3	882		-49	830
ν_3	OOH a-sym. bend	VDZ	1331	-47	1284	1265	-324	960		-6	1278
		VTZ	1330	-47	1283	1274	-324	960	947	-6	1277
		VQZ	1331	-47	1285		-324	961		-6	1278
ν_4	OOH sym. bend	VDZ	1448	-47	1402		-363	1038		-6	1396
		VTZ	1447	-46	1400	1394	-363	1037	1029	-6	1394
		VQZ	1448	-47	1401		-363	1038		-6	1396
ν_5	OH sym. str.	VDZ	3802	-193	3609	3610	-921	2688		-12	3597
		VTZ	3798	-193	3605	3618	-920	2685	2661	-12	3593
		VQZ	3800	-193	3607		-920	2686		-12	3595
ν_6	OH a-sym. str.	VDZ	3802	-192	3611	3611	-941	2669		-11	3600
		VTZ	3798	-192	3607	3619	-940	2667	2668	-11	3596
		VQZ	3800	-191	3609		-941	2668		-11	3598

[a] HOOH has been so widely studied over the years that for many of its vibrational modes, significantly different values have been reported by different sources, even for the gas phase. Since it is not the purpose of this paper to judge the relative merits of the experimental techniques used to obtain these values, we have reported two experimental values for some of the modes. Experimental values taken from refs.[267–271]

[b] Refs.[267,269,272]. Gas phase values are given unless otherwise indicated.

[c] In an Argon matrix.

Table 3.1: Spectroscopic features at the CCSD(T)-F12 level of theory with various basis sets for HOOH, DOOD, and $H^{18}O^{18}OH$ compared with experiment. All values are in cm^{-1}. Note that VnZ refers to the cc-pVnZ-F12 basis sets, as discussed in the text. Experimental values are from gas phase spectra unless otherwise indicated. Values for other possible isotopologues with H, D, ^{16}O, ^{17}O, and ^{18}O are included in the supplementary material.

	VDZ	VTZ	VQZ	expt.[a]
A_0	300482	300419	300688	301831
B_0	26025	26030	26070	26202
C_0	25315	25349	25386	25135

[a] Ref. [268]

Table 3.2: Experimental and theoretical rotational constants, in MHz, for HOOH at the CCSD(T)-F12/cc-pVnZ-F12 level of theory with zero-point and centrifugal distortion corrections included. The cc-pVnZ-F12 basis sets are represented in the table as simply VnZ.

sults for the VTZ and VQZ basis sets suggests that the VTZ basis set should be more than sufficient to eliminate most of the basis set incompleteness error for HOOOH and HO_4H to well below that of other sources of error, such as the exclusion of connected quadruples or core-correlation corrections.

Furthermore, the theoretically predicted fundamentals for HOOH are in very good agreement with the experimental values. In each case, the computed frequencies agree as well with the experimental results as the various experimental results agree with each other; if the experimental results are averaged (albeit arbitrarily), none of the computed values disagree with experiment by more than 2%, and all but ν_3 agree to better than 1% error. The agreement with experiment of the DOOD computed frequencies is a bit worse. The difficulty here can be attributed at least partially to errors in the experimental values, since the most recent gas phase IR study of DOOD (yielding ν_3 and ν_5) was conducted in 1955[267] and the most recent gas phase Raman study (yielding ν_2, ν_4, and ν_6) was conducted in 1974.[269] A number of matrix isolation studies have been conducted since then, but we prefer not to compare with these values whenever possible, since we suspect our error in most cases is less than the magnitudes of the various matrix shifts.

The computed zero-point and centrifugal distortion corrected rotational constants for HOOH are given in Table 3.2. The agreement between theory and experiment[267–271,273–275]

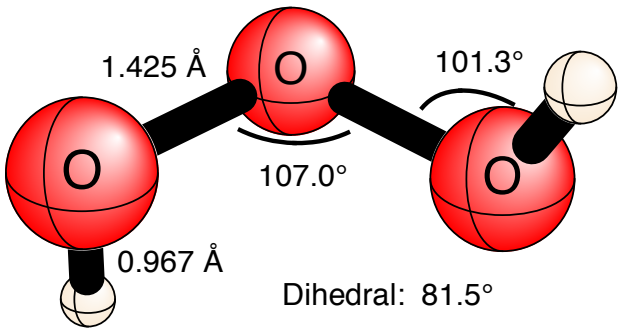

Figure 3.2: The CCSD(T)-F12/cc-pVTZ-F12 geometry of *trans*-HOOOH, the isomer for which experimental results are available. The structure has C_2 symmetry, and only unique geometric features are labeled.

is markedly bad, especially considering how good the agreement is in the case of HOOOH (Table 3.4, discussed below). However, this disagreement may be attributed to a breakdown of the rigid rotor approximation rather than error in the electronic structure computations. The large amplitude torsional motion in HOOH necessitates a full rovibrational analysis, which has been carried out in far greater detail elsewhere.[276,277] Because of this, we hesitate to draw any conclusions from this comparison to experimental data and instead delay this analysis until our discussion of HOOOH, which does not suffer from this difficulty to the same degree.

3.4.2 HOOOH BENCHMARK

The CCSD(T)-F12/VTZ geometry of HOOOH is shown in Figure 3.2, and computed vibrational frequencies are compared with experimental values in Table 3.3. Again, the general agreement is excellent, particularly considering the experiment was conducted in an argon matrix environment. In their *Science* paper, Engdahl and Nelander[232] state "[t]he strongest bands of H_2O_3 are the torsions [ν_1 and ν_2], the OH stretches [ν_8 and ν_9], and the antisym-

		Species	Harm.	Fund.	Expt.[a]
ν_1	sym. tors.	HOOOH	361	349	346
		DOOOD	261	254	274
		HOOOD	283	274	–
		HOO^{18}OH	361	344	346
ν_2	a-sym. tors.	HOOOH	415	385	387
		DOOOD	317	301	302
		HOOOD	394	370	369
		HOO^{18}OH	414	385	387
ν_3	OOO bend	HOOOH	531	511	509
		DOOOD	519	504	–
		HOOOD	525	507	–
		HOO^{18}OH	519	507	–
ν_4	a-sym. OO str.	HOOOH	811	774	776
		DOOOD	811	780	763
		HOOOD	811	778	772
		HOO^{18}OH	800	764	768
ν_5	sym. OO str.	HOOOH	909	881	821
		DOOOD	904	877	–
		HOOOD	907	879	815
		HOO^{18}OH	898	871	–
ν_6	sym. OOH bend	HOOOH	1397	1358	1347
		DOOOD	1033	1004	–
		HOOOD	1042	1012	–
		HOO^{18}OH	1392	1351	1344
ν_7	a-sym. OOH bend	HOOOH	1406	1367	1359
		DOOOD	1051	1023	1007
		HOOOD	1402	1362	1350
		HOO^{18}OH	1403	1360	1357
ν_8	a-sym. OH str.	HOOOH	3747	3549	3530
		DOOOD	2730	2626	2610
		HOOOD	2731	2626	2610
		HOO^{18}OH	3736	3539	3520
ν_9	sym. OH str.	HOOOH	3750	3553	3530
		DOOOD	2732	2628	2610
		HOOOD	3749	3552	3530
		HOO^{18}OH	3749	3551	3530

[a] Ref.[232]

Table 3.3: Spectroscopic features for HOOOH, DOOOD, DOOOH, and HOO^{18}OH predicted at the CCSD(T)-F12/cc-pVTZ-F12 level of theory. All values are in cm^{-1}. Note that the experimental results were obtained in Argon matrices. Values for all other possible isotopologues with H, D, ^{16}O, ^{17}O, and ^{18}O are included in the supplementary material.

metric OOH bends [ν_7]." In light of this remark, we think it wise to put the most weight into our comparison with the experimental results for these modes, since they are least likely to suffer from experimental error or be incorrectly assigned. For these five modes, the unsubstituted (HOOOH) fundamentals are in excellent agreement with the experiment, with errors of less than 1% in every case. Given the agreement of all of the other isotopologues with experiment for ν_1 and ν_2 and the agreement of the calculated HOOOD fundamental with the DOOOD experimental value, it is possible that the DOOD ν_1 frequency may be incorrectly assigned in the original experimental paper. However, it is more likely that a type I Fermi resonance ($2\omega_a \approx \omega_b$) between ω_1 and ω_3 is to blame for the discrepancy. (It is well-known that VPT2 may perform poorly when Fermi resonances are present.[263,278]) For ν_7, ν_8, and ν_9, all of the isotopologue fundamentals agree with experiment to better than 1% except ν_7 for DOOOD. Some of this error here may again be attributed to a type II Fermi resonance ($\omega_a + \omega_b \approx \omega_c$) between ω_1, ω_4, and ω_7.

Here we caution that not all errors in our method can be attributed to Fermi resonance, and not all Fermi resonances necessarily induce errors, though for the latter statement it is difficult (and beyond the scope of this work) to say whether this is an inherent property of VPT2 theory or a result of fortuitous error cancellation. For instance, HOOOD exhibits a type I Fermi resonance between ω_2 and ω_4 of roughly the same magnitude as the ones discussed in the preceding paragraph, yet the agreement between theory and experiment for both of these modes is spectacular. The largest contribution removed by the standard Fermi resonance correction for HOOOH is a 34 cm^{-1} contribution to ν_4 from a type II resonance between ω_1, ω_2, and ω_4. Yet the omission of the second order contribution (which is the purpose of the Fermi resonance correction[263]) greatly improves the computed value of this fundamental relative to experiment. The discrepancy between the Fermi resonance contribution and the resonance-corrected contribution merely represents an upper bound for the error caused by Fermi resonance to a given fundamental frequency, but it implies nothing

	HOOOH			DOOOD		
	VDZ	VTZ	Expt.[a]	VDZ	VTZ	Expt.[a]
A_0	51087	51119	51149	42985	43007	43043
B_0	10690	10708	10688	9711	9726	9709
C_0	9356	9370	9355	8746	8759	8745

[a] Ref. [234]

Table 3.4: Experimental and theoretical rotational constants, in MHz, for HOOOH and DOOOD at the CCSD(T)-F12/cc-pVnZ-F12 level of theory with zero-point and centrifugal distortion corrections included. The cc-pVnZ-F12 basis sets are represented in the table as simply VnZ.

about the tightness of this bound. On the other hand, an example of an error that cannot be attributed to Fermi resonance is that of ν_5 for the unsubstituted isotopologue. Though Fermi resonances exist in the terms contributing to this fundamental, the force constants associated with these resonances are small enough that no contribution from a term affected by resonance exceeds 1 cm^{-1}, and the sum of the terms removed by the resonance correction is less that 0.1 cm^{-1}. If the experimental ν_5 fundamental is correctly assigned, the error in this term must be attributed to missing core corrections, lack of quadruple and higher excitations in the coupled-cluster wavefunction, inherent inaccuracies in VPT2 theory, or most likely, some combination of these factors. In this respect, we suggest the possibility that this experimental frequency actually corresponds to the ν_7 mode of HO_4H (see Table 3.5 and discussion below), though we were unable to decipher from the description of experimental details provided[232] whether or not this is a reasonable possibility. The fact that the IR intensity of the ν_7 mode of HO_4H is predicted to be a factor of 10 larger than the intensity of the ν_5 mode of HOOOH supports this suggestion. The recent study by Levanov and coworkers[254] further supports this reasoning; they found the symmetric OO stretching peak at 878 cm^{-1} and assigned an 827 cm^{-1} peak to HOOOOH.

Theoretical rotational constants for HOOOH and DOOOD are compared to experiment

in Table 3.4. The agreement is extremely good, particularly for the A_0 value. Here we observe an interesting trend in the accuracy of the computed values for both HOOOH and DOOOD relative to basis set size. For the larger constant, A_0, the computed value improves with basis set, but for the smaller constants, B_0 and C_0, the computed value slightly worsens. (A somewhat similar trend exists for the HOOH rotational constants, but again we note our hesitancy to draw any conclusions based on the rigid rotor approximation for HOOH). From this trend it is tempting to recommend VTZ values for comparison with experimental HO_4H A_0 constants and VDZ value for B_0 and C_0 constants. However, we would advise against this. In addition to the obvious objection that this approach is a bad way to do science, we point out that the observed trend arises from a reduction in the amount of error cancellation, particularly with respect to the effects of core correlation and higher excitations, as discussed previously; we have no reason to believe that this trend will necessarily hold for HO_4H.

Geometric Properties

The predicted values for all five unique geometric features of HOOOH are in good agreement with the previously published experimental values obtained from the rotational spectrum.[234] The OO and OH bond lengths are predicted to be 0.003 Å shorter and 0.004 Å longer than the experimentally predicted values, respectively. The OOO bond angle agrees with experiment to the precision given, and the predicted OOH bond angle is only 0.2° larger. Finally, the predicted OOOH dihedral angle is only 0.3° smaller than the experimental value. This agreement further increases our confidence that the level of theory we have used to optimize geometric structures should be sufficient for most purposes.

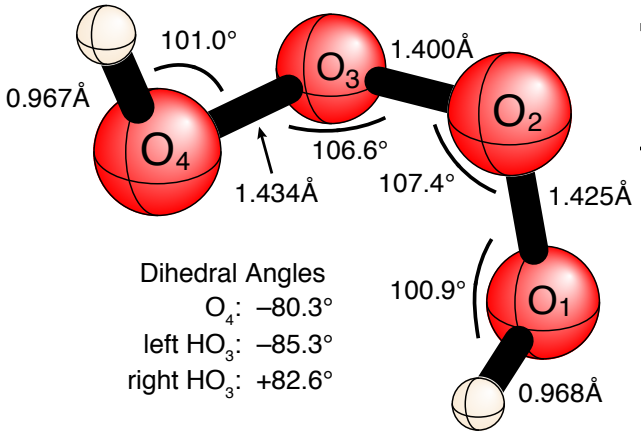

Figure 3.3: CCSD(T)-F12/cc-pVTZ-F12 geometry for chain isomer **1**, predicted to be the lowest energy chain structure of HO_4H. This structure has C_1 symmetry, and thus all geometric parameters are shown. The inset shows the view looking down the O2–O3 bond, useful for distinguishing the structures qualitatively.

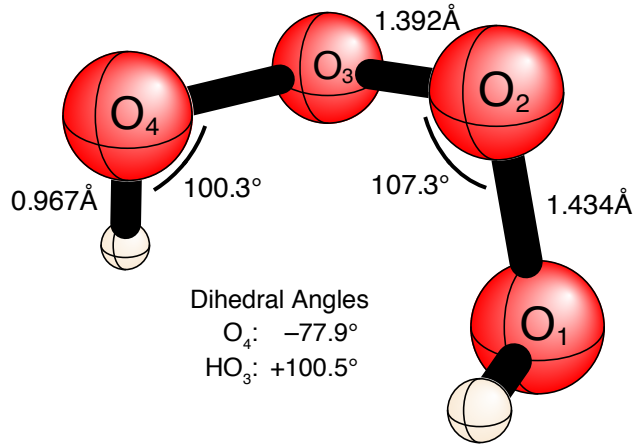

Figure 3.4: CCSD(T)-F12/cc-pVTZ-F12 geometry for chain isomer **2**, predicted to lie 0.63 kcal mol^{-1} above chain **1**. This structure has C_2 symmetry, and thus only unique geometric parameters are shown. The inset shows the view looking down the O2–O3 bond, useful for distinguishing the structures qualitatively.

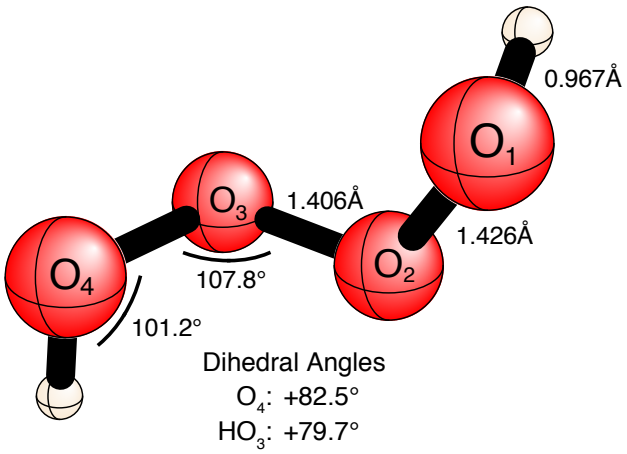

Figure 3.5: CCSD(T)-F12/cc-pVTZ-F12 geometry for chain isomer **3**, predicted to lie 0.87 kcal mol^{-1} above chain **1**. This structure has C_2 symmetry, and thus only unique geometric parameters are shown. The inset shows the view looking down the O2–O3 bond, useful for distinguishing the structures qualitatively.

3.4.3 HOOOOH

Geometric Analysis

As Anglada and coworkers previously noted,[227] HO_4H has three chain isomers that are local minima, which are pictured in Figures 3.3, 3.4, and 3.5 for what we will refer to as chains **1**, **2**, and **3**, respectively. The geometric parameters for chain **1** agree very well with those previously calculated by Denis and Ornellas,[235] with all bond lengths matching to an accuracy of 0.002 Å and all angles and torsions matching to an accuracy of 0.5°. All three structures agree qualitatively with the results of Anglada.[227] However, the lack of quantitative agreement prompted further investigation. Our CASSCF(14,12)/aug-cc-pVQZ computations indicate that no secondary reference contributes more than 3.5% to the final wavefunction, indicating the validity of our CCSD(T)-F12 methodology.[279] Thus, the quantitative differences in structural parameters between our results and those of Anglada,

et al. can be attributed to lack of sufficient correlation treatment rather than an insufficient multireference treatment in our computations. Other previous studies such as Fermann[253] and Fitzgerald.[252] did not have access to methodologies that would agree quantitatively with our results, but their structures for the chain minima are in qualitative agreement with ours.

Structural Analysis

Here we introduce a novel mode of structural analysis for the three HO_4H isomers, giving us further confidence that we have exhausted the possibilities for possible chain minima. When the isomers may be viewed with the O_2–O_3 bond perpendicular to the plane of the paper, as in Figure 3.6, the distinction between the three chains becomes immediately apparent.

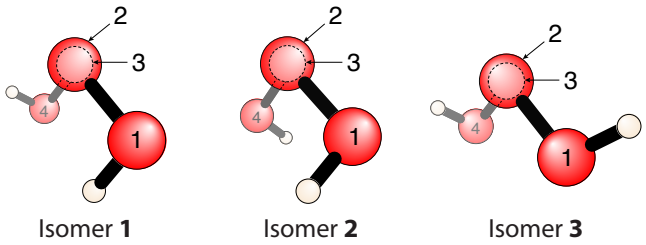

Figure 3.6: The three chain isomers, viewed with the O_2–O_3 bond perpendicular to the plane of the paper. Isomer 3 is portrayed in its stereoisomeric form.

If the slight deviation of the O–H bonds from parallel to the plane of the paper is taken to be unimportant to a qualitative understanding of the system, the three chains can be portrayed similarly to the well-known Newman projection paradigm from alkane stereochemistry,[280] as shown in Figure 3.7.

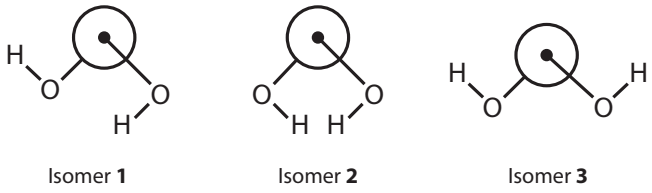

Figure 3.7: Newman-like projections of the three HO_4H chain isomers.

From this analysis, it becomes immediately apparent that any other potential chain minima would have to have a radically different geometry from the three presented here.

Comparison of Geometric Properties

The more interesting analysis here is the evolution of analogous geometric parameters with increasing polyoxide chain length and across the various chain isomers. Given that HOOH is known to be a reasonably stable molecule with an O–O bond length of 1.451 Å at the CCSD(T)-F12/VTZ level of theory, the bond lengths in the analogous computed structures of chains **1**, **2**, and **3** are strikingly short. Also of interest is the fact that the O_1–O_2 bond length in chain **1** is fairly similar to the O_1–O_2 and O_3–O_4 bond lengths in chain **3**, and the O_3–O_4 bond length in chain **1** is similar to the O_1–O_2 and O_3–O_4 bond lengths in chain **2**. This observation leads to the interesting interpretation that chain **1** is a "combination" of half chain **2** and half chain **3**, at least as far as bond lengths and angles are concerned, which can be seen qualitatively from Figures 3.6 and 3.7. As other authors have noted,[227,235,253,281] the most striking feature of all three chains is the short O_2–O_3 bond length, which prohibits the intuitively tempting interpretation of the system as two weakly interacting HO_2 radical moieties. The OOO and OOH bond angles as well as the OOOH dihedral angles in all three chains are remarkably similar to those in HOOOH. In short, there is nothing in the structural parameters of the HO_4H chain structures that would indicate their isolation should be significantly more difficult than HOOOH.

Spectroscopic Properties

Calculated fundamental frequencies for all three isomers as well as their DO_4D isotopologues are given in Table 3.5, and fundamental frequencies for additional isotopologues are given in the supplementary material. For each of the chain isomers, the OH stretching frequencies (ν_{11} and ν_{12}) are completely free from Fermi resonance, and thus we have a higher degree of

		Isomer **1**					Isomer **2**					Isomer **3**				
		HO_4H		DO_4D		irr.	HO_4H		DO_4D		irr.	HO_4H		DO_4D		
		harm.	fund.	harm.	fund.		harm.	fund.	harm.	fund.		harm.	fund.	harm.	fund.	
O_4 torsion	ν_1	175	173	164	162	a	175	172	167	164	a	162	159	155	152	
HO_3 torsions	ν_2	366	339	274	259	b	301	270	226	208	b	354	322	253	237	
	ν_3	411	381	303	287	a	428	414	326	309	a	389	357	291	272	
(various OOO bend and OO stretch combinations)*	ν_4	463	461	455	452	a	495	450	466	451	a	457	449	442	431	
	ν_5	621	602	612	595	b	618	596	611	592	b	610	592	621	600	
	ν_6	704	659	704	667	a	712	670	704	663	a	706	661	703	668	
	ν_7	861	831	860	828	b	874	832	870	830	b	877	844	869	833	
	ν_8	901	872	900	871	a	905	876	899	872	a	899	869	898	869	
HOO bends	ν_9	1387	1340	1028	999	b	1378	1332	1019	990	b	1406	1359	1039	1014	
	ν_{10}	1412	1365	1048	1021	a	1405	1357	1052	1021	a	1410	1364	1056	1031	
HO stretches	ν_{11}	3735	3537	2720	2615	b	3748	3550	2731	2625	b	3747	3550	2730	2626	
	ν_{12}	3750	3554	2733	2629	a	3750	3553	2732	2628	a	3749	3553	2731	2627	

* Due to the difficulty in assignment of these five modes, we prefer not to distinguish them.

Table 3.5: CCSD(T)-F12/cc-pVTZ-F12 fundamental vibrational frequencies for the HO_4H and DO_4D isotopologues of chain isomers **1**, **2**, and **3**. All values are given in cm^{-1}. (No irreducible representations are given for **1** since it has C_1 symmetry.) The modes are ν_1, O_4 torsion; ν_2 and ν_3, HO_3 torsions; ν_4 to ν_8, various OOO bends and OO stretches; ν_9 and ν_{10}, HOO bends; ν_{11} and ν_{12}, OH stretches. Values for all other possible isotopologues with H, D, ^{16}O, ^{17}O, and ^{18}O are included in the supplementary material.

confidence in assessing these modes. The lack of symmetry in chain **1** makes it a particularly difficult case for VPT2, since the number of possible Fermi resonances (which typically, though not always, arise from two or three harmonic frequencies with the same irreducible representation) is greatly increased relative to the C_2 chains. Indeed, if a cutoff of 50 cm^{-1} is used, there are 72 different resonance corrections included. However, the vast majority of the contributions excluded by these corrections are small—less than 1 cm^{-1}. We can get a general idea of how much Fermi resonance affects our final frequencies by looking at the sum of the Fermi-corrected contributions and comparing it to the sum of the uncorrected contributions. (The standard Fermi resonance correction essentially removes the contribution from the uncorrected term by reducing its contribution to first order in the perturbation, as described by Allen and coworkers.[263]) The worst total correction for chain **1** is ν_2, for which the terms removed sum to 30 cm^{-1}. Virtually all of this comes from the type I resonance between ω_2 and ω_6. The contribution of this resonance to ν_6 is only -13 cm^{-1} (the reason for this discrepancy can easily be seen from the form of the VPT2 equations; see Allen and coworkers[263]). Conveniently, this resonance does not occur for the DO_4D version of chain **1**. This affords us the opportunity to examine (albeit approximately) the value of this sort of term-by-term analysis of Fermi resonance contributions. In the case of ν_6, we see that this analysis has provided us with reasonable insight, since the sum of removed terms was 13 cm^{-1} in magnitude and the fundamentals for HO_4H and DO_4D differ by about 8 cm^{-1}, and most of this difference may be attributed to Fermi resonance since the harmonic frequencies for both isotopologues are approximately the same. (Refer to previous discussion of ν_4 in HOOOH for a case where this analysis does not quite work as well).

If the reader is willing to accept this sort of term-by-term Fermi resonance analysis as reasonable, then it is easy to pick out the frequencies which he or she should interpret with caution. For isomer **2**, ν_{10} on HO_4H has two separate 41 cm^{-1} corrections removed, from a type I resonance between ω_6 and ω_{10} and from a type II resonance between ω_4, ω_8, and ω_{10}.

For the DO_4D version of this same isomer, ν_2 has a -114 cm^{-1} contribution removed arising from a type I resonance between ω_2 and ω_4, while ν_4 has a 31 cm^{-1} correction from this same resonance. The ν_6 value for the HO_4H version of chain **3** has a 101 cm^{-1} contribution excluded due to a type I resonance between ω_6 and ω_{10}, while ν_{10} has a roughly -25 cm^{-1} contribution removed arising from this same resonance. For HOOOOH isomer **2** there is also a very large contribution from a type I resonance between ω_2 and ω_6, for which a 1214 cm^{-1} contribution is removed from ν_2 and a -410 cm^{-1} contribution is removed from ν_6. All of the Fermi resonance corrections included for the DO_4D isotopologues of chains **1** and **3** replace relatively small contributions, and thus we expect that any errors in these fundamentals do not arise from Fermi resonance. Again we caution that these corrections do not necessarily indicate quantitatively the errors in the computed values, but rather provide us with a mechanism by which we can suggest that the reader view certain computed fundamentals with a slightly higher degree of skepticism and certain others slightly more favorably, being assured that the most well-known cause of VPT2 error, Fermi resonance, does not affect the latter group.

The agreement of our results with the recent experimental study of Levanov and coworkers is excellent. Though the resolution of their study was not good enough to distinguish the three isomeric chain forms, the values they present for ν_4 (449 cm^{-1}), ν_5 (589 cm^{-1}), ν_7 (827 cm^{-1}), and ν_8 (865 cm^{-1}) each differ from our predicted values for at least one of the chains by less than 5 cm^{-1}. For the ν_6 fundamental, which Levanov and coworkers list as 624 cm^{-1}, the agreement is not terrible. Note that, as discussed above, the theoretical value of ν_6 suffers from significant Fermi resonances in all three isomers. The 35 cm^{-1} or so discrepancy could also be partially attributed to the strength of the perturbing medium in which the experiment was performed. Nonetheless, it is possible that this peak is incorrectly assigned in the experimental work.

Table 3.6 gives the computed rotational constants for all three chains with zero-point and

	Isomer **1**		Isomer **2**		Isomer **3**	
	HO_4H	DO_4D	HO_4H	DO_4D	HO_4H	DO_4D
A_0	19790	18176	19120	17077	20853	19907
B_0	5854	5509	5952	5706	5585	5089
C_0	5047	4753	5036	4754	4964	4634

Table 3.6: Computed rotational constants, in MHz, for HO_4H and DO_4D isotopologues of all three chain isomers at the CCSD(T)-F12/cc-pVTZ-F12 level of theory with zero-point and centrifugal distortion corrections included. More isotopologues, as well as values computed with the cc-pVDZ-F12 basis set, are included in the supplementary information.

centrifugal distortion corrections included. For chain **1**, which is the isomer investigated by Denis and Ornellas,[235] our computations represent a roughly −300 MHz revision to A_0, a 50 MHz revision to B_0, and very little change (15 MHz) to C_0. We have also recommended values for the rotational constants of chains **2** and **3**, along with their deuterated isotopologues, all of which should be well-separated enough to be distinguished from each other in many experiments. The rotational constants for all other isotopologues are included in the supplementary material.

Barriers and Relative Energies

The three HOOOOH chains are very nearly degenerate. Chain **1** is the minimum, but chains **2** and **3** only lie 0.6 kcal mol^{-1} and 0.9 kcal mol^{-1} higher in energy. For the sake of completeness, transition states were computed for isomerizations between the three chains. Here we simply note the CCSD(T)-F12/VDZ energies of the three transition states for discussion in future work. The forward barrier for the conversion from chain **1** to chain **2** is 4.0 kcal mol^{-1}, and the reverse barrier to this process is 3.4 kcal mol^{-1}. For the chain **2** to chain **3** isomerization process, the forward barrier is 10.1 kcal mol^{-1}, and the reverse barrier for the same isomerization is 9.9 kcal mol^{-1}. Finally, the barrier for conversion from chain **1** to chain **3** is 7.9 kcal mol^{-1} in the forward direction and 7.1 kcal mol^{-1} in the reverse

direction.

3.5 Conclusions

We have reported spectroscopic properties for HOOH, HOOOH, and HO_4H and their isotopologues by constructing a full quartic force field for each at the CCSD(T)-F12/cc-pVTZ-F12 level of theory. For many of the minor isotopologues, these data represent the first reported anharmonic vibrational frequencies. Despite the presence of several Fermi resonances, the computed QFFs provide reasonable fundamental frequencies in most instances. Based on the success of the rotational constants computed for HOOOH, the rotational constants provided for HO_4H are expected to be very reliable. We have also provided the first anharmonic spectroscopic predictions for the two other chain minima of HO_4H, both of which are energetically comparable to the C_1 minimum and thus may show up in an experimental spectrum. We hope our findings will further spur the theoretical and experimental excitement about polyoxide chains and ultimately that our data will lead to the experimental isolation of the HO_4H chain.

3.6 Acknowledgements

This research was supported by the Department of Energy, Office of Basic Energy Sciences, Chemistry Division, Fundamental Interactions Program, Grant No. DE-FG02-97-ER14748, and used resources of the National Energy Research Scientific Computing Center, which is supported by the Office of Science of the U. S. Department of Energy under Contract No. DE-AC02-05CH11231.

3.7 Supplementary Material

The supplementary material (239 pages) includes Cartesian geometric coordinates and normal coordinate force constants for all species, as well as predicted fundamental frequencies for all unique isotopologues with H, D, T, ^{16}O, ^{17}O, and ^{18}O substitutions for all species discussed. It is available on the internet on the page associated with the DOI 10.1063/1.3684231.

Chapter 4

Arbitrary Order El'yashevich–Wilson **B** Tensor Formulas for the Most Frequently Used Internal Coordinates in Molecular Vibrational Analyses*

*David S. Hollman and H. F. Schaefer, J. Chem. Phys. **137**, 164103 (2012). Reprinted here with permission of the American Institute of Physics.

4.1 Abstract

In recent years, internal coordinates have become the preferred means of expressing potential energy surfaces. The ability to transform quantities from chemically significant internal coordinates to primitive Cartesian coordinates and spectroscopically relevant normal coordinates is thus critical to the further development of computational chemistry. In the present work, general nth-order formulas are presented for the Cartesian derivatives of the five most commonly used internal coordinates—bond stretching, bond angle, torsion, out-of-plane angle, and linear bending. To compose such formulas in a reasonably understandable fashion, a new notation is developed that is a generalization of that which has been used previously for similar purposes. The notation developed leads to easily programmable and reasonably understandable arbitrary order formulas, yet it is powerful enough to express the arbitrary order $\mathbf{B}$ tensor of a general, N-point internal coordinate, as is done herein. The techniques employed in the derivation of such formulas are relatively straightforward, and could presumably be applied to a number of other internal coordinates as needed.

4.2 Introduction

One of the most fundamental concepts in modern molecular physics is that of the potential energy (hyper)surface (PES).[282–284] The PES is central to our understanding of reactions,[285–289] structure,[290] dynamics,[291–293] and a plethora of spectroscopic properties.[93,294–298] Given the difficulties associated with probing even the simplest of PESs experimentally,[299–301] the theoretical evaluation of PESs for molecular systems has become one of the most critical and widely utilized roles of computation in modern chemistry and molecular physics. The construction of PESs requires a reasonable choice of coordinates to be made. Indeed, the choice and use of intuitive internal coordinates is often critical to

the qualitative and quantitative interpretation of theoretical predictions for chemical systems.[302–306] However, it is rarely convenient (or even practical) to evaluate all properties of a system in curvalinear internal coordinates. For instance, the kinetic energy of a system is most easily formulated in terms of Cartesian coordinates, while normal coordinates are far more convenient for the computation of spectroscopic constants.

The ability to transform between internal, Cartesian, and normal coordinates is thus crucial to the computational study of molecular systems. As such, considerable effort has been put into the derivation of analytic forms of tensors that transform tensorial quantities expressed in one type of coordinates to another.[307–309] The non-linear transformation from a curvalinear representation to a rectalinear one is particularly challenging. The ubiquitous matrix for the linear component of the transformation from internal coordinates to Cartesian coordinates is the El'yashevich–Wilson **B** matrix,[310–312] and the extension of this transformation to non-linear terms thus involves the so-called **B** tensor. The further transformation from Cartesian coordinates to rectalinear normal coordinates is linear, and thus much more easily handled. An analogous tensor for the transformation from internal coordinates directly to normal coordinates is known as the **L** tensor, and has also been studied in significant detail elsewhere (see Hoy, Mills and Strey, reference 265).

Though the basic derivation of the **B** tensor elements at lower orders is fairly straightforward, the derivation of arbitrary order formulas needed for the transformation of higher-order tensorial quantities is much more challenging. More than fifteen years ago, complete arbitrary order formulas for the **B** tensors of the bond stretching and bond angle coordinates were developed by Allen, Császár, Szalay, and Mills (ACSM).[307] The research of ACSM also offers a formula for the arbitrary order **B** tensor elements of torsional coordinates involving only terminal atoms, but they state that the explicit formulas for the other torsional **B** tensor elements "are not compact." Compact formulas for these **B** tensor elements to arbitrary order are presented herein. In addition, we present formulas for arbitrary order **B** tensor

elements for the out-of-plane angle and linear bending coordinates, along with a notational system in which these formulas can be expressed compactly.

4.3 Theoretical Development

The general, nonlinear transformation between two distinct sets of n independent coordinates (often called *representations*) r and q can be expressed in component form as[313]

$$r_i = \sum_k^n X_i^k q_k + \frac{1}{2}\sum_{kl}^n X_i^{kl} q_k q_l + \frac{1}{6}\sum_{klm}^n X_i^{klm} q_k q_l q_m + \cdots \tag{4.1}$$

In keeping with notation initially established by Neto in the 1980s,[313–316] we will express transformation coefficients from r to q as $X_i^{\alpha\beta\cdots}$ (which are Christoffel symbols of the second kind). Typically,

$$X_i^{k_1 k_2 \cdots k_n} = \frac{\partial^n r_i}{\partial q_{k_1} \partial q_{k_2} \cdots \partial q_{k_n}} \tag{4.2}$$

and the symbol used in the place of X depends on the representations r and q. If, for instance, r is a curvalinear internal coordinate representation and q is a Cartesian representation, $\mathbf{B}$ is typically used in the place of X. Throughout the paper, we will use Greek letters α and β (in general α_i) to denote an arbitrary Cartesian axis (i.e., x, y, or z). We will use a, b, c, and d (in general a_i or b_i) to denote atoms composing a given internal coordinate. R_{ab} denotes a bond stretching coordinate between atoms a and b, and ϕ_{abc} denotes a bond angle coordinate from atom a through atom b to atom c. The symbols τ_{abcd}, γ_{abcd}, and θ_{abc} represent torsional coordinates, out-of-plane angle coordinates, and linear bending coordinates, respectively, all of which will be discussed in some detail below. The notation $\lambda_{a_1 a_2 \cdots a_N}$ denotes a general N-atom internal coordinate, and the symbol $\mathbf{e}_{ab}$ denotes a unit vector along the direction from atom a to atom b. Much of this notation is chosen to coincide with that of the aforementioned

ACSM paper.[307]

We make the following minor modifications to the formalism of Neto. First, rather than using an index in the internal representation as the subscript for $\mathbf{B}$, we use the coordinate itself, or indeed any function of the coordinate (noting that, of course, the internal coordinates themselves may be expressed as functions of the Cartesian coordinates of the atoms composing the coordinate). Thus modified, we find it easier to contemplate the notation directly in terms of equation (4.2) rather than equation (4.1). The use of the coefficients in equation (4.1) remains legitimate, but only when the subscript function is a coordinate that is part of the (complete) representation r. Other uses of the $\mathbf{B}$ notation in which the function does not have this property are used merely to facilitate the writing of the formulas. In every case where a composite function is used in the place of the coordinate, the formula for the $\mathbf{B}$ tensor elements of that composite function is given elsewhere in the paper. When we wish to express a vector of $\mathbf{B}$ transformation coefficients, we use the following notation:

$$\underline{\mathbf{b}}_f^{\mathbf{a_1},\ a_{2\alpha_2}a_{3\alpha_3}\cdots} \equiv \begin{pmatrix} \mathbf{B}_f^{a_{1x}a_{2\alpha_2}a_{3\alpha_3}\cdots} \\ \mathbf{B}_f^{a_{1y}a_{2\alpha_2}a_{3\alpha_3}\cdots} \\ \mathbf{B}_f^{a_{1z}a_{2\alpha_2}a_{3\alpha_3}\cdots} \end{pmatrix} \tag{4.3}$$

4.3.1 The u/ℓ-iterator notation

ACSM used what they called "brace notation" to express their general formulas. We have found it useful to make a slight generalization of their notation to express our formulas. To be precise, the notation we define here refers to a set of subsets of the power set of given set of indices,† but we find this formalism a bit too vast to conceptualize. Instead, we find it

†The power set of a set A is the set of all subsets A, including the empty set and A itself. To be even more technical, some of our iterators are not strictly described by this criterion, since some cases may have more than one empty "box", and the power set of a set only includes one empty set entry. To be absolutely correct, we would have to append some number of empty sets to the power set of which our notation describes a set of subsets. Given all of this formal complication, we certainly prefer to picture balls in boxes.

easier to conceptualize our notation in terms of the variety of ways to place balls in boxes. The balls may be labeled or unlabeled, corresponding to the first u or ℓ subscript, and the boxes may likewise be labeled or unlabeled, corresponding to the second u or ℓ subscript. This leads to a total of 4 possible "iterators" (hence the $\mathcal{I}$ notation). For instance,

$$\mathcal{I}_{\ell(3)u(2)}\left(i,j,k\right) = \Big\{ \big\{\{i,j,k\},\varnothing\big\},\ \big\{\{i,j\},\{k\}\big\},\ \big\{\{i,k\},\{j\}\big\},\ \big\{\{j,k\},\{i\}\big\} \Big\} \tag{4.4}$$

The above iterator indicates iteration over possible configurations of 3 labeled balls in 2 unlabeled boxes. The balls are labeled i, j, and k. Thus, the technical consideration of the notation as a "set of sets of sets of indices" can be rephrased as an "iterator over configurations of boxes containing balls," or an "iterator over the unique ways to put a certain number of total balls in a certain number of boxes." Throughout this work, we will use juxtaposition to indicate set composition in contexts where multiplication would be nonsensical and $\oplus$ to indicate explicit set-wise concatenation. Thus, the above expression could be written

$$\mathcal{I}_{\ell(3)u(2)}\left(ijk\right) = \big\{ \{ijk,\varnothing\},\ \{ij,k\},\ \{ik,j\},\ \{jk,i\} \big\} \tag{4.5}$$

The "labeled boxes" version of this same iterator would be

$$\mathcal{I}_{\ell(3)\ell(2)}\left(ijk\right) = \big\{ \{ijk,\varnothing\},\ \{\varnothing,ijk\},\ \{ij,k\},\ \{k,ij\},\ \{ik,j\},\ \{j,ik\},\ \{jk,i\},\ \{i,jk\} \big\} \tag{4.6}$$

Here we introduce one further notational item: each of these iterators have "barred" versions in which the u/ℓ indicating the box labeling or lack thereof has a bar above it. In this case,

n	k	$\mathcal{I}_{u(n)u(k)}$	$\mathcal{I}_{u(n)l(k)}$	$\mathcal{I}_{\ell(n)u(k)}$	$\mathcal{I}_{\ell(n)\ell(k)}$	n	k	$\mathcal{I}_{u(n)u(k)}$	$\mathcal{I}_{u(n)l(k)}$	$\mathcal{I}_{\ell(n)u(k)}$	$\mathcal{I}_{\ell(n)\ell(k)}$
1	1	1(1)	1(1)	1(1)	1(1)	4	1	1(1)	1(1)	1(1)	1(1)
1	2	1(0)	2(0)	1(0)	2(0)	4	2	3(2)	5(3)	8(7)	16(14)
1	3	1(0)	3(0)	1(0)	3(0)	4	3	4(1)	15(3)	14(6)	81(36)
1	4	1(0)	4(0)	1(0)	4(0)	4	4	5(1)	35(1)	15(1)	256(24)
1	5	1(0)	5(0)	1(0)	5(0)	4	5	5(0)	70(0)	15(0)	625(0)
1	6	1(0)	6(0)	1(0)	6(0)	4	6	5(0)	126(0)	15(0)	1296(0)
2	1	1(1)	1(1)	1(1)	1(1)	5	1	1(1)	1(1)	1(1)	1(1)
2	2	2(1)	3(1)	2(1)	4(2)	5	2	3(2)	6(4)	16(15)	32(30)
2	3	2(0)	6(0)	2(0)	9(0)	5	3	5(2)	21(6)	41(25)	243(150)
2	4	2(0)	10(0)	2(0)	16(0)	5	4	6(1)	56(4)	51(10)	1024(240)
2	5	2(0)	15(0)	2(0)	25(0)	5	5	7(1)	126(1)	52(1)	3125(120)
2	6	2(0)	21(0)	2(0)	36(0)	5	6	7(0)	252(0)	52(0)	7776(0)
3	1	1(1)	1(1)	1(1)	1(1)	6	1	1(1)	1(1)	1(1)	1(1)
3	2	2(1)	4(2)	4(3)	8(6)	6	2	4(3)	7(5)	32(31)	64(62)
3	3	3(1)	10(1)	5(1)	27(6)	6	3	7(3)	28(10)	122(90)	729(540)
3	4	3(0)	20(0)	5(0)	64(0)	6	4	9(2)	84(10)	187(65)	4096(1560)
3	5	3(0)	35(0)	5(0)	125(0)	6	5	10(1)	210(5)	202(15)	15625(1800)
3	6	3(0)	56(0)	5(0)	216(0)	6	6	11(1)	462(1)	203(1)	46656(720)

Table 4.1: Number of terms ("subsets of the power set of the indices") in the various iterators. The number of terms in the "barred" versions (see e.g. equation (4.7) in the text) are given in parentheses.

the iterator only runs over the configuration in which no box is empty. Thus:

$$\mathcal{I}_{\ell(3)\bar{\ell}(2)}\left(ijk\right) = \left\{\{ij,k\},\ \{k,ij\},\ \{ik,j\},\ \{j,ik\},\ \{jk,i\},\ \{i,jk\}\right\} \tag{4.7}$$

Table 4.1 gives the number of terms ("sets of sets" or "configurations") in each of the iterator forms introduced here. The relation between our notation and the notational paradigms of ACSM is discussed in Appendix A.

4.3.2 Brief examples of u/ℓ-iterator notation

The utility of u/ℓ-iterator notation is immediately apparent when we apply it to a couple of familiar general situations. For a general product of functions $h_p(\vec{v}) = f_1(\vec{v})f_2(\vec{v})\cdots f_p(\vec{v})$ where $v_i \in \vec{v}$ is a variable over which f_i is differentiable, the generalized nth order product rule may be stated:

$$\frac{\partial^n h_p(\vec{v})}{\partial v_1 \partial v_2 \cdots \partial v_n} = \sum_{s \in \mathcal{I}_{\ell(n)\ell(p)}(v_1 v_2 \cdots v_n)} f_1^{(s_1)}(\vec{v}) f_2^{(s_2)}(\vec{v}) \cdots f_p^{(s_p)}(\vec{v}) \tag{4.8}$$

where

$$f_i^{(\{v_1 \cdots v_k\})}(\vec{v}) \equiv \frac{\partial^k f_i}{\partial v_1 \cdots \partial v_k} \tag{4.9}$$

As an example, take $h(x_1, x_2, x_3)$ to be a funtion in three dimensions that is a product of functions $f_1(x_1, x_2, x_3)$, $f_2(x_1, x_2, x_3)$, and $f_3(x_1, x_2, x_3)$. Then for any $\{x_i, x_j\}$ with $i, j \in \{1, 2, 3\}$, we have

$$\begin{aligned}\mathcal{I}_{\ell(2)\ell(3)}(x_i, x_j) = \big\{ &\{x_i x_j, \varnothing, \varnothing\},\ \{x_i, x_j, \varnothing\},\ \{x_j, x_i, \varnothing\},\ \{x_i, \varnothing, x_j\},\ \{x_j, \varnothing, x_i\},\\ &\{\varnothing, x_i x_j, \varnothing\},\ \{\varnothing, x_i, x_j\},\ \{\varnothing, x_j, x_i\},\ \{\varnothing, \varnothing, x_i x_j\}\big\}\end{aligned} \tag{4.10}$$

and thus

$$\begin{aligned}\frac{\partial^2 h}{\partial x_i \partial x_j} = &\frac{\partial^2 f_1}{\partial x_i \partial x_j} f_2 f_3 + \frac{\partial f_1}{\partial x_i}\frac{\partial f_2}{\partial x_j} f_3 + \frac{\partial f_1}{\partial x_j}\frac{\partial f_2}{\partial x_i} f_3 + \frac{\partial f_1}{\partial x_i} f_2 \frac{\partial f_3}{\partial x_j} + \frac{\partial f_1}{\partial x_j} f_2 \frac{\partial f_3}{\partial x_i}\\ &+ f_1 \frac{\partial^2 f_2}{\partial x_i \partial x_j} f_3 + f_1 \frac{\partial f_2}{\partial x_i}\frac{\partial f_3}{\partial x_j} + f_1 \frac{\partial f_2}{\partial x_j}\frac{\partial f_3}{\partial x_i} + f_1 f_2 \frac{\partial^2 f_3}{\partial x_i \partial x_j}\end{aligned} \tag{4.11}$$

In a similar fashion, the generalized chain rule for a function $h_c(\vec{v}) = f(g(\vec{v}))$ can be expressed as

$$\frac{\partial^n h_c(\vec{v})}{\partial v_1 \partial v_2 \cdots \partial v_n} = \sum_{k=1}^{n} \left[\left(\frac{d^k f(u)}{du^k} \right)_{u=g(\vec{v})} \left(\sum_{s \in \mathcal{I}_{\ell(n)\bar{u}(k)}(v_1 v_2 \cdots v_n)} \prod_{i=1}^{k} g^{(s_i)}(\vec{v}) \right) \right] \tag{4.12}$$

4.3.3 The utility of the u/ℓ-iterator notation

Strictly speaking, the notation defines only sets of sets of sets (i.e., unordered, as opposed to a formal iterator which would be ordered). We use the term "iterator" to emphasize the connection to the simplest implementation of the formulas: in most modern programming languages, arbitrary iterators can be defined to abstract away the complexity involved in generating complicated iteration patterns such as the ones described here. The utility of this approach should not be overlooked. The practical importance of compactness and elegance in any mathematical formula lies in the ease of implementation, particularly when it comes to formulas that are significantly beyond simple physical interpretation (as is the case for the higher-order B-tensor formulas). Presenting the formulas in terms of the four most basic combinatorial problems leads directly to a simple and modular implementation of each of the formulas; the iterators themselves are the most complicated part of our formalism, but they may be implemented and tested independently of the formulas themselves.

4.4 B tensor formulas

In his important review of anharmonic force field methods,[305] Attila Császár lists five internal coordinate types which he calls "customary": bond stretching, angle bending, torsion, out-of-plane bending, and linear angle bending. Though complete, arbitrary order formulas for the first two of these have already been published,[307] we include them here for com-

pleteness and because they are frequently referenced from the other formulas. The formulas for the remaining coordinates are presented here for the first time. All formulas have been checked‡ using a computer algebra system.[317]

4.4.1 Translational invariance

We can significantly reduce the amount of work that needs to be done for each coordinate by invoking a relation derived from the translational invariance conditions. For a general N-point coordinate $\lambda_{a_1 a_2 \cdots a_N}$, the $\mathbf{B}$ tensor elements involving atom a_1 coordinates can be given in terms of the elements of coordinates for atoms a_2 through a_N as follows:

$$\begin{aligned}
&\mathbf{B}_{\lambda_{a_1 a_2 \cdots a_N}}^{a_{1\alpha_1} a_{1\alpha_2} \cdots a_{1\alpha_{m_1}} a_{2\alpha_{(m_1+1)}} \cdots a_{2\alpha_{m_2}} a_{3\alpha_{(m_2+1)}} \cdots a_{N-1\alpha_{m_{(N-1)}}} a_{N\alpha_{(m_{(N-1)}+1)}} \cdots a_{N\alpha_{m_N}}} \\
&\quad = (-1)^{m_1} \sum_{b_1 b_2 \cdots b_{m_1}} \mathbf{B}_{\lambda_{a_1 a_2 \cdots a_N}}^{b_{1\alpha_1} b_{2\alpha_2} \cdots b_{m_1\alpha_{m_1}} a_{2\alpha_{(m_1+1)}} \cdots a_{2\alpha_{m_2}} a_{3\alpha_{(m_2+1)}} \cdots a_{N-1\alpha_{m_{(N-1)}}} a_{N\alpha_{(m_{(N-1)}+1)}} \cdots a_{N\alpha_{m_N}}}
\end{aligned} \tag{4.13}$$

where all b_i run over the set of atoms $\{a_k | k = 2,\ 3,\ \ldots,\ N\}$ independently.[307] For instance, in the case of a bond angle coordinate ϕ_{abc} going from atom a through atom b to atom c (discussed in further detail below), the following relations involving the middle atom b may be obtained:

$$\mathbf{B}_{\phi_{abc}}^{b_{\alpha_1}} = -\mathbf{B}_{\phi_{abc}}^{a_{\alpha_1}} - \mathbf{B}_{\phi_{abc}}^{c_{\alpha_1}} \tag{4.14}$$

$$\mathbf{B}_{\phi_{abc}}^{b_{\alpha_1} a_{\alpha_2}} = -\mathbf{B}_{\phi_{abc}}^{a_{\alpha_1} a_{\alpha_2}} - \mathbf{B}_{\phi_{abc}}^{c_{\alpha_1} a_{\alpha_2}} \tag{4.15}$$

$$\mathbf{B}_{\phi_{abc}}^{b_{\alpha_1} b_{\alpha_2}} = \mathbf{B}_{\phi_{abc}}^{a_{\alpha_1} a_{\alpha_2}} + \mathbf{B}_{\phi_{abc}}^{c_{\alpha_1} a_{\alpha_2}} + \mathbf{B}_{\phi_{abc}}^{a_{\alpha_1} c_{\alpha_2}} + \mathbf{B}_{\phi_{abc}}^{c_{\alpha_1} c_{\alpha_2}} \tag{4.16}$$

$$\mathbf{B}_{\phi_{abc}}^{b_{\alpha_1} b_{\alpha_2} c_{\alpha_3}} = \mathbf{B}_{\phi_{abc}}^{a_{\alpha_1} a_{\alpha_2} c_{\alpha_3}} + \mathbf{B}_{\phi_{abc}}^{c_{\alpha_1} a_{\alpha_2} c_{\alpha_3}} + \mathbf{B}_{\phi_{abc}}^{a_{\alpha_1} c_{\alpha_2} c_{\alpha_3}} + \mathbf{B}_{\phi_{abc}}^{c_{\alpha_1} c_{\alpha_2} c_{\alpha_3}} \tag{4.17}$$

‡See Supplementary Material document No. _____ for a *Mathematica* 8 script demonstrating the verification of the new formulas in this paper as well as the formulas themselves.

and so on. Equation (4.13) is extremely useful for coordinates such as the bond angle and out-of-plane bending, where differentiating with respect to a central atom substantially complicates the higher derivatives.

4.4.2 Bond stretching

Given a bond stretching coordinate $R_{ab} \equiv |\alpha_b - \alpha_a| = \sqrt{(b_x - a_x)^2 + (b_y - a_y)^2 + (b_z - a_z)^2}$, it is elementary to show that the first order $\mathbf{B}$ tensor for this coordinate is:[307]

$$\mathbf{B}^{a_\alpha}_{R_{ab}} \equiv \frac{\partial R_{ab}}{\partial \alpha_a} = R^{-1}_{ab}(\alpha_a - \alpha_b) = -(\mathbf{e}_{ab})_\alpha = (\mathbf{e}_{ba})_\alpha \tag{4.18}$$

We mention this fact here because it gives us an important general relation to be used later:

$$\mathbf{e}_{a_1 a_2} = \underline{\mathbf{b}}^{\mathbf{a_2}}_{R_{a_1 a_2}} \tag{4.19}$$

for any a_1, a_2. Further direct differentiation gives, for atom a:[307]

$$\mathbf{B}^{a_\alpha a_\beta}_{R_{ab}} \equiv \frac{\partial R_{ab}}{\partial \alpha_a \partial \beta_a} = -R^{-1}_{ab}\left(\mathbf{B}^{a_\alpha}_{R_{ab}}\mathbf{B}^{a_\beta}_{R_{ab}} - \delta_{\alpha\beta}\right) \tag{4.20}$$

and for all orders greater than two:

$$\mathbf{B}^{a_{\alpha_1} a_{\alpha_2} \cdots a_{\alpha_n}}_{R_{ab}} = -R^{-1}_{ab} \sum_{s \in \mathcal{I}_{\ell(n)\bar{u}(2)}\left(a_{\alpha_1} a_{\alpha_2} \cdots a_{\alpha_n}\right)} \mathbf{B}^{s_1}_{R_{ab}}\mathbf{B}^{s_2}_{R_{ab}} \tag{4.21}$$

The mixed $a-b$ elements may be obtained by translational invariance using equation (4.13).

4.4.3 Bond angle

As with the bond stretching coordinate, we note the following formula for the first order $\mathbf{B}$ tensor of a bond angle ϕ_{abc} in passing, because it leads to an important general relation we will later exploit. For a bond angle ϕ_{abc} from atom a through atom b to atom c [i.e. $\phi_{abc} = \arccos(\mathbf{e}_{ba} \cdot \mathbf{e}_{bc})$], we have

$$\mathbf{B}^{a_\alpha}_{\phi_{abc}} = R_{ab}^{-1} \csc\phi_{abc}(\cos\phi_{abc}\mathbf{e}_{ba} - \mathbf{e}_{bc})_\alpha = -\csc\phi_{abc}\left(\underline{\mathbf{b}}^{\mathbf{a},\ a_\alpha}_{R_{ab}} \cdot \underline{\mathbf{b}}^{\mathbf{c}}_{R_{bc}}\right) \tag{4.22}$$

where the latter form comes from direct differentiation of $cos(\phi_{abc}) = \mathbf{e}_{ba} \cdot \mathbf{e}_{bc}$ and equation (4.19). We can immediately glean the following useful general relations:

$$\mathbf{e}_{a_1a_2} = \left(\underline{\mathbf{b}}^{\mathbf{a_2}}_{\phi_{a_2a_1a_3}} R_{a_1a_2}\sin\phi_{a_2a_1a_3} + \mathbf{e}_{a_1a_3}\right)\sec\phi_{a_2a_1a_3} \tag{4.23}$$

$$= \mathbf{e}_{a_1a_3}\cos\phi_{a_2a_1a_3} - \underline{\mathbf{b}}^{\mathbf{a_3}}_{\phi_{a_2a_1a_3}} R_{a_1a_3}\sin\phi_{a_2a_1a_3} \tag{4.24}$$

where a_1 and a_2 are unique atoms and a_3 is any atom not collinear with a_1 and a_2.

Drawing on the work of ACSM[307] one final time, we find the general form of the bond angle $\mathbf{B}$ tensor involving the terminal atoms a and c to be:

$$\mathbf{B}^{a_{\alpha_1}a_{\alpha_2}\cdots a_{\alpha_p}c_{\alpha_{(p+1)}}\cdots c_{\alpha_n}}_{\phi_{abc}} = -\csc\phi_{abc}\left(\underline{\mathbf{b}}^{\mathbf{a},\ a_{\alpha_1}\cdots a_{\alpha_p}}_{R_{ab}} \cdot \underline{\mathbf{b}}^{\mathbf{c},\ c_{\alpha_{(p+1)}}\cdots a_{\alpha_n}}_{R_{bc}}\right) + \sum_{k=2}^{n} f_k(\phi_{abc}) \sum_{s\in\mathcal{I}_{\ell(n)\bar{u}(k)}\left(a_{\alpha_1}\cdots c_{\alpha_n}\right)} \prod_{i=1}^{k} \mathbf{B}^{s_i}_{\phi_{abc}} \tag{4.25}$$

where

$$f_k(\phi) = \begin{cases} (-1)^{(k+1)/2} & \text{if } k \text{ is odd} \\ (-1)^{k/2}\cot\phi & \text{if } k \text{ is even} \end{cases} \tag{4.26}$$

(Previous work by ACSM[307] gives the odd piece of this function as 1 rather than the value above, causing their formula to be incorrect for fifth order and beyond). The remaining elements involving the central b atom can be obtained by translational invariance using equation (4.13).

4.4.4 Torsion

The most difficult and involved of the coordinates presented herein is the torsional coordinate τ_{abcd}. We label atoms a, b, c, and d in the customary manner, such that τ_{abcd} is the angle between the planes defined by abc and bcd. In other words:

$$\cos \tau_{abcd} = \frac{(\mathbf{e}_{ba} \times \mathbf{e}_{bc}) \cdot (\mathbf{e}_{cb} \times \mathbf{e}_{cd})}{\sin \phi_{abc} \sin \phi_{bcd}} \tag{4.27}$$

One can decompose the general $\mathbf{B}$ tensor problem into several cases:

1. $a - b - c$ *elements*: $\mathbf{B}$ tensor elements involving at least one coordinate on a terminal atom a and some combination of other coordinates on the two central atoms b and c neighboring a

2. $a - d$ *elements*: $\mathbf{B}$ tensor elements involving at least one coordinate on a terminal atom a and at least one other coordinate on the other terminal atom d and any combination of other coordinates

3. $b - b$ *elements*: $\mathbf{B}$ tensor elements involving coordinates only on atom b, the atom immediately adjacent to an (arbitrarily chosen) terminal atom a

Noting that the $d - c - b$ case is merely a relabeled version of the $a - b - c$ case, all other cases may be obtained by translational invariance using equation (4.13).

THE $a-b-c$ ELEMENTS

We find it easiest to start with the first-order terminal atom $\underline{\mathbf{b}}$ expression given by

$$\underline{\mathbf{b}}^{\mathbf{a}}_{\tau_{abcd}} = R_{ab}^{-1} \csc^2 \phi_{abc} \left(\mathbf{e}_{ba} \times \mathbf{e}_{bc} \right) \tag{4.28}$$

Using equation (4.23) for $\mathbf{e}_{ba}$ and equation (4.19) for $\mathbf{e}_{bc}$ and rearranging, we get

$$\sin(2\phi_{abc}) \mathbf{B}^{a_{\alpha_1}}_{\tau_{abcd}} = 2(\underline{\mathbf{b}}^{\mathbf{a}}_{\phi_{abc}} \times \underline{\mathbf{b}}^{\mathbf{c}}_{R_{bc}})_{\alpha_1} \tag{4.29}$$

Noting that the product rule for cross products works exactly analogously to that of scalar products, we have

$$\begin{aligned} \sin(2\phi_{abc}) \mathbf{B}^{a_{\alpha_1} \cdots a_{\alpha_p} b_{\alpha_{(p+1)}} \cdots b_{\alpha_q} c_{\alpha_{(q+1)}} \cdots c_{\alpha_n}}_{\tau_{abcd}} &= 2 \left(\sum_{t \in \mathcal{I}_{\ell(n-p)\ell(2)}\left(b_{\alpha_{(p+1)}} \cdots c_{\alpha_n}\right)} \underline{\mathbf{b}}^{\mathbf{a},\ \{a_{\alpha_2} \cdots a_{\alpha_p}\} \oplus t_1}_{\phi_{abc}} \times \underline{\mathbf{b}}^{\mathbf{c},\ t_2}_{R_{bc}} \right)_{\alpha_1} \\ &\quad - \mathbf{B}^{a_{\alpha_1}}_{\tau_{abcd}} \mathbf{B}^{a_{\alpha_2} \cdots c_{\alpha_n}}_{\sin(2\phi_{abc})} - \left(\sum_{s \in \mathcal{I}_{\ell(n-1)\bar{\ell}(2)}\left(a_{\alpha_2} \cdots c_{\alpha_n}\right)} \mathbf{B}^{s_1}_{\sin(2\phi_{abc})} \mathbf{B}^{\{a_{\alpha_1}\} \oplus s_2}_{\tau_{abcd}} \right) \end{aligned} \tag{4.30}$$

where a void derivative is simply the undifferentiated function (i.e., $\mathbf{B}^{\varnothing}_{\sin(2\phi_{abc})} = \sin(2\phi_{abc})$) and a void, non-barred iterator still contains one term (i.e., there is exactly one way to place 0 balls in 2 boxes: $\mathcal{I}_{\ell(0)\ell(2)}(\varnothing) = \{\{\varnothing, \varnothing\}\}$). Also in equation (4.30), $a_{\alpha_2} \cdots c_{\alpha_n}$ is short for $a_{\alpha_2} a_{\alpha_3} \cdots a_{\alpha_p} b_{\alpha_{(p+1)}} b_{\alpha_{(p+2)}} \cdots b_{\alpha_q} c_{\alpha_{(q+1)}} c_{\alpha_{(q+2)}} \cdots c_{\alpha_n}$; analogous shortenings are made in other parts of this equation and throughout the remainder of this paper. Note further that in equation (4.30) we have $n \geq q \geq p > 0$ (in other words, as previously stated, at least one coordinate must be on terminal atom a). Equation (4.30) contains the first instance in which we have taken advantage of our notational generalization to allow function subscripts of $\mathbf{B}$. In this case, the $\mathbf{B}$ tensor of the composite function $\sin(2\phi_{abc})$ can easily be computed using

equation (4.12):

$$\mathbf{B}_{\sin(2\phi_{abc})}^{a_{\alpha_1}\cdots a_{\alpha_p} b_{\alpha_{(p+1)}}\cdots b_{\alpha_q} c_{\alpha_{(q+1)}}\cdots c_{\alpha_n}} = \sum_{k=1}^{n}\left(2^k \sin\left(2\phi_{abc}+\frac{k\pi}{2}\right) \sum_{s\in\mathcal{I}_{\ell(n)\bar{u}(k)}\left(a_{\alpha_1}\cdots c_{\alpha_n}\right)} \prod_{i=1}^{k} \mathbf{B}_{\phi_{abc}}^{s_i}\right) \tag{4.31}$$

The $a-d$ elements

As can be easily seen from equation (4.28), any cross-terms involving a and d will be rigorously zero, since no part of this equation depends on atom d coordinates.

The $b-b$ elements

Starting from the first-order expression for $\underline{\mathbf{b}}_{\tau_{abcd}}^{\mathbf{b}}$, given by

$$\underline{\mathbf{b}}_{\tau_{abcd}}^{\mathbf{b}} = R_{ab}^{-1}\csc^2\phi_{abc}\left(\mathbf{e}_{bc}\times\mathbf{e}_{ba}\right) - R_{bc}^{-1}\cot\phi_{abc}\csc\phi_{abc}\left(\mathbf{e}_{bc}\times\mathbf{e}_{ba}\right) + R_{bc}^{-1}\cot\phi_{bcd}\csc\phi_{bcd}\left(\mathbf{e}_{cb}\times\mathbf{e}_{cd}\right) \tag{4.32}$$

we can use equations (4.24) and (4.19) on the first term and (4.23) and (4.19) on the second and third terms to get

$$\underline{\mathbf{b}}_{\tau_{abcd}}^{\mathbf{b}} = \csc\phi_{abc}\left(\underline{\mathbf{b}}_{\phi_{abc}}^{\mathbf{a}}\times\underline{\mathbf{b}}_{R_{ba}}^{\mathbf{a}}\right) - \csc\phi_{abc}\left(\underline{\mathbf{b}}_{\phi_{abc}}^{\mathbf{c}}\times\underline{\mathbf{b}}_{R_{ba}}^{\mathbf{a}}\right) + \csc\phi_{bcd}\left(\underline{\mathbf{b}}_{\phi_{bcd}}^{\mathbf{b}}\times\underline{\mathbf{b}}_{R_{cd}}^{\mathbf{d}}\right) \tag{4.33}$$

Using equation (4.8) on each term, we obtain

$$\begin{aligned}\mathbf{B}_{\tau_{abcd}}^{b_{\alpha_1} b_{\alpha_2}\cdots b_{\alpha_n}} = &\left(\sum_{s\in\mathcal{I}_{\ell(n-1)\ell(2)}\left(b_{\alpha_2}\cdots b_{\alpha_n}\right)} \mathbf{B}_{\csc\phi_{bcd}}^{s_1}\left(\underline{\mathbf{b}}_{\phi_{bcd}}^{\mathbf{b},\ s_2}\times\underline{\mathbf{b}}_{R_{cd}}^{\mathbf{d}}\right)\right)_{\alpha_1} \\ &- \left(\sum_{t\in\mathcal{I}_{\ell(n-1)\ell(3)}\left(b_{\alpha_2}\cdots b_{\alpha_n}\right)} \mathbf{B}_{\csc\phi_{abc}}^{t_1}\left(\underline{\mathbf{b}}_{\phi_{abc}}^{\mathbf{a},\ t_2}\times\underline{\mathbf{b}}_{R_{ba}}^{\mathbf{a},\ t_3} + \underline{\mathbf{b}}_{\phi_{abc}}^{\mathbf{c},\ t_2}\times\underline{\mathbf{b}}_{R_{ba}}^{\mathbf{a},\ t_3}\right)\right)_{\alpha_1}\end{aligned} \tag{4.34}$$

This result requires the arbitrary order $\mathbf{B}$ tensor for the function $\csc\phi_{abc}$. Using equation (4.12), we quickly find

$$\mathbf{B}_{\csc(\phi_{abc})}^{a_{\alpha_1}\cdots a_{\alpha_p} b_{\alpha_{(p+1)}}\cdots b_{\alpha_q} c_{\alpha_{(q+1)}}\cdots c_{\alpha_n}} = \sum_{k=1}^{n} \left(\frac{d^k \csc u}{du^k} \right)_{u=\phi_{abc}} \sum_{\mathcal{I}_{\ell(n)\bar{u}(k)}\left(a_{\alpha_1}\cdots c_{\alpha_n}\right)} \prod_{i=1}^{k} \mathbf{B}_{\phi_{abc}}^{s_i} \tag{4.35}$$

A number of formulas are known for $d^k \csc u / du^k$, dating back to at least 1924.[318,319] Our own formula is presented here because it is easiest to program; we have not seen this formula in any other source, but we have not done enough mathematical research to claim discovery of it with any certainty:

$$\frac{d^n \csc u}{du^n} = (-1)^n \sum_{k=0}^{\lfloor n/2 \rfloor} t_{n,k} \cot^{n-2k} u \csc^{2k+1} u \tag{4.36}$$

where $t_{n,k}$ is given by

$$t_{n,k} = \begin{cases} 1 & \text{if } k = 0 \\ (2k+1)t_{n-1,k} + (n-2k+1)t_{n-1,k-1} & \text{if } k \leq \lfloor n/2 \rfloor \\ 0 & \text{if } k > \lfloor n/2 \rfloor \end{cases} \tag{4.37}$$

(Incidentally, the non-zero $t_{n,k}$ form Sloane's integer sequence A008971,[320] and it is the number of permutations of the first n integers with k increasing runs of length at least 2).

4.4.5 Out-of-plane angle

The easiest way to approach the out-of-plane $\mathbf{B}$ tensor elements is to start from the value function, apply equation (4.12) and then equation (4.8). The value of the out-of-plane angle γ_{abcd} (where d is the central atom and γ_{abcd} is the angle between the vector $\mathbf{e}_{da}$ and the plane

defined by bdc) is given by

$$\gamma_{abcd} = \arcsin\left[\csc\left(\phi_{bdc}\right)\mathbf{e}_{da}\cdot\left(\mathbf{e}_{db}\times\mathbf{e}_{dc}\right)\right] = \arcsin\left(\sin\gamma_{abcd}\right) \tag{4.38}$$

Using equation (4.12), one finds

$$\mathbf{B}_{\gamma_{abcd}}^{a_{\alpha_1}\cdots a_{\alpha_p}b_{\alpha_{(p+1)}}\cdots b_{\alpha_q}c_{\alpha_{(q+1)}}\cdots c_{\alpha_n}} = \sum_{k=1}^{n}\left(\frac{d^k\arcsin u}{du^k}\right)_{u=\sin(\gamma_{abcd})}\sum_{\mathcal{I}_{\ell(n)\bar{u}(k)}\left(a_{\alpha_1}\cdots c_{\alpha_n}\right)}\prod_{i=1}^{k}\mathbf{B}_{\sin(\gamma_{abcd})}^{s_i} \tag{4.39}$$

where, using equation (4.8) and equation (4.19), we have

$$\mathbf{B}_{\sin(\gamma_{abcd})}^{a_{\alpha_1}\cdots a_{\alpha_p}b_{\alpha_{(p+1)}}\cdots b_{\alpha_q}c_{\alpha_{(q+1)}}\cdots c_{\alpha_n}} = \underline{\mathbf{b}}_{R_{da}}^{\mathbf{a},\ a_{\alpha_1}\cdots a_{\alpha_n}}\cdot\left[\sum_{\substack{s\in\mathcal{I}_{\ell(q-p)\ell(2)}\left(b_{\alpha_{(p+1)}}\cdots b_{\alpha_q}\right)\\ t\in\mathcal{I}_{\ell(n-q)\ell(2)}\left(c_{\alpha_{(q+1)}}\cdots c_{\alpha_n}\right)}}\mathbf{B}_{\csc\phi_{bdc}}^{s_1\oplus t_1}\left(\underline{\mathbf{b}}_{R_{db}}^{\mathbf{b},\ s_2}\times\underline{\mathbf{b}}_{R_{dc}}^{\mathbf{c},\ t_2}\right)\right] \tag{4.40}$$

and $\mathbf{B}_{\csc\phi_{bdc}}^{a_{\alpha_1}\cdots c_{\alpha_n}}$ is given in equation (4.35). Several formulas for $d^k\arcsin u/du^k$ are known,[321] one of which is

$$\frac{d^n\arcsin(u)}{du^n} = 2^{1-n}(n-1)!\sum_{k=0}^{\lfloor(n-1)/2\rfloor}\binom{n-1}{k}\binom{2n-2k-2}{n-1}u^{n-2k-1}(1-u^2)^{k-n+\frac{1}{2}} \tag{4.41}$$

All out-of-plane angle $\mathbf{B}$ tensor elements involving atom d can be obtained exploiting translational invariance using equation (4.13).

4.4.6 Linear bending

One way to define a linear bending internal coordinate is to take $\theta_{abc}^{(A)}$ to be the angle from atom a through atom b to atom c in the plane perpendicular to a given, fixed unit vector

$\mathbf{e}_A$. In this case, we have the following expression for $\theta^{(A)}_{abc}$:

$$\theta^{(A)}_{abc} = \arcsin\left[\mathbf{e}_A \cdot (\mathbf{e}_{bc} \times \mathbf{e}_{ba})\right] = \arcsin\left(\sin\theta^{(A)}_{abc}\right) \tag{4.42}$$

Proceeding in exactly the same manner as for the out-of-plane angle, one finds for terminal atoms a and c

$$\mathbf{B}^{a_{\alpha_1}\cdots a_{\alpha_p} c_{\alpha_{(p+1)}}\cdots c_{\alpha_n}}_{\theta^{(A)}_{abc}} = \sum_{k=1}^{n} \left(\frac{d^k \arcsin u}{du^k}\right)_{u=\sin\theta^{(A)}_{abc}} \sum_{\mathcal{I}_{\ell(n)\bar{u}(k)}\left(a_{\alpha_1}\cdots c_{\alpha_n}\right)} \prod_{i=1}^{k} \mathbf{B}^{s_i}_{\sin\theta^{(A)}_{abc}} \tag{4.43}$$

where

$$\mathbf{B}^{a_{\alpha_1}\cdots a_{\alpha_p} c_{\alpha_{(p+1)}}\cdots c_{\alpha_n}}_{\sin\theta^{(A)}_{abc}} = \mathbf{e}_A \cdot \left(\underline{\mathbf{b}}^{\mathbf{c},\ c_{\alpha_{(p+1)}}\cdots c_{\alpha_n}}_{R_{bc}} \times \underline{\mathbf{b}}^{\mathbf{a},\ a_{\alpha_1}\cdots a_{\alpha_p}}_{R_{ba}}\right) \tag{4.44}$$

and with the arbitrary order derivative of $\arcsin u$ given in the out-of-plane angle section. The elements involving coordinates on central atom b may then be computed utilizing translational invariance with equation (4.13).

4.4.7 General N-atom coordinate

From the discussion above, particularly the last two coordinates, it should be clear that the notation developed in this paper leads to a relatively general and comparatively simple strategy for determining analytic formulas for arbitrary order $\mathbf{B}$ tensor elements of a given coordinate. We thus endeavor to summarize this strategy notationally by presenting a formula for the arbitrary order $\mathbf{B}$ tensor elements of a *general* coordinate. We define our general coordinate $\lambda_{a_1 a_2 \cdots a_N}$ as follows:

$$\lambda_{a_1 a_2 \cdots a_N} = \sum_{i}^{t^{(s)}} \prod_{j}^{t^{(m)}_i} f_{ij}(\mathbf{k}_{ij}) \tag{4.45}$$

where $t^{(s)}$ is the number of summands in the (arbitrary) coordinate value formula, $t_i^{(m)}$ is the number of multiplicands in the ith summand, $\mathbf{k}_{ij} \subseteq \{a_{1x}a_{1y}a_{1z}a_{2x}\cdots a_{Ny}a_{Nz}\}$, and all f_{ij} are arbitrarily differentiable over the domain of $\lambda_{a_1a_2\cdots a_N}$. We define the following notation:

$$J_{im} \equiv \{\ j \mid \{a_{mx}, a_{my}, a_{mz}\} \subseteq \mathbf{k}_{ij}\ \}_{\text{ord}} \tag{4.46}$$

$$\tilde{J}_{ij} \equiv \{\ \mu \mid \{a_{\mu x}, a_{\mu y}, a_{\mu z}\} \subseteq \mathbf{k}_{ij}\ \}_{\text{ord}} \tag{4.47}$$

where $\{\dots\}_{\text{ord}}$ indicates an ordered set with respect to the indices it is composed of. Then the arbitrary order $\mathbf{B}$ tensor for coordinate can be written

$$\mathbf{B}^{a_{1\alpha_1}a_{1\alpha_2}\cdots a_{1\alpha_{m_1}}a_{2\alpha_{(m_1+1)}}\cdots a_{2\alpha_{m_2}}a_{3\alpha_{(m_2+1)}}\cdots a_{p\alpha_{(m_{p-1})}}a_{p\alpha_{m_p}}}_{\lambda_{a_1a_2\cdots a_N}} = \sum_i^{t^{(s)}} \sum_{\mathcal{S}\in\mathscr{G}_i} \prod_j^{t^{(m)}} \mathbf{B}_{f_{ij}(k_{ij})}^{\oplus_{h\in\tilde{J}_{ij}}\mathcal{S}_{h,\eta(h,i,j)}} \tag{4.48}$$

where

$$\mathscr{G}_i \equiv \bigotimes_\nu^N \mathcal{I}_{\ell(m_\nu - m_{(\nu-1)})\ell(\|J_{i\nu}\|)} \left(a_{\nu\alpha_{(m_{(\nu-1)}+1)}} \cdots a_{\nu\alpha_{m_\nu}}\right) \tag{4.49}$$

and $\eta(h,i,j)$ is the position of j in J_{ih}. For a given f_{ij}, we can apply equation (4.12) (recursively, if necessary) to obtain the $\mathbf{B}$ tensor formulas for that function.

4.5 Conclusions

We have provided arbitrary order formulas for the $\mathbf{B}$ tensors of the five customary internal coordinates. Our notation directly suggests a simple, modular implementation while remaining compact enough to easily express the general formulas derived in this work. Analytic forms of $\mathbf{B}$ tensors are particularly important compared to their $\mathbf{L}$ tensor counterparts because the alternative to analytic forms—numeric finite difference—is far less stable in the former case than in the latter. Furthermore, use of numeric methods for $\mathbf{B}$ tensor elements

can lead to orientation-dependent results if the implementation is not carried out carefully. The most obvious application of this work is the transformation of higher order force fields, as noted by Allen and Császár.[306] In our work, we have found it easier to program the arbitrary order formulas than to explicitly program even the (well-known) fourth order formulas. The transformation of quartic force fields is critical for computation of anharmonic vibrational properties using second-order vibrational perturbation theory, for instance.[263] It is our hope that the formulas presented here will spur further development of software that utilizes curvalinear internal coordinates and, consequently, more prominent use of localized internal coordinates in chemical application studies.

4.6 Acknowledgments and Supporting Information

The *Mathematica* script demonstrating the verification of the new formulas in this paper as well as the formulas themselves is included in the supplementary material. It is available on the internet on the page associated with the DOI 10.1063/1.4759170. This research was supported by the Department of Energy, Office of Basic Energy Sciences, Chemistry Division, Fundamental Interactions Program, Grant No. DE-FG02-97-ER14748, and used resources of the National Energy Research Scientific Computing Center, which is supported by the Office of Science of the U. S. Department of Energy under Contract No. DE-AC02-05CH11231. The authors would like to acknowledge the contributions of Wesley D. Allen, who graciously offered us his scratch work from reference 307 which got us started on this paper. We also thank Dr. Jeremiah Wilke for many helpful discussions.

4.7 Appendix A: Relation of notational paradigms

This appendix assumes the reader is familiar with reference 307. ACSM[307] used a partition operator labeled $\mathscr{P}_{\mathscr{N}_K}^{(K,m_n)}$ which gives the $\mathscr{N}_k$th partition of a list of m_n indices into K segments. Summation over this operator is exactly equivalent to summation over our iterator $\mathcal{I}_{u(n)\bar{u}(k)}$ (i.e., summation over the arrangements of n unlabeled balls in K non-empty unlabeled boxes). However, they almost exclusively use this operator in concert with the brace-notation brackets. In that case, we have the notational equivalence

$$\sum_{\mathscr{N}_K}^{\mathscr{L}(K,n)} F\left\{\mathscr{P}_{\mathscr{N}_K}^{(K,n)}\left(a_{1\alpha_1}a_{2\alpha_2}\cdots a_{n\alpha_n}\right)\right\} = \sum_{s\in\mathcal{I}_{\ell(n)\bar{u}(k)}\left(a_{1\alpha_1}a_{2\alpha_2}\cdots a_{n\alpha_n}\right)} \prod_{i=1}^{k} F(s_i) \tag{4.50}$$

for some function F and where the left-hand side of the equals sign uses notation from ACSM and the right-hand side uses notation from the present research.

Chapter 5

Explicitly Correlated Atomic Orbital Basis Second Order Møller–Plesset Theory*

*David S. Hollman and H. F. Schaefer, J. Chem. Phys. **138**, 064107 (2013). Reprinted here with permission of the American Institute of Physics.

Abstract

The scope of problems treatable by *ab initio* wavefunction methods has expanded greatly through the application of local approximations. In particular, atomic orbital (AO) based wavefunction methods have emerged as powerful techniques for exploiting sparsity and have been applied to biomolecules as large as 1707 atoms [Maurer et al., *J. Chem. Phys.* **136**, 144107 (2012)]. Correlated wavefunction methods, however, converge notoriously slowly to the basis set limit and, excepting the use of large basis sets, will suffer from a severe basis set incompleteness error (BSIE). The use of larger basis sets is prohibitively expensive for AO basis methods since, for example, second-order Møller-Plesset perturbation theory (MP2) scales linearly with the number of atoms, but still scales as $\mathcal{O}(N^5)$ in the number of functions per atom. Explicitly-correlated F12 methods have been shown to drastically reduce BSIE for even modestly-sized basis sets. In this work, we therefore explore an atomic orbital based formulation of explicitly-correlated MP2-F12 theory. We present working equations for the new method, which produce results identical to the widely-used molecular orbital (MO) version of MP2-F12 without resorting to a delocalized MO basis. We conclude with a discussion of several possible approaches to *a priori* screening of contraction terms in our method and the prospects for a linear scaling implementation of AO-MP2-F12. The discussion includes concrete examples involving noble gas dimers and linear alkane chains.

5.1 Introduction

The importance of electron correlation effects has long been known for quantum mechanical computations of molecular system properties. In the past decade, wave function methods have increasingly been applied to large biomolecules and biochemical systems.[322–326] Even the simplest correlated method, second order Møller-Plesset theory (MP2),[195] scales formally as $\mathcal{O}(N^5)$, making it prohibitively expensive for use with large systems. However, electron correlation is a local effect, and should be treatable in a computational effort that scales linearly with system size; it is in large part the use of delocalized molecular orbitals (MOs) that leads to this unphysical scaling. As such, substantial effort has been put into the development of methods that scale linearly with system size.[111,327–338] These so-called "linear-scaling methods" typically use some localization criterion for defining localized occupied MOs and some set of non-orthogonal, projected atomic orbitals for the virtual space. Atomic orbital (AO) basis methods further use a set of localized, non-orthogonal AOs to span even the occupied space, along with some screening technique for determining *a priori* which blocks of integrals are zero.[108,109,112,339,340]

In general, wavefunction methods have unrivaled accuracy but scale formally worse than density functional theory (DFT). In addition, correlated methods suffer form a more severe basis set incompleteness error (BSIE). Recent studies, however, have shown DFT is often qualitatively incorrect, particularly for noncovalent effects[289] and properties such as NMR shieldings.[341–343] To make the computational cost of wavefunction methods more competitive, we need to ameliorate both the unphysical scaling and the slow basis set convergence. Though the AO basis methods discussed above address the unphysical scaling, BSIE remains a substantial problem. Even though AO-MP2 computations scale linearly in the number of atoms, they still scale as $\mathcal{O}(N^5)$ in the number of basis functions *per atom*. The residual error in correlation energy only falls off as $\mathcal{O}(\ell_{\text{max}}^{-3})$, where ℓ_{max} is the maximum angular

momentum of the basis set.[32,49] For a typical basis set series such as the cc-pVnZ basis sets of Dunning and co-workers,[25] the number of basis functions N_{AO} increases as ℓ_{max}^3. The error therefore only decays as $\mathcal{O}(t^{-1/5})$ in the total computational time![†]

One approach to improving basis set convergence of wavefunction methods in recent years has been the use of explicitly correlated methods. These explicitly correlated R12 (and later, F12) corrections[5,42–45,344–348] have been developed for a number of conventional *ab initio* methods, including MP2,[49–65] coupled cluster singles and doubles (CCSD),[66–76] CCSD with perturbative triples,[77–84] multireference perturbation theory,[61] and multireference configuration interaction.[85,86] The utility of F12 methods stems from their ability to better approximate the shape of the wavefunction around the electron-electron coalescence cusp.[32,33] Unlike conventional methods, F12 methods include a term that is an explicit function of the distance r_{12} between two electrons. Studies have shown that the use of only a triple-ζ basis set with explicitly correlated methods can lead to results of the same accuracy as a quintuple-ζ[349] or possibly even a hextuple-ζ[74] basis with conventional methods. The success of R12/F12 methods can be seen in the fact that they are now used in a breadth of quantum chemical computations.[87–95]

Explicitly correlated methods therefore provide a powerful and natural extension to AO-basis methods. F12 methods, as stated above, improve basis set convergence by better approximating the interelectronic cusp. This cusp is fundamentally a short-range phenomenon, and the convergence of the wavefunction in regions further away from the cusp is quite good otherwise.[5] AO basis methods principally draw their success from the ability to treat local phenomena locally, without delocalizing the effects of said phenomena across the whole molecule in question. Moreover, if it could be shown that F12-type interactions degrade with distance substantially more rapidly than conventional interactions, explicitly correlated

[†]Note that this is different from the result for MO basis MP2, which only scales as $\mathcal{O}(N^4)$ in the number of basis functions *per atom*, and thus the error decays as $\mathcal{O}(t^{-1/4})$.

corrections could be added to conventional AO basis methods at minimal extra cost.

Progress in MO-based local MP2-F12 methods has been made in recent years.[58,63] This approach uses one of several techniques to create a set of localized, orthogonal MOs. While effective, these methods still require the diagonalization of an effective Fock operator to generate the local MOs, which can be prohibitively expensive for sufficiently large molecules. The high cost of the diagonalization step has pushed researchers to explore reformulations of Hartree-Fock theory (and ultimately, MP2 theory) based on an AO-basis density matrix without reference to molecular orbitals.[350,351] The recent success of AO basis MP2 for the treatment of very large systems[352,353] merits further investigation into the viability of recasting explicitly correlated methods in the AO basis.

In this work, we present working equations for two of the most widely used approximations[52] to MO basis MP2-F12 theory. For the first time, we recast these equations in the AO basis and discuss the implications of and difficulties with this reformulation. The resulting equations lead to *exactly the same result* as the widely used MO version of the method. With the equations recast in terms of local quantities, screening techniques such as those of Lambrecht and Ochsenfeld[108,109,112,340] become feasible, and we present a discussion of the new method's practicality with these considerations in mind. We conclude by discussing future directions of explicitly correlated AO basis methods.

5.2 Theoretical Background

5.2.1 Notation

Throughout this paper, we will use the following indexing conventions:

$\mu,\ \nu,\ \varrho,\ \sigma,\ \ldots$	AO orbital indices
$\mu'',\ \nu'',\ \varrho'',\ \sigma'',\ \ldots$	AO auxiliary indices
$\mu',\ \nu',\ \varrho',\ \sigma',\ \ldots$	General AO indices
$p,\ q,\ r,\ s,\ \ldots$	MO orbital indices
$p'',\ q'',\ r'',\ s'',\ \ldots$	MO complementary auxiliary space
$p',\ q',\ r',\ s',\ \ldots$	General MO indices
$i,\ j,\ k,\ l,\ \ldots$	MO occupied indices
$a,\ b,\ c,\ d,\ \ldots$	MO virtual indices
$\beta,\ldots$	Infinite MO RI basis
$x,\ y,\ w,\ z,\ \ldots$	Geminal generating space

The symbols η, λ, κ, δ, ζ, and ϑ will also be used as AO orbital indices (with corresponding primed and double primed versions for auxiliary and general AO indices, respectively).

In keeping with convention,[4,329] matrix elements of an operator $\hat{O}$ will be expressed in tensor notation:

$$O_{\mu\nu} \equiv \langle\mu|\hat{O}|\nu\rangle = \int \chi_\mu(r_1)\hat{O}\chi_\nu(r_1)d\tau_1 \tag{5.1}$$

if $\hat{O}$ is a one electron operator and

$$O_{\mu\nu,\varrho\sigma} \equiv \langle\chi_\mu(r_1)\chi_\nu(r_2)|\hat{O}|\chi_\varrho(r_1)\chi_\sigma(r_2)\rangle \tag{5.2}$$

if $\hat{O}$ is a two electron operator. Following the notation of Head-Gordon, Maslen, and White (HMW),[329] we will use subscripts to denote covariant indices in a non-orthogonal basis and superscripts to denote contravariant indices. To summarize the formalism of HMW briefly, basis functions (atomic orbitals, in our case) $|\mu\rangle \equiv |\chi_\mu(r)\rangle$ are covariant; MO coefficient tensors are contravariant in the AO basis index and either covariant or contravariant in the

MO index (since the MO indices represent an orthogonal basis). If a symbol that appears as both a covariant and a contravariant index in a given product, summation is implied unless otherwise noted (Einstein summation convention). [‡] Matrix elements over covariant orbitals are covariant, as shown in equations (5.1) and (5.2). The covariant metric that converts a single index from contravariant to covariant is the overlap tensor $S_{\mu\nu} \equiv \langle \chi_\mu | \chi_\nu \rangle$.[§] Thus, for some (one electron) operator $\hat{O}$ we have[¶]

$$O_{\mu\nu} = O_\mu^\sigma S_{\sigma\nu} = O^{\varrho\sigma} S_{\mu\varrho} S_{\sigma\nu} \tag{5.3}$$

The contravariant metric tensor is the inverse overlap matrix,

$$S^{\mu\nu} \equiv (S^{-1})_{\mu\nu} \tag{5.4}$$

and by analogy to equation (5.3), we have

$$O^{\mu\nu} = O_\sigma^\mu S^{\sigma\nu} = O_{\varrho\sigma} S^{\mu\varrho} S^{\sigma\nu} \tag{5.5}$$

[‡]There is a bit of a tension between whether one should abide by the covariant–contravariant contraction rule strictly or avoid confusing the reader by using C_i^μ and $C^{\mu i}$ to mean the same thing. We opt for the former, but the reader should be aware that other authors opt for the latter for equally valid reasons.

[§]Throughout the paper, we will use $|\mu\rangle$ and $|\chi_\mu\rangle$ interchangeably, depending on whether we wish to be compact or emphasize the covariant nature of the basis function. Similarly, $|i\rangle$ and $|\phi_i\rangle$ may be used interchangeably, even though in the orthogonal MO basis no such covariant implication is necessary.

[¶]Readers familiar with the work of HMW [329] will note here that we have been slightly sloppy with respect to index ordering and bra-ket formalism. HMW always identifies the bra with the first index of a second rank tensor and the ket with the second. Thus, the first part of equation (5.3) should be written $O_{\mu\nu} = O_\mu^{\bullet\sigma} S_{\sigma\nu}$. Since practical implementations of the methods presented in this paper typically involve real orbitals and Hermitian operators, and since we work with the assumption in this paper that all orbitals are real, we dispense with this additional detail here.

5.2.2 The Hylleraas Functional and MP2-F12 Theory

The typical starting point for discussion of MP2-F12 related methods is the Hylleraas functional:[354]

$$\langle \mathbf{\Psi}^{(1)} | \hat{H}^{(0)} - E^{(0)} | \mathbf{\Psi}^{(1)} \rangle + 2 \langle \mathbf{\Psi}^{(1)} | \hat{H} | \mathbf{\Psi}^{(0)} \rangle \geq E^{(2)}[\mathbf{\Psi}^{(1)}] \tag{5.6}$$

which can be expressed in terms of pair correlation functions as

$$\langle u_{ij} | \hat{f}_1 + \hat{f}_2 - \varepsilon_i - \varepsilon_j | u_{ij} \rangle + 2 \langle u_{ij} | \frac{1}{r_{12}} | ij \rangle \geq e_{ij}^{(2)} \tag{5.7}$$

where $\hat{f}_1$ and $\hat{f}_2$ are the Fock operators on electrons 1 and 2, ε_i and ε_j are the eigenvalues corresponding to (occupied) orbitals i and j, and $E^{(2)} = \sum_{ij} e_{ij}^{(2)}$. For conventional MP2 theory, we use the ansatz

$$|u_{ij}\rangle_{\mathrm{MP2}} = \tfrac{1}{2} \sum_{ab} t_{ij}^{ab} \, |ab\rangle \tag{5.8}$$

where t_{ij}^{ab} are variationally optimized amplitudes. For closed shell molecules, this formulation is equivalent to that of Møller and Plesset.[195] In MP2-F12 theory, an explicitly correlated term is added to the MP2 ansatz to get

$$|u_{ij}\rangle_{\mathrm{MP2F12}} = \tfrac{1}{2} \sum_{ab} t_{ij}^{ab} \, |ab\rangle + \tfrac{1}{2} \sum_{xy} \tilde{t}_{ij}^{xy} \hat{Q}_{12} F(r_{12}) \, |xy\rangle \tag{5.9}$$

where $\hat{Q}_{12}$ (known as the "strong orthogonality projector") is a projection operator that ensures the first order wavefunction is orthogonal to the reference wavefunction, which is a condition of the Hylleraas formulation, and $F(r_{12})$ is a function (called the "correlation factor") that depends explicitly on the interelectronic coordinate r_{12}.[48] Typically, only the

occupied orbitals are necessary to construct the geminal space (i.e., $\{x\} = \{i\}$), but for excited states and response properties virtual orbitals are also necessary.[57,355–357] For simplicity, however, we will assume in this paper that the occupied orbitals are used to construct the geminal space. The extension of our method to a generalized geminal space is relatively straightforward. In modern F12 theories, one typically uses[5,46–48]

$$\hat{Q}_{12} = (1 - \hat{o}_1)(1 - \hat{o}_2) - \hat{v}_1\hat{v}_2 \tag{5.10}$$

$$\hat{F}_{12} \equiv F(r_{12}) = \tfrac{1}{\gamma}\big(1 - \exp(-\gamma r_{12})\big) \tag{5.11}$$

where $\hat{o} \equiv \sum_i |i\rangle\langle i|$ (with i being a function of electron 1 for $\hat{o}_1$ and electron 2 for $\hat{o}_2$), $\hat{v} \equiv \sum_a |a\rangle\langle a|$, and γ is a length-scale parameter that accounts for how strongly the interelectronic interaction is screened by the surrounding electron density.[‖] The amplitudes $\tilde{t}_{ij}^{xy}$ are in theory also variationally optimized parameters, though in practical applications these are almost always fixed.[51] The use of this ansatz with the Hylleraas functional formalism leads to the following closed-shell, spin-adapted equations for the MP2-F12 energy and amplitude residuals[49,52]

$$E_{MP2F12} = t_{ij}^{ab}(2g_{ab}^{ij} - g_{ab}^{ji}) + \tilde{t}_{ij}^{xy}(2V_{xy}^{ij} - V_{xy}^{ji}) \tag{5.12}$$

$$R_{ij}^{ab} = t_{ij}^{ac}f_c^b + t_{ij}^{cb}f_c^a - t_{ik}^{ab}f_j^k - t_{kj}^{ab}f_i^k + g_{ij}^{ab} + \tilde{t}_{ij}^{xy}C_{xy}^{ab} \tag{5.13}$$

$$\tilde{R}_{ij}^{xy} = V_{ij}^{xy} + B_{wz}^{xy}\tilde{t}_{ij}^{wz} - X_{wz}^{xy}(f_i^k\tilde{t}_{kj}^{wz} + f_j^k\tilde{t}_{ik}^{wz}) + C_{ab}^{xy}t_{ij}^{ab} \tag{5.14}$$

[‖]This version of the strong orthogonality projector is typically referred to as ansatz 2, though some authors[49] label this as ansatz 3. Since we will only be discussing theories derived from this ansatz, we thought it best to omit discussion of other ansätze here.

where $\hat{f}$ is the Fock operator and

$$g_{ij}^{ab} = \langle ij|\frac{1}{r_{12}}|xy\rangle \tag{5.15}$$

$$V_{ij}^{xy} = \langle ij|\frac{1}{r_{12}}\hat{Q}_{12}\hat{F}_{12}|xy\rangle \tag{5.16}$$

$$X_{wz}^{xy} = \langle wz|\hat{F}_{12}\hat{Q}_{12}\hat{F}_{12}|xy\rangle \tag{5.17}$$

$$B_{wz}^{xy} = \langle wz|\hat{F}_{12}\hat{Q}_{12}(\hat{f}_1 + \hat{f}_2)\hat{Q}_{12}\hat{F}_{12}|xy\rangle \tag{5.18}$$

$$C_{xy}^{ab} = \langle xy|\hat{F}_{12}\hat{Q}_{12}(\hat{f}_1 + \hat{f}_2)|ab\rangle \tag{5.19}$$

The V intermediate may be thought of as the F12 generalization of the electron repulsion integrals. The X intermediate is the geminal overlap matrix, and the B intermediate is the F12 generalization of the energy denominator or resolvent.

In the interest of simplicity and to focus our efforts on the use of the atomic orbital basis rather than the details of MP2-F12 theory, we will here discuss only the recasting of a couple of commonly used F12 approximations—often labeled approximation 3*C and 3C by other authors.[49,52] In the 3*C approximation, it is assumed that the virtual orbitals are eigenfunctions of the true Fock operator and thus $f_{ap''} = 0$, which leads to $C_{xy}^{ab} = 0$. This assumption is known as the Extended Brillouin Condition (EBC). Fixed F12 amplitudes using the Ten-no rational generator[51] are also used, which leads to an action of the amplitudes that is equivalent to

$$\tilde{t}_{ij}^{xy}\,|xy\rangle = \tfrac{3}{8}\,|xy\rangle + \tfrac{1}{8}\,|yx\rangle \tag{5.20}$$

With $C_{xy}^{ab} = 0$, the amplitude equations completely decouple, and the energy can be expressed

as a sum of the conventional and explicitly correlated energies:

$$E_{\mathrm{MP2F12}} = E_{\mathrm{MP2}} + E_{\mathrm{F12}}, \tag{5.21}$$

$$E_{\mathrm{MP2}} = t_{ij}^{ab}(2g_{ab}^{ij} - g_{ab}^{ji}) \tag{5.22}$$

$$E_{\mathrm{F12}} = \tilde{t}_{ij}^{xy}(2V_{xy}^{ij} - V_{xy}^{ji}) \tag{5.23}$$

Since the amplitudes are no longer being variationally optimized, we include the F12 residuals in the energy expression, equation (5.23), to get

$$E_{\mathrm{F12}} = \tilde{t}_{ij}^{xy}(2V_{xy}^{ij} - V_{xy}^{ji} + 2\tilde{R}_{xy}^{ij} - \tilde{R}_{xy}^{ji}) \tag{5.24}$$

Applying the fixed amplitude formalism from equation (5.20) gives us the working (MO) expression

$$E_{\mathrm{F12}} = \sum_{ij} \left(\tfrac{5}{8} V_{ij}^{ij} - \tfrac{1}{8} V_{ij}^{ji} + \tfrac{5}{8} \tilde{R}_{ij}^{ij} - \tfrac{1}{8} \tilde{R}_{ij}^{ji} \right) \tag{5.25}$$

where we have broken with Einstein convention and included explicit summations for clarity. Similar manipulations of equation (5.14) give us

$$\tilde{R}_{ij}^{xy} = V_{ij}^{xy} + \tfrac{3}{8} B_{ij}^{xy} + \tfrac{1}{8} B_{ij}^{yx} - \tfrac{3}{8} X_{wj}^{xy} f_i^w - \tfrac{1}{8} X_{jz}^{xy} f_i^z - \tfrac{3}{8} X_{iz}^{xy} f_j^z - \tfrac{1}{8} X_{wi}^{xy} f_j^w \tag{5.26}$$

Intermediates

Direct evaluation of expressions for the V and X intermediates leads to notorious three electron integrals, so it is common to use resolutions of the identity (RI) to factor these terms into products of two electron integrals. These RI approximations are equivalent to

expressing the projection operators in $\hat{Q}_{12}$ as

$$\hat{o}_1 = \sum_{i\beta} |i\beta\rangle \langle i\beta| \tag{5.27}$$

$$\hat{o}_2 = \sum_{i\beta} |\beta i\rangle \langle \beta i| \tag{5.28}$$

$$\hat{v}_1\hat{v}_2 = \sum_{ab} |ab\rangle \langle ab| \tag{5.29}$$

which is exact if $\{\beta\}$ is a complete, infinite basis (this resolution of the identity is sometimes called a "spectral decomposition"). Given the finitude of computers, it is conventional to approximate $\{\beta\}$ using an RI basis $\{p'\}$ that includes the orbital basis $\{p\}$ and the complementary auxiliary basis (CABS) $\{p''\}$.[348] The strong orthogonality projector in equation (5.10) can then be written as (noting, again, that repeated indices still indicate summation)

$$\hat{Q}_{12} = 1 - \hat{P}_{12} \tag{5.30}$$

$$\hat{P}_{12} = \hat{o}_1\hat{p}'_2 + \hat{p}'_1\hat{o}_2 - \hat{o}_1\hat{o}_2 + \hat{v}_1\hat{v}_2 \tag{5.31}$$

$$= |ip'\rangle \langle ip'| + |p'i\rangle \langle p'i| - |ij\rangle \langle ij| + |ab\rangle \langle ab| \tag{5.32}$$

$$= |ip''\rangle \langle ip''| + |p''i\rangle \langle p''i| + |pq\rangle \langle pq| \tag{5.33}$$

where $\hat{p}' \equiv \sum_{p'} |p'\rangle \langle p'|$ and we have used $\{p\} = \{i\} \cup \{a\}$ and $\{p'\} = \{p\} \cup \{p''\}$. Using this version of the strong orthogonality projector, we immediately get the working MO expression for the V intermediate:

$$V_{ij}^{xy} = (Fg)_{ij}^{xy} - F_{ij}^{p''k} g_{p''k}^{xy} - F_{ij}^{kp''} g_{kp''}^{xy} - F_{ij}^{pq} g_{pq}^{xy} \tag{5.34}$$

where

$$(Fg)_{ij}^{xy} \equiv \langle ij|\frac{\hat{F}_{12}}{r_{12}}|xy\rangle \tag{5.35}$$

are integrals that can be computed analytically (as are the integrals over the operator $\hat{F}_{12}$). The expression for the geminal overlap matrix elements may be obtained similarly:

$$X_{wz}^{xy} = \tilde{F}_{wz}^{xy} - F_{wz}^{p''i}F_{p''i}^{xy} - F_{wz}^{ip''}F_{ip''}^{xy} - F_{wz}^{pq}F_{pq}^{xy} \tag{5.36}$$

where

$$\tilde{F}_{ij}^{xy} \equiv \langle ij|\hat{F}_{12}^2|xy\rangle \tag{5.37}$$

are integrals that can be computed analytically.

The B intermediate is substantially more complicated. In the interest of maintaining focus on the stated purpose of this paper, we will give working (programmable) equations for the B matrix elements and refer the reader to Ref. 52 for a detailed derivation. We define the operator $\widehat{\mathcal{S}_{pq}^{rs}}$ by its action on some four-index tensor T_{pq}^{rs}

$$\widehat{\mathcal{S}_{pq}^{rs}}T_{pq}^{rs} = T_{pq}^{rs} + T_{qp}^{sr} + (T_{pq}^{rs} + T_{qp}^{sr})^\dagger \tag{5.38}$$

$$= T_{pq}^{rs} + T_{qp}^{sr} + T_{rs}^{pq} + T_{sr}^{qp} \tag{5.39}$$

The expression for the B matrix elements can then be written (adapted from Ref. 52 and

Ref. 57)

$$B_{wz}^{xy} = [DC]_{wz}^{xy} - \tfrac{1}{2}\widehat{\mathcal{S}_{xy}^{wz}}\big(F_{iq'}^{xy}(f+k)_{r'}^{k'}F_{wz}^{ir'} + F_{as}^{xy}f_{r}^{s}F_{wz}^{ar} + F_{as}^{xy}k_{q'}^{s}F_{wz}^{aq'} + 2F_{as''}^{xy}f_{q}^{s''}F_{wz}^{aq}$$
$$+ F_{as''}^{xy}k_{r'}^{s''}F_{wz}^{ar'} - F_{r''j}^{xy}f_{n}^{j}F_{wz}^{r''n} + F_{r''j}^{xy}k_{p'}^{j}F_{wz}^{r''p'} + 2F_{r''j}^{xy}f_{p'}^{j}F_{wz}^{r''p'}$$
$$+ F_{ab}^{xy}f_{p''}^{a}F_{wz}^{bp''} + F_{r''b}^{xy}k_{p'}^{b}F_{wz}^{r''p'} + F_{r''s''}^{xy}k_{p'}^{s''}F_{wz}^{r''p'} - \tilde{F}_{wz}^{xp'}(f+k)_{p'}^{y}\big) \quad (5.40)$$

where k is the exchange operator (and hence $(f+k)$ is the exchange-free Fock operator) and $[DC]_{wz}^{xy}$ are the double commutator integrals

$$[DC]_{wz}^{xy} \equiv \langle wz|[[\hat{F}_{12},(\hat{f}+\hat{k})],\hat{F}_{12}]|xy\rangle \quad (5.41)$$

which can be computed analytically. We note here that our brief introduction of this matter (particularly of the B matrix) glosses over a substantial amount of historical development and discussion of competing approximations. For a discussion of these topics, we refer the reader to recent reviews of explicitly correlated methods.[5,49,345]

5.2.3 AO-MP2 Theory

The use of the atomic orbital basis for MP2 theory is also well established in the literature.[108,111,330,332,334] Beginning with a series of papers by Almlöf and Häser[327,358,359] and continuing with significant contributions from Ayala and Scuseria[330,332,334] as well as Ochsenfeld and coworkers,[108,109,111,340] the basic strategy for AO-MP2 theory involves a Laplace transform of the energy denominator coupled with a technique for screening inte-

grals and the use of density-matrix like projectors:

$$\mathcal{P}^{\mu\nu} = \sum_i C_i^\mu C^{\nu i} \tag{5.42}$$

$$\mathcal{Q}^{\mu\nu} = \sum_a C_a^\mu C^{\nu a} \tag{5.43}$$

We begin with the closed shell, spin-adapted MP2 expression in the canonical MO basis:

$$E_{\mathrm{MP2}} = \sum_{ijab} \frac{\langle ij|ab\rangle \left(2\langle ij|ab\rangle - \langle ij|ba\rangle\right)}{\varepsilon_i + \varepsilon_j - \varepsilon_a - \varepsilon_b} \tag{5.44}$$

where ϵ_p is the energy of the molecular orbital p. Almlöf noted in 1991[358] that the energy denominator (and thus canonical MOs altogether) could be avoided using a Laplace transform of the form

$$\frac{1}{\Delta_{ij}^{ab}} = \int_0^\infty \exp(-\Delta_{ij}^{ab} t) dt \tag{5.45}$$

$$\Delta_{ij}^{ab} \equiv \varepsilon_a + \varepsilon_b - \varepsilon_i - \varepsilon_j \tag{5.46}$$

This integral can then be approximated using a Gaussian quadrature

$$\frac{1}{\Delta_{ij}^{ab}} \approx \sum_\alpha^\tau \omega_{(\alpha)} \exp(-\Delta_{ij}^{ab} t_{(\alpha)}) \tag{5.47}$$

Häser and Almlöf found that fewer than eight quadrature points $\{\omega_{(\alpha)}, t_{(\alpha)}\}$ were needed to achieve microhartree accuracy. Using pseudo-density matrices which partially fold in the

Gaussian quadrature

$$\mathcal{P}^{\mu\nu}_{(\alpha)} = \sum_i C^\mu_i C^{\nu i} \exp(\varepsilon_i t_{(\alpha)}) \tag{5.48}$$

$$\mathcal{Q}^{\mu\nu}_{(\alpha)} = \sum_a C^\mu_a C^{\nu a} \exp(-\varepsilon_a t_{(\alpha)}) \tag{5.49}$$

the MP2 energy expression can be rewritten

$$E_{\mathrm{MP2}} = -\sum_\alpha^\tau \omega_{(\alpha)} e^{\mathrm{MP2}}_{(\alpha)} \tag{5.50}$$

$$e^{\mathrm{MP2}}_{(\alpha)} = g_{\mu\nu,\varrho\sigma} \mathcal{P}^{\mu\lambda}_{(\alpha)} \mathcal{P}^{\nu\eta}_{(\alpha)} \mathcal{Q}^{\varrho\delta}_{(\alpha)} \mathcal{Q}^{\sigma\zeta}_{(\alpha)} (2g_{\lambda\eta,\delta\zeta} - g_{\lambda\eta,\zeta\delta}) \tag{5.51}$$

As an important aside, we note that the pseudo-density matrices can be obtained without any reference to MO quantities using $\mathcal{P}_{(\alpha)} = \exp(t_{(\alpha)}\mathcal{P}f)\mathcal{P}$ and $\mathcal{Q}_{(\alpha)} = \exp(t_{(\alpha)}\mathcal{Q}f)\mathcal{Q}$, where f is the Fock matrix and $\mathcal{P}$ from equation (5.42) as well as $\mathcal{Q}$ from (5.43) can be computed directly.[330,340,350,360,361] This is an important point because it leads to linear scaling AO-MP2 if sufficient screening techniques are used for the $g_{\mu\nu,\varrho\sigma}$ integrals.

5.3 AO-MP2-F12 Equations

Combining the methodologies from the previous section, the recasting of the MP2-F12 equations is possible. In addition to the density-like projectors in equations (5.42) and (5.43), we define a CABS space projector

$$\mathcal{O}^{\mu'\nu'} = \sum_{p''} C^{\mu'}_{p''} C^{\nu' p''} \tag{5.52}$$

Here we make note of several details. First, note that $\{\mu'\} = \{\mu\} \cup \{\mu''\}$, and that the CABS space projector $\mathcal{O}$ is the only one of the three projectors with contributions from the

auxiliary basis $\{\mu''\}$. Second, the contravariant metric (overlap) tensor $S^{\mu'\nu'}$ can be written

$$S^{\mu'\nu'} = C^{\mu'}_{p'} S^{p'q'} C^{\nu'}_{q'} \tag{5.53}$$

$$= C^{\mu'}_{i} S^{ij} C^{\nu'}_{j} + C^{\mu'}_{a} S^{ab} C^{\nu'}_{b} + C^{\mu'}_{p''} S^{p''q''} C^{\nu'}_{q''} \tag{5.54}$$

$$= \mathcal{P}^{\mu'\nu'} + \mathcal{Q}^{\mu'\nu'} + \mathcal{O}^{\mu'\nu'} \tag{5.55}$$

where the orthogonality of the MO space and the unitarity of the MO coefficients have been used. Also, as previously noted, the $C^{\mu''}_{p}$ block is zero, as are the $\mathcal{P}^{\mu'\nu''}$, $\mathcal{P}^{\mu''\nu'}$, $\mathcal{Q}^{\mu'\nu''}$, and $\mathcal{Q}^{\mu''\nu'}$ blocks. Finally, since $C^{\mu}_{p''}$ is not in general zero, the contravariant overlap matrix in the orbital basis (which we will denote $\mathcal{S}^{\mu\nu}$) is not a sub-block of the full RI basis overlap matrix $S^{\mu\nu}$. (Note that this sub-block relationship *does* exist for the covariant overlap tensors). However, we do have

$$\mathcal{S}^{\mu\nu} = \mathcal{P}^{\mu\nu} + \mathcal{Q}^{\mu\nu} \tag{5.56}$$

which will be used in the recasting of some of our equations.

5.3.1 The Energy Expression and the Residuals

Since the 3C* F12 approximation decouples the energy expression, we need only recast equation (5.25) and the residuals in equation (5.26). Noting that the full expression for the first term in (5.25) is written with explicit summations as

$$\frac{5}{8} \sum_{ij} \langle ij | \hat{g}_{12} \hat{Q}_{12} \hat{F}_{12} | ij \rangle \tag{5.57}$$

we can use the definition of the molecular orbitals $|i\rangle = \sum_\mu C_i^\mu |\mu\rangle$ to rewrite this as

$$\frac{5}{8} \sum_{ij\mu\nu\varrho\sigma} C_i^\mu C_j^\nu \langle \mu\nu | \hat{g}_{12} \hat{Q}_{12} \hat{F}_{12} | \varrho\sigma \rangle C_i^\varrho C_j^\sigma = \tfrac{5}{8} \mathcal{P}^{\mu\varrho} V_{\mu\nu,\varrho\sigma} \mathcal{P}^{\nu\sigma} \tag{5.58}$$

Similar manipulations of the other terms lead to

$$E_{\mathrm{F12}} = \tfrac{5}{8} \mathcal{P}^{\mu\varrho} V_{\mu\nu,\varrho\sigma} \mathcal{P}^{\nu\sigma} - \tfrac{1}{8} \mathcal{P}^{\mu\varrho} V_{\mu\nu,\sigma\varrho} \mathcal{P}^{\nu\sigma} + \tfrac{5}{8} \mathcal{P}^{\mu\varrho} \tilde{R}_{\mu\nu,\varrho\sigma} \mathcal{P}^{\nu\sigma} - \tfrac{1}{8} \mathcal{P}^{\mu\varrho} \tilde{R}_{\mu\nu,\sigma\varrho} \mathcal{P}^{\nu\sigma} \tag{5.59}$$

The expression for the residuals in equation (5.26) can be recast in the AO basis as

$$\begin{aligned} \tilde{R}_{\mu\nu,\varrho\sigma} = V_{\mu\nu,\varrho\sigma} + \tfrac{3}{8} B_{\mu\nu,\varrho\sigma} + \tfrac{1}{8} B_{\mu\nu,\sigma\varrho} - \tfrac{3}{8} X_{\varrho\sigma,\kappa\nu} \mathcal{P}^{\kappa\lambda} f_{\mu\lambda} - \tfrac{1}{8} X_{\varrho\sigma,\nu\kappa} \mathcal{P}^{\kappa\lambda} f_{\mu\lambda} \\ - \tfrac{3}{8} X_{\varrho\sigma,\mu\kappa} \mathcal{P}^{\kappa\lambda} f_{\nu\lambda} - \tfrac{1}{8} X_{\varrho\sigma,\kappa\mu} \mathcal{P}^{\kappa\lambda} f_{\nu\lambda} \end{aligned} \tag{5.60}$$

5.3.2 The V and X Intermediates

The recasting of the V and X intermediates to the AO basis is accomplished similarly. The V intermediate becomes

$$V_{\mu\nu,\varrho\sigma} = (Fg)_{\mu\nu,\varrho\sigma} - F_{\varrho\sigma,\zeta'\eta} \mathcal{O}^{\zeta'\lambda'} \mathcal{P}^{\eta\delta} g_{\mu\nu,\lambda'\delta} - F_{\varrho\sigma,\eta\zeta'} \mathcal{O}^{\zeta'\lambda'} \mathcal{P}^{\eta\delta} g_{\mu\nu,\delta\lambda'} - F_{\varrho\sigma,\delta\lambda} \mathcal{Q}^{\delta\kappa} \mathcal{Q}^{\lambda\eta} g_{\mu\nu,\kappa\eta} \tag{5.61}$$

By exactly the same process, the X matrix becomes

$$X_{\mu\nu,\varrho\sigma} = \tilde{F}_{\mu\nu,\varrho\sigma} - F_{\varrho\sigma,\zeta'\eta} \mathcal{O}^{\zeta'\lambda'} \mathcal{P}^{\eta\delta} F_{\mu\nu,\lambda'\delta} - F_{\varrho\sigma,\eta\zeta'} \mathcal{O}^{\zeta'\lambda'} \mathcal{P}^{\eta\delta} F_{\mu\nu,\delta\lambda'} - F_{\varrho\sigma,\delta\lambda} \mathcal{Q}^{\delta\kappa} \mathcal{Q}^{\lambda\eta} F_{\mu\nu,\kappa\eta} \tag{5.62}$$

5.3.3 The B Intermediate

Though we could just apply the same general process to equation (5.40), we found that more useful expressions were obtained by first factorizing the MO expression and then recasting the factorized equations to the AO basis.

We rearrange equation (5.40) as follows:

$$B_{wz}^{xy} = [DC]_{wz}^{xy} - \tfrac{1}{2}\widehat{\mathcal{S}_{xy}^{wz}}\big(F_{iq'}^{xy}\Gamma_{wz}^{iq'} + F_{as}^{xy}\Lambda_{wz}^{as} + F_{as''}^{xy}\Xi_{wz}^{as''} + F_{r''j}^{xy}\Theta_{wz}^{r''j} + F_{r''b}^{xy}\Omega_{wz}^{r''b} + F_{r''s''}^{xy}\Omega_{wz}^{r''s''} - F_{wz}^{xp'}(f+k)_{p'}^{y}\big) \quad (5.63)$$

where

$$\Gamma_{xy}^{mp'} = F_{xy}^{mr'}f_{r'}^{p'} + F_{xy}^{mr'}k_{r'}^{p'} \quad (5.64)$$

$$\Theta_{xy}^{q''m} = F_{xy}^{q''r'}k_{r'}^{m} - F_{xy}^{q''n}f_{n}^{m} + 2F_{xy}^{q''p'}f_{p'}^{m} \quad (5.65)$$

$$\Lambda_{xy}^{cp} = F_{xy}^{cr}f_{r}^{p} + F_{xy}^{cq'}k_{q'}^{p} \quad (5.66)$$

$$\Xi_{xy}^{cp''} = 2F_{xy}^{cq}f_{q}^{p''} + F_{xy}^{cr'}k_{r'}^{p''} - F_{xy}^{cb}f_{b}^{p''} \quad (5.67)$$

$$\Omega_{xy}^{p''q'} = F_{xy}^{p''r'}k_{r'}^{q'} \quad (5.68)$$

Note that the reintroduction of MO basis intermediates here is merely for notational convenience; it has no effect on the sparsity of the resulting intermediates. By avoiding these intermediates and grouping terms in the AO basis, one could arrive at the same formulation. Utilizing this factorized form, we can obtain the AO versions of the B matrix equations

$$B_{\mu\nu,\varrho\sigma} = [DC]_{\mu\nu,\varrho\sigma} - \tfrac{1}{2}\widehat{\mathcal{S}_{\mu\nu}^{\varrho\sigma}}\big(F_{\mu\nu,\lambda\kappa'}\mathcal{P}^{\lambda\eta}S^{\kappa'\delta'}\Gamma_{\varrho\sigma,\eta\delta'} + F_{\mu\nu,\lambda\kappa}\mathcal{Q}^{\lambda\eta}\mathcal{Q}^{\kappa\delta}\Lambda_{\varrho\sigma,\eta\delta} + F_{\mu\nu,\lambda\kappa'}\mathcal{Q}^{\lambda\eta}\mathcal{O}^{\kappa'\delta'}\Xi_{\varrho\sigma,\eta\delta'} + F_{\mu\nu,\lambda'\kappa}\mathcal{O}^{\lambda'\eta'}\mathcal{P}^{\vartheta\delta}\Theta_{\varrho\sigma,\eta'\delta} + F_{\mu\nu,\lambda'\vartheta}\mathcal{O}^{\lambda'\eta'}\mathcal{Q}^{\vartheta\delta}\Omega_{\varrho\sigma,\eta'\delta} + F_{\mu\nu,\lambda'\vartheta'}\mathcal{O}^{\lambda'\eta'}\mathcal{O}^{\vartheta'\delta'}\Omega_{\varrho\sigma,\eta'\delta'} + \tilde{F}_{\mu\nu,\varrho\lambda'}S^{\lambda'\eta'}(f+k)_{\sigma\eta'}\big) \quad (5.69)$$

where the following symbols are used as shorthand:

$$\Gamma_{\mu\nu,\varrho\sigma'} = F_{\mu\nu,\varrho\lambda'} S^{\lambda'\kappa'} f_{\sigma'\kappa'} + F_{\mu\nu,\varrho\lambda'} S^{\lambda'\kappa'} k_{\sigma'\kappa'} \tag{5.70}$$

$$\Theta_{\mu\nu,\varrho'\sigma} = F_{\mu\nu\varrho'\lambda'} S^{\lambda'\kappa'} k_{\kappa'\sigma} - F_{\mu\nu,\varrho'\lambda} P^{\lambda\kappa} f_{\kappa\sigma} + 2F_{\mu\nu\varrho'\lambda'} S^{\lambda'\kappa'} f_{\kappa'\sigma} \tag{5.71}$$

$$\Lambda_{\mu\nu,\varrho\sigma} = F_{\mu\nu,\varrho\lambda} \mathcal{Q}^{\lambda\kappa} f_{\kappa\sigma} + F_{\mu\nu\varrho\lambda'} S^{\lambda'\kappa'} k_{\kappa'\sigma'} \tag{5.72}$$

$$\Xi_{\mu\nu,\varrho\sigma'} = 2F_{\mu\nu,\varrho\lambda} \mathcal{Q}^{\lambda\kappa} f_{\kappa\sigma'} + F_{\mu\nu,\varrho\lambda'} S^{\lambda'\kappa'} k_{\kappa'\sigma'} - F_{\mu\nu,\varrho\lambda} \mathcal{Q}^{\lambda\kappa} f_{\kappa\sigma'} \tag{5.73}$$

$$\Omega_{\mu\nu,\varrho'\sigma'} = F_{\mu\nu,\varrho'\lambda'} S^{\lambda'\kappa'} k_{\kappa'\sigma'} \tag{5.74}$$

5.3.4 Forgoing the EBC: The 3C Approximation

Clearly, if we do not assume the EBC and thus proceed without the approximation $C_{ab}^{xy} \approx 0$, equations (5.13) and (5.14) no longer decouple and equation (5.21) no longer holds. As it turns out, this make the recasting of the MO equations challenging and leads to a method that is much less computationally efficient. Nonetheless, the derivation of the AO-MP2-F12(3C) equations is important because it demonstrates the applicability of explicitly correlated AO basis techniques to iterative post-Hartree-Fock methods and provides important insight for the future development of explicitly correlated AO basis coupled-cluster methods.

AO basis coupled-cluster techniques date back to at least 1999,[331] when Scuseria and Ayala presented working equations for AO basis coupled-cluster doubles (CCD) theory. A consequence of their derivation is the demonstration that AO basis MP2 can be carried out iteratively and without a Laplace transformation. Adapting the Scuseria-Ayala amplitude equations to our notation and method, we arrive at the following iterative equations for the

covariant amplitudes:

$$t_{\mu\nu,\varrho\sigma} = t_{\mu\nu,\varrho\sigma} + \frac{R_{\mu\nu,\varrho\sigma}}{\Delta_{\mu\nu,\varrho\sigma}} \quad \text{(no sum in second term)} \tag{5.75}$$

$$\begin{aligned} R_{\mu\nu,\varrho\sigma} = {} & \mathcal{P}_{\mu}^{\lambda}\mathcal{P}_{\nu}^{\zeta}\mathcal{Q}_{\varrho}^{\kappa}\mathcal{Q}_{\sigma}^{\eta}g_{\lambda\zeta,\kappa\eta} + t_{\mu\nu,\delta\sigma}\mathcal{Q}^{\delta\zeta}f_{\zeta\varrho} + t_{\mu\nu,\varrho\delta}\mathcal{Q}^{\delta\zeta}f_{\zeta\sigma} \\ & - t_{\delta\nu,\varrho\sigma}\mathcal{P}^{\delta\zeta}f_{\zeta\mu} - t_{\mu\delta,\varrho\sigma}\mathcal{P}^{\delta\zeta}f_{\zeta\nu} + \mathcal{P}_{\mu}^{\lambda}\mathcal{P}_{\nu}^{\zeta}\mathcal{Q}_{\varrho}^{\kappa}\mathcal{Q}_{\sigma}^{\eta}\left(\tfrac{3}{8}C_{\lambda\zeta,\kappa\eta} + \tfrac{1}{8}C_{\lambda\zeta,\eta\kappa}\right) \end{aligned} \tag{5.76}$$

$$\Delta_{\mu\nu,\varrho\sigma} = \underline{f}_{\mu}^{\mu} + \underline{f}_{\nu}^{\nu} - \overline{f}_{\varrho}^{\varrho} - \overline{f}_{\sigma}^{\sigma} \quad \text{(no sum over } \mu,\nu,\varrho, \text{ or } \sigma) \tag{5.77}$$

where the quantities in the resolvent, $\Delta_{\mu\nu,\varrho\sigma}$, are diagonal elements of intermediate matrices given by

$$\underline{f}_{\nu}^{\mu} = \mathcal{P}^{\mu\lambda}f_{\lambda\nu} \tag{5.78}$$

$$\overline{f}_{\sigma}^{\varrho} = \mathcal{Q}^{\varrho\lambda}f_{\lambda\sigma} \tag{5.79}$$

Recall that the mixed covariant/contravariant density matrices $\mathcal{P}_{\mu}^{\lambda}$ and $\mathcal{Q}_{\varrho}^{\kappa}$ are obtained using the overlap metric:

$$\mathcal{P}_{\mu}^{\lambda} = \mathcal{P}^{\mu\zeta}S_{\zeta\lambda} \tag{5.80}$$

$$\mathcal{Q}_{\varrho}^{\kappa} = \mathcal{Q}^{\varrho\zeta}S_{\zeta\varrho} \tag{5.81}$$

The coupling tensor $C_{\mu\nu,\varrho\sigma}$ can be recast from the MO expression given in reference 49 using the technique from section 5.3.1:

$$C_{ab}^{xy} = f_{a}^{p''}F_{p''b}^{xy} + f_{b}^{p''}F_{ap''}^{xy} \tag{5.82}$$

becomes

$$C_{\mu\nu,\varrho\sigma} = F_{\vartheta'\nu,\varrho\sigma}\mathcal{O}^{\vartheta'\lambda'}f_{\mu\lambda'} + F_{\mu\vartheta',\varrho\sigma}\mathcal{O}^{\vartheta'\lambda'}f_{\nu\lambda'} \tag{5.83}$$

In the context of linear scaling AO basis methods, equation (5.75) is not very helpful, since it requires an $\mathcal{O}(N_{AO}^4)$ operation that is not convenient for screening. This deficiency can be remedied using a Laplace transform and Gaussian quadrature, as with the conventional MP2 case.[327] The approach we have implemented is as follows. We start with a guess for the amplitudes

$$(t\Delta)^{(\text{initial})}_{\mu\nu,\varrho\sigma} = \mathcal{P}^{\lambda}_{\mu}\mathcal{P}^{\zeta}_{\nu}\mathcal{Q}^{\kappa}_{\varrho}\mathcal{Q}^{\eta}_{\sigma}g_{\lambda\zeta,\kappa\eta} \tag{5.84}$$

where we have used $(t\Delta)$ on the left-hand side to symbolize the t amplitude guess before division by the resolvent Δ. This expression can, of course, be factored into four (formally) $\mathcal{O}(N_{AO}^5)$ contractions over sparse quantities. In fact, many of the expressions in the following discussion can be similarly factored, but in the interest of brevity, we will not do so here. Given a set of τ Gaussian quadrature points $\{t_{(\alpha)}, \omega_{(\alpha)}\}$, we construct the Laplace-transformed *contravariant* amplitudes:

$$t^{\mu\nu,\varrho\sigma} = -\sum_{\alpha}^{\tau}(t\Delta)^{(\text{initial})}_{\lambda\zeta,\delta\vartheta}\,\underline{\mathcal{Q}}^{\mu\lambda}_{(\alpha)}\underline{\mathcal{Q}}^{\nu\zeta}_{(\alpha)}\overline{\mathcal{Q}}^{\varrho\delta}_{(\alpha)}\overline{\mathcal{Q}}^{\sigma\vartheta}_{(\alpha)} \tag{5.85}$$

where

$$\underline{\mathcal{Q}}^{\mu\lambda}_{(\alpha)} = \omega^{1/4}_{(\alpha)}\mathcal{Q}^{\mu\lambda}\exp(t_{(\alpha)}\underline{f}^{\mu}) \quad (\text{no sum over } \mu) \tag{5.86}$$

$$\overline{\mathcal{Q}}^{\varrho\delta}_{(\alpha)} = \omega^{1/4}_{(\alpha)}\mathcal{Q}^{\varrho\delta}\exp(-t_{(\alpha)}\overline{f}^{\varrho}) \quad (\text{no sum over } \varrho) \tag{5.87}$$

This first step needs to be done only once, before the iterations begin, to establish a reason-

able starting guess. We then back-transform $t^{\mu\nu,\varrho\sigma}$ to obtain covariant amplitudes:

$$t_{\mu\nu,\varrho\sigma} = t^{\lambda\delta,\zeta\vartheta} S_{\lambda\mu} S_{\delta\nu} S_{\zeta\varrho} S_{\vartheta\sigma} \tag{5.88}$$

and use these amplitudes with equation (5.76) to obtain covariant residuals. Then, using the same technique as in the construction of the starting guess, we incorporate the resolvent into the residuals:

$$(R/\Delta)^{\mu\nu,\varrho\sigma} = -\sum_{\alpha}^{\tau} R_{\lambda\zeta,\delta\vartheta} \underline{\mathcal{Q}}^{\mu\lambda}_{(\alpha)} \underline{\mathcal{Q}}^{\nu\zeta}_{(\alpha)} \overline{\mathcal{Q}}^{\varrho\delta}_{(\alpha)} \overline{\mathcal{Q}}^{\sigma\vartheta}_{(\alpha)} \tag{5.89}$$

and add the result to the contravariant amplitudes to complete the iteration

$$t^{\mu\nu,\varrho\sigma}_{(\text{new})} = t^{\mu\nu,\varrho\sigma}_{(\text{old})} + (R/\Delta)^{\mu\nu\varrho\sigma} \tag{5.90}$$

We iterate in this manner until the norm of the (covariant) residual vector $R_{\mu\nu\varrho\sigma}$ is less than some threshold (in our experience, 10^{-10} was sufficient to achieve machine-precision agreement with the MO result for small molecules). The energy may be computed on a per-iteration basis to check for convergence, but it need not be. To compute the conventional portion of the energy, we transform by the appropriate density matrices and contract with the electron repulsion integrals:

$$E_{MP2} = t_{\lambda\zeta,\delta\vartheta} \mathcal{P}^{\lambda\mu} \mathcal{P}^{\zeta\nu} \mathcal{Q}^{\delta\varrho} \mathcal{Q}^{\vartheta\sigma} \left(2g_{\mu\nu,\varrho\sigma} - g_{\mu\nu,\sigma\varrho}\right) \tag{5.91}$$

Incorporating $C_{\mu\nu,\varrho\sigma}$ into the F12 residuals $\tilde{R}_{\mu\nu,\varrho\sigma}$ for approximation 3C is much simpler,

since we have used the fixed F12 amplitudes.[51] Equation (5.60) becomes

$$\tilde{R}_{\mu\nu,\varrho\sigma} = V_{\mu\nu,\varrho\sigma} + \tfrac{3}{8}B_{\mu\nu,\varrho\sigma} + \tfrac{1}{8}B_{\mu\nu,\sigma\varrho} - \tfrac{3}{8}X_{\varrho\sigma,\kappa\nu}\mathcal{P}^{\kappa\lambda}f_{\mu\lambda} - \tfrac{1}{8}X_{\varrho\sigma,\nu\kappa}\mathcal{P}^{\kappa\lambda}f_{\mu\lambda} - \tfrac{3}{8}X_{\varrho\sigma,\mu\kappa}\mathcal{P}^{\kappa\lambda}f_{\nu\lambda} - \tfrac{1}{8}X_{\varrho\sigma,\kappa\mu}\mathcal{P}^{\kappa\lambda}f_{\nu\lambda} + C_{\mu\nu,\lambda\vartheta}\mathcal{Q}^{\lambda\kappa}\mathcal{Q}^{\vartheta\zeta}t_{\kappa\vartheta,\varrho\sigma} \quad (5.92)$$

where the only additional term is the final one, and the optimized covariant amplitudes $t_{\kappa\vartheta,\varrho\sigma}$ come from the iterative procedure described above. Finally, an additional cancellation leads to a slightly simpler form of the Ξ factor in the B intermediate, and equation (5.73) becomes:

$$\Xi_{\mu\nu,\varrho\sigma'} = 2F_{\mu\nu,\varrho\lambda}\mathcal{C}^{\lambda\kappa}f_{\kappa\sigma'} + F_{\mu\nu,\varrho\lambda'}S^{\lambda'\kappa'}k_{\kappa'\sigma'} \quad (5.93)$$

Practicality of the 3C Approximation

As Scuseria and Ayala note in their AO basis CCD paper,[331] the convergence of the iterative determination of the $t_{\mu\nu\varrho\sigma}$ amplitudes (equations (5.88)-(5.90)) can be quite slow and erratic. In our implementation, we were only able to get convergence for computations with F12 basis sets such as the cc-pVDZ-F12[258] basis by using relatively small damping factors and very careful DIIS extrapolation.[362] (Scuseria and Ayala mention the use of similar strategies for AO basis CCD).[331] Even with extrapolation, convergence for H_2 with the cc-pVDZ-F12[258] basis and the cc-pVDZ-F12/OPTRI[259] auxiliary basis required over 600 iterations and a damping factor of 0.03. Though we make no claims that our convergence techniques are optimal, it appears that the AO-MP2-F12(3C) method is of greater theoretical value than practical value, particularly given that Werner, Adler, and Manby[49] found that the decoupled 3*C approximation actually *outperforms* the 3C approximation in terms of root mean square error, even though the latter is more rigorous.

5.4 Computational Methods

A prototype code using the equations in the previous section was written using the `PSI4` package[363] with its new interface to the `Python` programming language.[364] This interface, which utilizes `NumPy`[365] for some numerical back-end functionality, allows the programmer to enter equations in Einstein summation formalism, such that the written form of the `Python` code for the program is nearly identical to the written form of the equations presented in this research. Our program verifies that the equations derived here exactly reproduce the MO basis result, as expected. The source code is freely available from the authors upon request. Several larger computations for the figures in the next section were carried out using a modified version of the `MPQC` package.[207]

5.5 Discussion

There are two important points to make about the nature of the equations themselves before we discuss their content. First, as alluded to in the previous section, the energies computed with these equations *are identical to the MO basis results.* The equations have merely been recast to make them more amenable to computation of local phenomena in a local basis, rather than a delocalized molecular orbital basis that leads to an unphysical scaling of computational effort. This is not the case, for instance, with many local orbital approximations,[58,63,64,72,100,328,335,337] which define localized MO domains. This leads to the second point: as with AO-MP2 theory, there are no "local domains" to be defined (or computed), as is the case with AO-MP2 theory. Ochsenfeld and coworkers give a thorough discussion of the importance of this point elsewhere in the literature,[109,111,340] and we will not discuss this issue further here.

The formal scaling of the equations without any *a priori* screening of integrals or sparse

matrix methods appears to be $\mathcal{O}(N^6)$ in equation (5.69). However, in a careful implementation of our method, this formal scaling can be reduced to $\mathcal{O}(N^5)$ simply by factorization. Consider the contribution to the energy of the second to last term ($F_{\mu\nu,\lambda'\vartheta'}\mathcal{O}^{\lambda'\eta'}\mathcal{O}^{\vartheta'\delta'}\Omega_{\varrho\sigma,\eta'\delta'}$) in equation (5.69) via equation (5.60) and the second to last term ($\frac{5}{8}\mathcal{P}^{\mu\varrho}\tilde{R}_{\mu\nu,\varrho\sigma}\mathcal{P}^{\nu\sigma}$) of equation (5.59). For this term only (neglecting the $\widehat{\mathcal{S}^{\varrho\sigma}_{\mu\nu}}$ for the moment), we have

$$E_{F12} \leftarrow -\tfrac{5}{16}\mathcal{P}^{\mu\varrho}F_{\mu\nu,\lambda'\vartheta'}\mathcal{O}^{\lambda'\eta'}\mathcal{O}^{\vartheta'\delta'}\Omega_{\varrho\sigma,\eta'\delta'}\mathcal{P}^{\nu\sigma} \tag{5.94}$$

Utilizing intermediates ${}^{(1)}\mathcal{I}$, ${}^{(2)}\mathcal{I}$, ${}^{(3)}\mathcal{I}$, and ${}^{(4)}\mathcal{I}$, we can factorize this contribution to the energy as follows:

$${}^{(1)}\mathcal{I}^{\varrho}_{\nu,\lambda'\vartheta'} = F_{\mu\nu,\lambda'\vartheta'}\mathcal{P}^{\mu\varrho} \tag{5.95}$$

$${}^{(2)}\mathcal{I}^{\varrho,\sigma}_{\lambda'\vartheta'} = {}^{(1)}\mathcal{I}^{\varrho}_{\nu,\lambda'\vartheta'}\mathcal{P}^{\nu\sigma} \tag{5.96}$$

$${}^{(3)}\mathcal{I}^{\varrho\sigma\eta'}_{\vartheta'} = {}^{(2)}\mathcal{I}^{\varrho,\sigma}_{\lambda'\vartheta'}\mathcal{O}^{\lambda'\eta'} \tag{5.97}$$

$${}^{(4)}\mathcal{I}^{\varrho\sigma\eta'\delta'} = {}^{(3)}\mathcal{I}^{\varrho\sigma\eta'}_{\vartheta'}\mathcal{O}^{\vartheta'\delta'} \tag{5.98}$$

$$E_{F12} \leftarrow -\tfrac{5}{16}\left({}^{(4)}\mathcal{I}^{\varrho\sigma\eta'\delta'}\Omega_{\varrho\sigma,\eta'\delta'}\right) \tag{5.99}$$

The first four contractions in this factorization are $\mathcal{O}(N^5)$; the last one is $\mathcal{O}(N^4)$. Note the similarity of this approach to that of conventional MO basis MP2 theory.

However, even though AO-MP2-F12 scales as formally as $\mathcal{O}(N^5)$ when sparsity is ignored, there is substantial sparsity that can be taken advantage of to significantly reduce this scaling. It is well known that $\mathcal{P}$ and $\mathcal{Q}$ are sparse quantities.[330,340,350,360,361] It follows from equation (5.56) that $\mathcal{B}$ should also be a sparse matrix. As discussed below, the F12 integrals F, $\tilde{F}$, (Fg), and $[DC]$ are also sparse, local quantities in the AO basis.

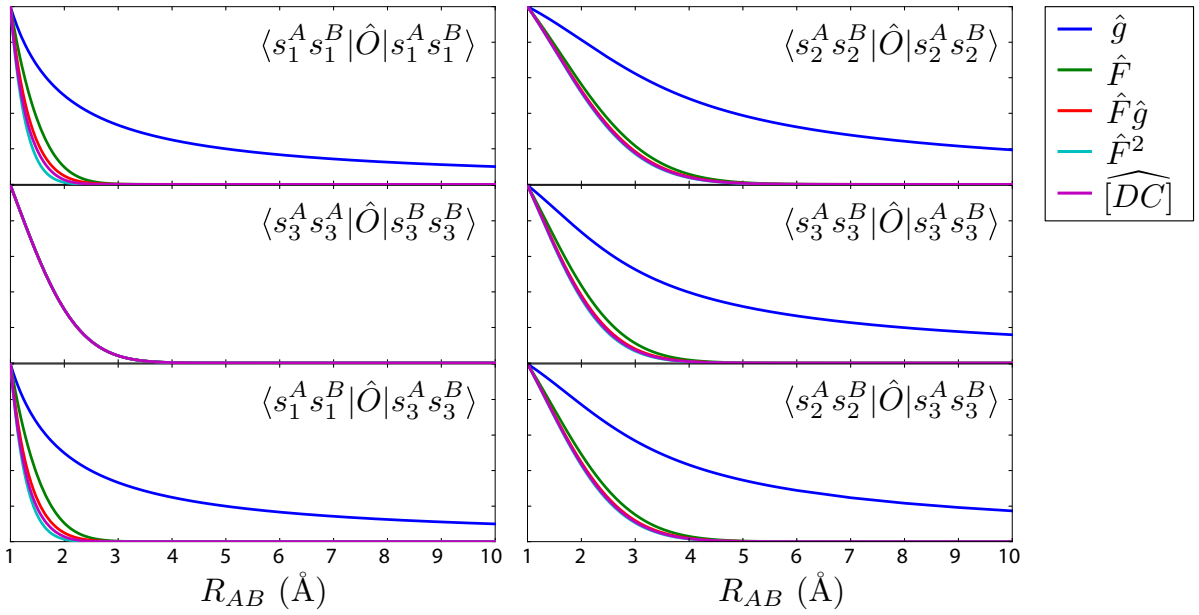

Figure 5.1: Representative two electron integral magnitudes of Argon dimer at various internuclear separations R_{AB} for the five two electron operators (represented generically as $\hat{O}$) relevant to this research. The magnitudes of all the integrals are normalized to the magnitude of the electron repulsion integral ($\hat{O} = \hat{g}$) at 1 Å to better compare the rates of decay (and since they are roughly the same order of magnitude to begin with). Functional forms of the Gaussian basis functions s_1, s_2, and s_3 (from the cc-pVDZ-F12[258] and cc-pVDZ-F12/OPTRI[259] basis sets) are given on the right side of the figure; superscripts denote the atom center A or B that the function is centered on.

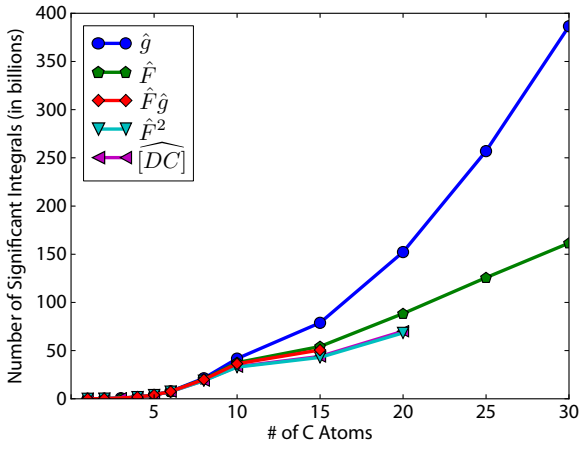

Figure 5.2: The number of significant integrals (magnitude larger than 10^{-8}) for the various two electron operators relevant to the present research for increasingly large linear alkanes (C_nH_{2n+2}) using the cc-pVDZ-F12[258] basis set.

5.5.1 F12 Integrals

It has previously been established in the literature[5,366] that the magnitude of the F12 integral for a given quartet $\{\mu, \nu, \varrho, \sigma\}$ decreases more rapidly than the electron repulsion integral (ERI) for the same quartet. We demonstrate this for several quartets in computations of Ar dimer in Figure 5.1. This is not surprising, given the exponential fundamental of the F12 integrals compared to the inverse linear fundamental of the ERIs. In Figure 5.2, we plot the number of significant integrals of each of the relevant types for increasingly large alkane chains. Given the success ERI screening has experienced in the literature,[108,109,112,339,340] we expect that similar screening techniques could be developed for each of the F12 fundamentals.

5.5.2 Screening Approximations

Utilizing Projector Sparsity

First, we point out that along with occupied and virtual projectors $\mathcal{P}$ and $\mathcal{Q}$, the CABS projector $\mathcal{O}$ is also sparse, as shown empirically for the Ne dimer in Figure 5.3. This sparsity follows from the sparsity of the overlap tensor (and hence its inverse), as well as the occupied and virtual projectors. One could further screen the two electron integrals in the contractions over the CABS space by only computing the two electron integrals that have a large enough contribution from the projection matrices *and* a large enough estimate from whatever two electron integral screening technique is used. This is not a new concept; the use of density matrix screening in linear scaling self-consistent field computations, for instance, has met with substantial success in the literature.[350,367,368] As a concrete example, consider the second term of the V intermediate, $-F_{\varrho\sigma,\zeta'\eta}\mathcal{O}^{\zeta'\lambda'}\mathcal{P}^{\eta\delta}g_{\mu\nu,\lambda'\delta}$. The most reasonable implementation of a linear scaling version of our method involves considering tensors as collections of blocks of, say, shells of orbitals or all the orbitals on a given atomic center. The most efficient approach would involve a hierarchy several layers deep of such blocks. For the sake of dis-

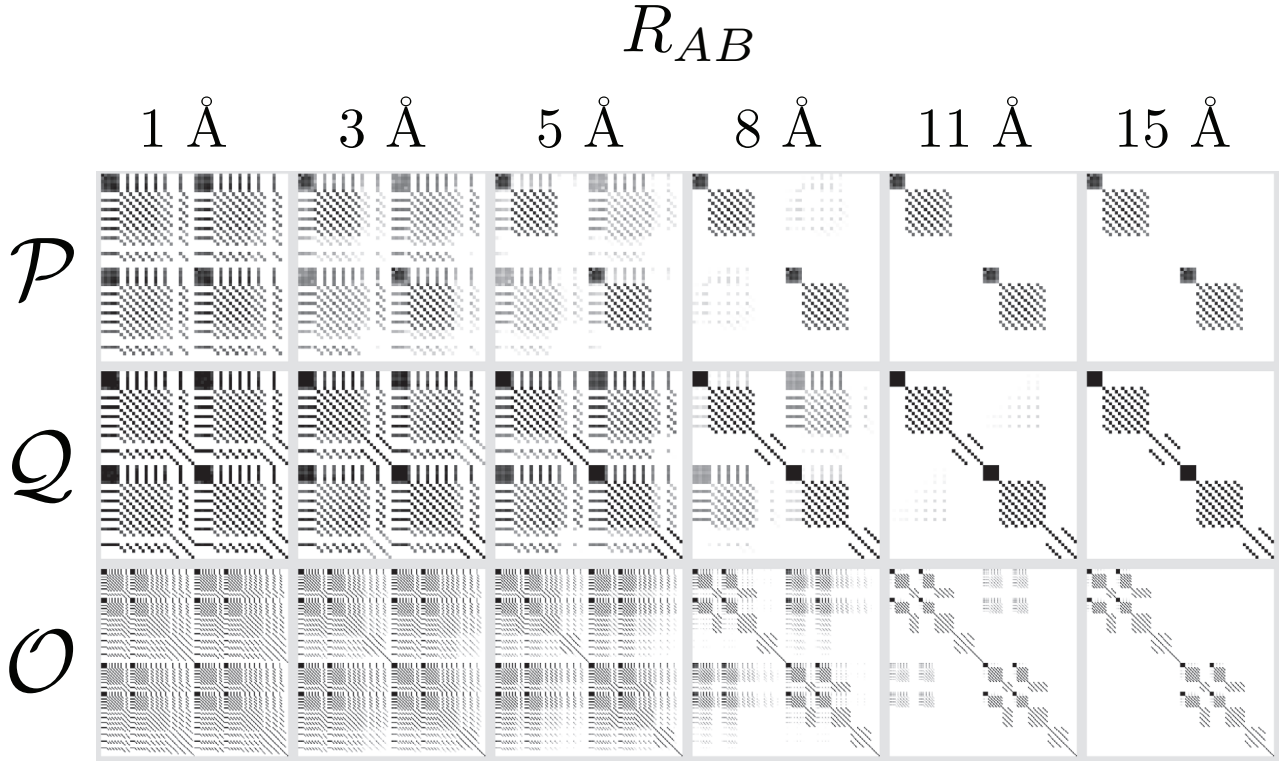

Figure 5.3: Snapshots of the various density-like projectors for Ne dimer at increasing internuclear separation R_{AB} with the cc-pVDZ-F12 + cc-pVDZ-F12/OPTRI[258,259] basis set. The color scale is logarithmic, with 10^{-8} represented in white and 1 represented in black. The indices in $\mathcal{P}$ (from equation (5.42)) and $\mathcal{Q}$ (from equation (5.43)) only span the orbital basis set; the indices in $\mathcal{O}$ (defined in equation (5.52)) span the full RI space. In all three projectors, the indices are grouped by atom center.

cussion, consider a block of indices defined by the notation $\tilde{\xi} \subseteq \{\xi\}$, where ξ is some index in the term under consideration (to be explicit, in our example $\xi \in \{\varrho, \sigma, \zeta', \eta, \lambda', \delta, \mu, \nu\}$). We first obtain estimates $\aleph^F$ for the elements of the integrals in the block $F_{\tilde{\varrho}\tilde{\sigma},\tilde{\zeta}'\tilde{\eta}}$. For instance, if Schwarz screening is used, we have $\aleph^F_{\varrho\sigma,\zeta'\eta} = (F_{\varrho\zeta',\varrho\zeta'}F_{\sigma\eta,\sigma\eta})^{1/2}$ (where repeated indices do *not* indicate summation). Non-rigorous (but effective) distance-based screening techniques which take advantage of the short-range F12 kernels have been developed previously,[58] and these techniques could be made rigorous by analogy to existing distance-based ERI screening techniques.[108,112] For each block, we store a maximum estimate $\tilde{\aleph}^F_{\tilde{\varrho}\tilde{\sigma},\tilde{\zeta}'\tilde{\eta}}$ such that for all $\varrho \in \tilde{\varrho}$, $\sigma \in \tilde{\sigma}$, $\zeta' \in \tilde{\zeta}'$, and $\eta \in \tilde{\eta}$, $\tilde{\aleph}^F_{\tilde{\varrho}\tilde{\sigma},\tilde{\zeta}'\tilde{\eta}} \geq |F_{\varrho\sigma,\zeta'\eta}|$. Similarly, we can store a maximum estimate for a block of g, $\tilde{\aleph}^g_{\tilde{\mu}\tilde{\nu},\tilde{\lambda}'\tilde{\delta}}$. We can also store block-wise maxima for $\mathcal{O}^{\tilde{\zeta}'\tilde{\lambda}'}$ and $\mathcal{P}^{\tilde{\eta}\tilde{\delta}}$, which we will denote $\tilde{\beth}^{\mathcal{O}}_{\tilde{\zeta}'\tilde{\lambda}'}$ and $\tilde{\beth}^{\mathcal{P}}_{\tilde{\eta}\tilde{\delta}}$, respectively. We may then rigorously avoid the computation of the integral blocks $F_{\tilde{\varrho}\tilde{\sigma},\tilde{\zeta}'\tilde{\eta}}$ and $g_{\tilde{\mu}\tilde{\nu},\tilde{\lambda}'\tilde{\delta}}$ if

$$|\tilde{\zeta}'||\tilde{\eta}|\tilde{\aleph}^F_{\tilde{\varrho}\tilde{\sigma},\tilde{\zeta}'\tilde{\eta}}\tilde{\beth}^{\mathcal{O}}_{\tilde{\zeta}'\tilde{\lambda}'}\tilde{\beth}^{\mathcal{P}}_{\tilde{\eta}\tilde{\delta}}\tilde{\aleph}^g_{\tilde{\mu}\tilde{\nu},\tilde{\lambda}'\tilde{\delta}}|\tilde{\lambda}'||\tilde{\delta}| < \epsilon \tag{5.100}$$

where repeated indices do *not* indicate summation in the above expression, $|\tilde{\xi}|$ indicates the size of the set $\tilde{\xi}$, and ϵ is some threshold set by the user as a control of the error.** Further screening of this individual term could be performed by screening out its direct contribution to the energy, i.e., including the two density matrix projectors in equation (5.59) in this discussion. This whole procedure leads to a massive scaling in the number of index blocks, but with a careful, hierarchical approach this number need not scale with the size of the system. Moreover, the index blocks screened over need not be from the same level in the blocking hierarchy. For instance, in the above example, if $\tilde{\lambda}'$ and $\tilde{\delta}$ span the entirety of the index spaces $\{\lambda'\}$ and $\{\delta\}$, respectively, and the relation still holds, then no sub-blocks

**Of course, the inclusion of the orders of the index sets in the above expression substantially loosens the tightness of the upper bound in the above expression and ignores substantial error cancellation. Empirical tests could be conducted to show that some much smaller scale factor is sufficient; we include them here for the sake of completeness and rigor.

of $g_{\tilde{\mu}\tilde{\nu},\tilde{\lambda}'\tilde{\delta}}$ need be investigated at the next level down for that term, and the scaling in the number of blocks is substantially decreased. The efficiency of this technique could be improved further by blocking tight and diffuse functions separately.

Direct Evaluation of Three-Electron Integrals

Of some concern is the diffuseness of the basis sets used for F12 computations, particularly for the RI portion. The diffuseness of RI basis sets in linear scaling methods is a well known problem in the literature, and for density fitting of conventional methods this problem has largely been solved.[337] However, the above discussion leads to another possibility for reducing or eliminating the problem of the diffuseness of RI basis sets. In the projected basis we use for AO-MP2-F12, the number of significant three electron integrals should not increase any more quickly than the number of two electron integrals. Thus, the direct evaluation of three electron integrals could partially or completely circumvent the need for a resolution of the identity over a basis of diffuse orbitals. Indeed, Wind and coworkers[50,369] have already investigated this possibility in the context of MO basis linear MP2-R12. The expansion of their work to F12 methods should be possible. However, the use of projection matrices for additional *a priori* screening makes their ideas more viable than ever before. Consider, for instance, the three electron integral $\langle xym|\hat{g}_{12}\hat{F}_{23}|mji\rangle$, which contributes to the V intermediate. The contribution to the energy from this term via the first term of equation (5.25) is (for sake of discussion, we will only examine the contribution via this term, since the others are similar):

$$\tfrac{5}{8}\sum_{ijm}\langle ijm|\hat{g}_{12}\hat{F}_{23}|mji\rangle \tag{5.101}$$

Recast in the AO basis, this term is

$$\frac{5}{8} \sum_{\mu\nu\varrho\sigma\zeta\lambda} \mathcal{P}^{\mu\varrho}\mathcal{P}^{\nu\sigma}\mathcal{P}^{\zeta\lambda} \langle \mu\nu\zeta|\hat{g}_{12}\hat{F}_{23}|\lambda\sigma\varrho\rangle \tag{5.102}$$

However, using the discussion above, the (expensive) three electron integrals would only need to be computed for a given block if

$$|\tilde{\mu}||\tilde{\nu}||\tilde{\zeta}|\tilde{\mathbf{\Delta}}^{\mathcal{P}}_{\tilde{\mu}\tilde{\varrho}}\tilde{\mathbf{\Delta}}^{\mathcal{P}}_{\tilde{\nu}\tilde{\sigma}}\tilde{\mathbf{\Delta}}^{\mathcal{P}}_{\tilde{\zeta}\tilde{\lambda}}\tilde{\aleph}^{g_{12}F_{23}}_{\tilde{\mu}\tilde{\nu}\tilde{\zeta},\tilde{\lambda}\tilde{\sigma}\tilde{\varrho}}|\tilde{\varrho}||\tilde{\sigma}||\tilde{\lambda}| > \epsilon \tag{5.103}$$

where again summation over repeated indices is *not* implied. In general, this should only be the case if the blocks $\tilde{\mu}$ and $\tilde{\varrho}$ are on atoms or clusters close enough to each other, the blocks $\tilde{\nu}$ and $\tilde{\sigma}$ are close enough to each other, *and* the blocks $\tilde{\zeta}$ and $\tilde{\lambda}$ are close enough to each other. This condition should be less likely than in the two particle case. Furthermore, the three electron operator $\hat{g}_{12}\hat{F}_{23}$ should (intuitively) be more local than either of the two electron operators taken separately. There is, of course, the matter of determining $\tilde{\aleph}^{g_{12}F_{23}}_{\tilde{\mu}\tilde{\nu}\tilde{\zeta},\tilde{\lambda}\tilde{\sigma}\tilde{\varrho}}$ efficiently, but such problems should have relatively similar solutions to the two electron case.

F12 Basis Sets

The increased diffuseness of basis sets used for F12 is not unique to the RI basis; the primary basis sets used in F12 computations are also more diffuse than those used in conventional methods. The seminal 1985 work of Kutzelnigg[42] demonstrated that the primary benefit of explicitly correlated terms is in eliminating the need for high angular momentum functions. F12 basis sets thus include extra low angular momentum functions in order to maintain basis set balance, thus maximizing the accuracy for a given $\ell_{\max}$. The subject of F12 basis set design has been the topic of substantial research in the literature.[258,259,370] A discussion of

whether existing basis sets present an optimal trade-off between accuracy and efficiency in the context of AO-MP2-F12 should be pursued as the method is further developed.

5.6 Conclusions

In conclusion, we have provided a recasting in the AO basis of the MP2-F12 method within two widely-used approximations of Kedžuch, Milko, and Noga.[52] A prototype code has been written that implements these equations and demonstrates that they yield exactly the same result as the MO basis version of the method, to machine precision in the case of the F12 portion of the energy. We have addressed many of the anticipated difficulties with an efficient implementation of our method, leaving a few potential issues which need substantial expounding as the method develops. Of these issues, the two most obvious are (1) the discussion of efficient techniques for screening ("estimating") the two and potentially three electron integrals involved in our method, and (2) investigation of the sparsity and decay properties of the density-like projectors. It is the hope of the authors that our presentation of these equations will spark further work on an efficient implementation and further discussion of the use of AO basis techniques for a wide variety of computational chemistry problems.

5.7 Acknowledgements

This research was supported by the National Science Foundation, Grant No. CHE-1054286. The authors would like to thank Professors E. F. Valeev and C. Ochsenfeld for their valuable insight and helpful discussion.

Chapter 6

Concluding Remarks

Since the first computations on helium in the 1920s, electron correlation has been at the heart of *ab initio* quantum chemistry. As the availability of computational resources continues to increase, the need to examine methods that push the boundaries of computational accuracy and molecular system size becomes more poignant. The ideas presented herein loosely represent a microcosm of several recent trends in molecular quantum mechanics research — the realization that many DFT methods fail even qualitatively for a number of systems of chemical interest; the use of high-accuracy wavefunction methods to interpret, correct, and guide experiment through the accurate and reliable determination of spectroscopic parameters; the increased use of explicitly correlated wavefunctions to handle BSIE and study larger systems quantitatively with errors at or below chemical accuracy; improvements in auxiliary methods not concerned directly with the solution to the electronic Schrödinger equation but still crucial for the interaction between theory and experiment; and the derivation and use of new local correlation methods that have low order scaling with system size but are nonetheless mathematically rigorous. If the heart of quantum chemistry is the many-body electron correlation problem, the soul is the intricate dance between theory and experiment, between rigor and practicality, between elegance and feasibility. This dance has been played out here in many forms. In chapter 2, this storyline was played out in the demonstration that a higher than usual level of rigor is required for a particular system and, by analogical extension, a particular class of systems — noncovalent aromatic–radical interactions. Chapter 3 showed the interplay between theory and experiment by providing computed spectroscopic parameters for several experimentally unstudied systems. Here also the reverse aspect of this interaction was played out in the reassignment of several peaks from previous experimental spectra. Chapter 4 presented elegant formulas that push the bounds of implementational feasibility while demonstrating the constant push, catalyzed by new experimental techniques, to develop correspondingly accurate theoretical methods. Finally, chapter 5 presented a new theoretical method applicable to large molecules that walks the fine line between rigor and

practicality in an attempt to optimize the latter without sacrificing the former. The balance point between rigor and practicality is an ever-moving fulcrum, spurred onward by the constant increase in available computing power. The challenge quantum chemists face is to position themselves in research areas that have the flexibility to follow this movement. Explicitly correlated AO basis methods are ideally suited in this regard, and the potential for the research presented herein to be extended and expounded to a point of prominence in *ab initio* quantum chemistry is exciting.

Chapter 7

Bibliography

Bibliography

[1] D. P. Tew, W. Klopper, and T. Helgaker, J. Comput. Chem. **28**, 1307 (2007).

[2] W. Kutzelnigg, G. Del Re, and G. Berthier, Phys. Rev. **172**, 49 (1968).

[3] J. J. Sakurai, *Modern Quantum Mechanics*, Addison-Wesley Pub. Co, Reading, Mass, 1994.

[4] T. Helgaker, P. Jørgensen, and J. Olsen, *Molecular Electronic-Structure Theory*, Wiley, Chichester New York, 2000.

[5] C. Hättig, W. Klopper, A. Köhn, and D. P. Tew, Chem. Rev. **112**, 4 (2012).

[6] M. Born and R. Oppenheimer, Ann. Phys. **389**, 457 (1927).

[7] W. Pauli, Z. Physik **36**, 336 (1926).

[8] E. Schrödinger, Phys. Rev. **28**, 1049 (1926).

[9] J. C. Slater, Phys. Rev. **31**, 333 (1928).

[10] E. A. Hylleraas, Z. Physik **54**, 347 (1929).

[11] E. A. Hylleraas, Z. Physik **65**, 209 (1930).

[12] J. Neumann, *Mathematical foundations of quantum mechanics*, Princeton University Press, Princeton N.J, 1955.

[13] Ref. 4, p. 221.

[14] Ref. 3, pp. 454–455.

[15] J. C. Slater, Phys. Rev. **34**, 1293 (1929).

[16] Ref. 4, pp. 112–115.

[17] P. Dirac, Mathematical Proceedings of the Cambridge Philosophical Society **35**, 416 (1939).

[18] C. Roothaan, Rev. Mod. Phys. **23**, 69 (1951).

[19] Ref. 4, p. 433.

[20] J. A. Miller and S. J. Klippenstein, Inorg. Chem. **33**, 654 (2001).

[21] S. Canneaux et al., J. Phys. Chem. A **112**, 6045 (2008).

[22] A. Szabo and N. S. Ostlund, *Modern quantum chemistry : introduction to advanced electronic structure theory*, Macmillan, New York, 1982.

[23] W. J. Hehre, J. Chem. Phys. **56**, 2257 (1972).

[24] P. C. Hariharan and J. A. Pople, Theor. Chim. Acta **28**, 213 (1973).

[25] T. H. Dunning, J. Chem. Phys. **90**, 1007 (1989).

[26] Ref. 4, p. 183.

[27] P. N. Ascik, J. J. Wilke, A. C. Simmonett, Y. Yamaguchi, and H. F. Schaefer, J. Chem. Phys. **134**, 074110 (2011).

[28] J. J. Wilke, W. D. Allen, and H. F. Schaefer, J. Chem. Phys. **128**, 074308 (2008).

[29] W. Kohn, *Nobel Lectures in Chemistry, 1996-2000*, World Scientific, River Edge, N.J, 2003.

[30] I. Shavitt and R. J. Bartlett, *Many-body methods in chemistry and physics : MBPT and coupled-cluster theory*, Cambridge University Press, Cambridge New York, 2009.

[31] W. D. Allen, A. L. L. East, and A. G. Császár, *Structures and Conformations of Non-Rigid Molecules*, pages 343–374, Kluwer, Dordrecht, 1993.

[32] W. Kutzelnigg and J. D. Morgan, J. Chem. Phys. **96**, 4484 (1992).

[33] T. Kato, Comm. Pure Appl. Math. **10**, 151 (1957).

[34] R. T. Pack, J. Chem. Phys. **45**, 556 (1966).

[35] D. P. Tew, J. Chem. Phys. **129**, 014104 (2008).

[36] T. Helgaker and W. Klopper, Theor. Chim. Acta **103**, 180 (2000).

[37] Y. I. Kurokawa, H. Nakashima, and H. Nakatsuji, Phys. Chem. Chem. Phys. **10**, 4486 (2008).

[38] M. Puchalski and K. Pachucki, Phys. Rev. A **73**, 022503 (2006).

[39] M. Puchalski, D. Kędziera, and K. Pachucki, Phys. Rev. A **80**, 032521 (2009).

[40] G. Büsse, H. Kleindienst, and A. Lüchow, Int. J. Quantum Chem. **66**, 241 (1998).

[41] W. Klopper and W. Kutzelnigg, Chem. Phys. Lett. **134**, 17 (1987).

[42] W. Kutzelnigg, Theor. Chim. Acta **68**, 445 (1985).

[43] W. Kutzelnigg and W. Klopper, J. Chem. Phys. **94**, 1985 (1991).

[44] W. Klopper and W. Kutzelnigg, J. Chem. Phys. **94**, 2020 (1991).

[45] V. Termath, W. Klopper, and W. Kutzelnigg, J. Chem. Phys. **94**, 2002 (1991).

[46] W. Klopper and C. C. M. Samson, J. Chem. Phys. **116**, 6397 (2002).

[47] S. Ten-No, Chem. Phys. Lett. **398**, 56 (2004).

[48] D. P. Tew and W. Klopper, J. Chem. Phys. **123**, 074101 (2005).

[49] H.-J. Werner, T. B. Adler, and F. R. Manby, J. Chem. Phys. **126**, 164102 (2007).

[50] P. Wind, W. Klopper, and T. Helgaker, Theor. Chim. Acta **107**, 173 (2002).

[51] S. Ten-No, J. Chem. Phys. **121**, 117 (2004).

[52] S. Kedžuch, M. Milko, and J. Noga, Int. J. Quantum Chem. **105**, 929 (2005).

[53] F. R. Manby, H.-J. Werner, T. B. Adler, and A. J. May, J. Chem. Phys. **124**, 94103 (2006).

[54] J. Noga, S. Kedžuch, and J. Šimunek, J. Chem. Phys. **127**, 034106 (2007).

[55] E. Kordel, C. Villani, and W. Klopper, Mol. Phys. **105**, 2565 (2007).

[56] G. Knizia and H.-J. Werner, J. Chem. Phys. **128**, 154103 (2008).

[57] J. J. Wilke and H. F. Schaefer, J. Chem. Phys. **131**, 244116 (2009).

[58] T. B. Adler, H.-J. Werner, and F. R. Manby, J. Chem. Phys. **130**, 054106 (2009).

[59] D. Bokhan, S. Bernadotte, and S. Ten-No, J. Chem. Phys. **131**, 084105 (2009).

[60] S. Höfener and W. Klopper, Mol. Phys. **108**, 1783 (2010).

[61] T. Shiozaki and H.-J. Werner, J. Chem. Phys. **133**, 141103 (2010).

[62] J. Yang, Y. Kurashige, F. R. Manby, and G. K. L. Chan, J. Chem. Phys. **134**, 044123 (2011).

[63] D. P. Tew, B. Helmich, and C. Hättig, J. Chem. Phys. **135**, 074107 (2011).

[64] C. Hättig, D. P. Tew, and B. Helmich, J. Chem. Phys. **136**, 204105 (2012).

[65] D. Bokhan and D. N. Trubnikov, J. Chem. Phys. **136**, 204110 (2012).

[66] E. F. Valeev, Phys. Chem. Chem. Phys. **10**, 106 (2007).

[67] T. Shiozaki, M. Kamiya, S. Hirata, and E. F. Valeev, J. Chem. Phys. **129**, 071101 (2008).

[68] T. Shiozaki, M. Kamiya, S. Hirata, and E. F. Valeev, Phys. Chem. Chem. Phys. **10**, 3358 (2008).

[69] A. Köhn, G. W. Richings, and D. P. Tew, J. Chem. Phys. **129**, 201103 (2008).

[70] M. Torheyden and E. F. Valeev, Phys. Chem. Chem. Phys. **10**, 3410 (2008).

[71] D. P. Tew, W. Klopper, and C. Hättig, Chem. Phys. Lett. **452**, 326 (2008).

[72] T. B. Adler and H.-J. Werner, J. Chem. Phys. **130**, 241101 (2009).

[73] A. Köhn and D. P. Tew, J. Chem. Phys. **133**, 174117 (2010).

[74] J. J. Wilke and H. F. Schaefer, J. Chem. Theory Comput. **7**, 2416 (2011).

[75] H.-J. Werner, G. Knizia, and F. R. Manby, Mol. Phys. **109**, 407 (2011).

[76] T. B. Adler and H.-J. Werner, J. Chem. Phys. **135**, 144117 (2011).

[77] D. Bokhan, S. Ten-No, and J. Noga, Phys. Chem. Chem. Phys. **10**, 3320 (2008).

[78] A. Köhn, J. Chem. Phys. **133**, 174118 (2010).

[79] M. S. Marshall and C. D. Sherrill, J. Chem. Theory Comput. **7**, 3978 (2011).

[80] G. Knizia, T. B. Adler, and H.-J. Werner, J. Chem. Phys. **130**, 054104 (2009).

[81] A. Köhn, J. Chem. Phys. **130**, 131101 (2009).

[82] T. Shiozaki, M. Kamiya, S. Hirata, and E. F. Valeev, J. Chem. Phys. **130**, 054101 (2009).

[83] E. F. Valeev and T. D. Crawford, J. Chem. Phys. **128**, 244113 (2008).

[84] T. B. Adler, G. Knizia, and H.-J. Werner, J. Chem. Phys. **127**, 221106 (2007).

[85] T. Shiozaki and H.-J. Werner, J. Chem. Phys. **134**, 184104 (2011).

[86] T. Shiozaki, G. Knizia, and H.-J. Werner, J. Chem. Phys. **134**, 034113 (2011).

[87] G. Rauhut, G. Knizia, and H.-J. Werner, J. Chem. Phys. **130**, 054105 (2009).

[88] P. Botschwina, R. Oswald, and G. Rauhut, Phys. Chem. Chem. Phys. **13**, 7921 (2011).

[89] P. Halvick, T. Stoecklin, F. Lique, and M. Hochlaf, J. Chem. Phys. **135**, 044312 (2011).

[90] A. Yachmenev, S. N. Yurchenko, T. Ribeyre, and W. Thiel, J. Chem. Phys. **135**, 074302 (2011).

[91] D. Lauvergnat, M. L. Senent, L. Jutier, and M. Hochlaf, J. Chem. Phys. **135**, 074301 (2011).

[92] V. M. Rodriguez-Betancourtt, V. M. Quezada-Navarro, M. Neff, and G. Rauhut, Chem. Phys. **387**, 1 (2011).

[93] D. S. Hollman and H. F. Schaefer, J. Chem. Phys. **136**, 084302 (2012).

[94] P. Botschwina and R. Oswald, J. Phys. Chem. A **114**, 9782 (2010).

[95] K. Kahn, B. Kirtman, J. Noga, and S. Ten-No, J. Chem. Phys. **133**, 074106 (2010).

[96] P. Pulay, Chem. Phys. Lett. **100**, 151 (1983).

[97] S. Saebo and P. Pulay, Chem. Phys. Lett. **113**, 13 (1985).

[98] P. Pulay and S. Saeb, Theor. Chim. Acta **69**, 357 (1986).

[99] S. Saebo and P. Pulay, J. Chem. Phys. **88**, 1884 (1988).

[100] S. Saebo and P. Pulay, J. Chem. Phys. **86**, 914 (1987).

[101] S. F. Boys, *Quantum Theory of Atoms, Molecules and the Solid State*, pages 253–280, Academic, New York, 1968.

[102] C. Edmiston and K. Ruedenberg, J. Chem. Phys. **43**, S97 (1965).

[103] J. Pipek and P. G. Mezey, J. Chem. Phys. **90**, 4916 (1989).

[104] F. Neese, F. Wennmohs, and A. Hansen, J. Chem. Phys. **130**, 114108 (2009).

[105] M. Schütz, J. Chem. Phys. **113**, 9986 (2000).

[106] M. Schütz and H.-J. Werner, J. Chem. Phys. **114**, 661 (2001).

[107] M. Schütz, J. Chem. Phys. **116**, 8772 (2002).

[108] D. S. Lambrecht and C. Ochsenfeld, J. Chem. Phys. **123**, 184101 (2005).

[109] D. S. Lambrecht, B. Doser, and C. Ochsenfeld, J. Chem. Phys. **123**, 184102 (2005).

[110] C. Ochsenfeld and J. Kussmann, Reviews in ... (2007).

[111] B. Doser, D. S. Lambrecht, J. Kussmann, and C. Ochsenfeld, J. Chem. Phys. **130**, 064107 (2009).

[112] S. A. Maurer, D. S. Lambrecht, D. Flaig, and C. Ochsenfeld, J. Chem. Phys. **136**, 144107 (2012).

[113] S. A. Maurer, D. S. Lambrecht, J. Kussmann, and C. Ochsenfeld, J. Chem. Phys. **138**, 014101 (2013).

[114] K. B. Hewett, L. C. Anderson, M. P. Rosynek, and J. H. Lunsford, J. Am. Chem. Soc. **118**, 6992 (1996).

[115] C. M. Marks and L. D. Schmidt, Chem. Phys. Lett. **178**, 358 (1991).

[116] Z. S. Li, C. Hu, J. Zetterberg, M. Linvin, and M. Alden, J. Chem. Phys. **127**, 084310 (2007).

[117] C. L. Darling and H. B. Schlegel, J. Phys. Chem. **98**, 8910 (1994).

[118] S. Y. Lee, S. R. Turns, and R. J. Santoro, Combust. Flame **156**, 2264 (2009).

[119] E. R. Stadtman, Science **257**, 1220 (1992).

[120] M. Suthanthiran et al., Nature **307**, 276 (1984).

[121] C. Richter, J. W. Park, and B. N. Ames, Proc. Natl. Acad. Sci. USA **85**, 6465 (1988).

[122] D. C. Malins, N. L. Polissar, and S. J. Gunselman, Proc. Natl. Acad. Sci. USA **93**, 2557 (1996).

[123] B. Halliwell and J. Gutteridge, *Free Radicals in Biology and Medicine*, Oxford University Press Oxford, 2007.

[124] C. von Sonntag, *The Chemical Basis of Radiation Biology*, Taylor & Francis London, 1987.

[125] F. Rohrer and H. Berresheim, Nature **442**, 184 (2006).

[126] J. Lelieveld, Nature **466**, 925.

[127] W. H. Brune, Science **256**, 1154 (1992).

[128] R. G. Prinn et al., Science **292**, 1882 (2001).

[129] S. A. Montzka et al., Science **288**, 500 (2000).

[130] B. J. Finlayson-Pitts and J. N. Pitts, Science **276**, 1045 (1997).

[131] G. Ghigo and G. Tonachini, J. Am. Chem. Soc. **120**, 6753 (1998).

[132] T. Lay, J. Bozzelli, and J. Seinfeld, J. Phys. Chem. **100**, 6543 (1996).

[133] D. R. Blake and F. S. Rowland, Science **269**, 953 (1995).

[134] K. Mopper and X. L. Zhou, Science **250**, 661 (1990).

[135] W. Cooper, R. Curry, and K. O'Shea, *Environmental Applications of Ionizing Radiation*, Wiley-Interscience, 1998.

[136] J. F. Ogilvie, Nature **204**, 572 (1964).

[137] G. L. Vaghjiani and A. R. Ravishankara, Nature **350**, 406 (1991).

[138] S. Mitroka, S. Zimmeck, D. Troya, and J. M. Tanko, J. Am. Chem. Soc. **132**, 2907 (2010).

[139] S. Li, J. Matthews, and A. Sinha, Science **319**, 1657 (2008).

[140] F. A. Villamena, C. M. Hadad, and J. L. Zweier, J. Am. Chem. Soc. **126**, 1816 (2004).

[141] S. Jorgensen, V. F. Andersen, E. J. K. Nilsson, O. J. Nielsen, and M. S. Johnson, Chem. Phys. Lett. **490**, 116 (2010).

[142] P. Vassilev, M. J. Louwerse, and E.-J. Baerends, Chem. Phys. Lett. **398**, 212 (2004).

[143] C. F. Williams, S. K. Pogrebnya, and D. C. Clary, J. Chem. Phys. **126**, 154321 (2007).

[144] A. T. Benjelloun, A. Daoudi, and H. Chermette, J. Chem. Phys. **121**, 7207 (2004).

[145] B. Sclavi, M. Sullivan, M. R. Chance, M. Brenowitz, and S. A. Woodson, Science **279**, 1940 (1998).

[146] G. M. Heilek and H. F. Noller, Science **272**, 1659 (1996).

[147] J. Cadet et al., Mutat. Res.-Fund. Mol. M. **424**, 9 (1999).

[148] L. Flowers, S. T. Ohnishi, and T. M. Penning, Biochemistry **36**, 8640 (1997).

[149] M. M. Huycke, V. Abrams, and D. R. Moore, Carcinogenesis **23**, 529 (2002).

[150] R. M. Wright, J. L. McManaman, and J. E. Repine, Free Radical Bio. Med. **26**, 348 (1999).

[151] P. T. A. Reilly, R. A. Gieray, W. B. Whitten, and J. M. Ramsey, J. Am. Chem. Soc. **122**, 11596 (2000).

[152] K. Siegmann and K. Sattler, J. Chem. Phys. **112**, 698 (2000).

[153] B. Saha, S. Irle, and K. Morokuma, J. Chem. Phys. **132**, 224303 (2010).

[154] C. Shen et al., J. Hazard. Mater. **179**, 197 (2010).

[155] B. Shukla and M. Koshi, Phys. Chem. Chem. Phys. **12**, 2427 (2010).

[156] A. Violi and A. Venkatnathan, J. Chem. Phys. **125**, 054302 (2006).

[157] D. Baulch et al., J. Phys. Chem. Ref. Data **21**, 411 (1992).

[158] N. K. Tran, S. M. Steinberg, and B. J. Johnson, Atmos Environ **34**, 1845 (2000).

[159] A. Mardyukov, E. Sanchez-Garcia, R. Crespo-Otero, and W. Sander, Angew. Chem. Int. Edit. **48**, 4804 (2009).

[160] V. V. Lobanov, N. A. Vysotskaya, E. A. Rabovskaya, and V. I. Bogillo, Theor. Exp. Chem. **22**, 17 (1986).

[161] B. V. Cheney, J. Mol. Struc. **364**, 219 (1996).

[162] I. V. Tokmakov and M. C. Lin, J. Phys. Chem. A **106**, 11309 (2002).

[163] C. Barckholtz, T. Barckholtz, and C. M. Hadad, J. Phys. Chem. A **105**, 140 (2001).

[164] C. C. Chen, J. Bozzelli, and J. T. Farrell, J. Phys. Chem. A **108**, 4632 (2004).

[165] M. P. DeMatteo et al., J. Am. Chem. Soc. **127**, 7094 (2005).

[166] T. Seta, M. Nakajima, and A. Miyoshi, J. Phys. Chem. A **110**, 5081 (2006).

[167] R. Knispel, R. Koch, M. Siese, and C. Zetzsch, Ber. Bunsen. Phys. Chem. **94**, 1375 (1990).

[168] R. Perry, R. Atkinson, and J. N. Pitts Jr, J. Phys. Chem. **81**, 296 (1977).

[169] S. Madronich and W. Felder, J. Phys. Chem. **89**, 3556 (1985).

[170] F. Tully et al., J. Phys. Chem. **85**, 2262 (1981).

[171] K. Lorenz and R. Zellner, Ber. Bunsen. Phys. Chem. **87**, 629 (1983).

[172] T. J. Wallington, D. M. Neuman, and M. J. Kurylo, Inorg. Chem. **19**, 725 (1987).

[173] F. Witte, E. Urbanik, and C. Zetzsch, J. Phys. Chem. **90**, 3251 (1986).

[174] S.-C. Lin, T.-C. Kuo, and Y.-P. Lee, J. Chem. Phys. **101**, 2098 (1994).

[175] Y. He, W. Mallard, and W. Tsang, J. Phys. Chem. **92**, 2196 (1988).

[176] T. Ohta and T. Ohyama, Bull. Chem. Soc. Jpn. **58**, 3029 (1985).

[177] J. Manion and R. Louw, J. Phys. Chem. **94**, 4127 (1990).

[178] A. Goumri, J. F. Pauwels, and P. Devolder, Can. J. Chem. **69**, 1057 (1991).

[179] H. F. Schaefer, J. Phys. Chem. **89**, 5336 (1985).

[180] M. W. Feyereisen, G. Fitzgerald, and A. Komornicki, Chem. Phys. Lett. **208**, 359 (1993).

[181] F. Weigend and M. Häser, Theor Chem Acc **97**, 331 (1997).

[182] R. A. DiStasio, R. P. Steele, Y. M. Rhee, Y. Shao, and M. Head-Gordon, J. Comput. Chem. **28**, 839 (2007).

[183] F. Weigend, M. Häser, H. Patzelt, and R. Ahlrichs, Chem. Phys. Lett. **294**, 143 (1998).

[184] K. Raghavachari, G. W. Trucks, J. A. Pople, and M. Head-Gordon, Chem. Phys. Lett. **157**, 479 (1989).

[185] P. J. Knowles, C. Hampel, and H.-J. Werner, J. Chem. Phys. **99**, 5219 (1993).

[186] J. D. Watts, J. Gauss, and R. J. Bartlett, J. Chem. Phys. **98**, 8718 (1993).

[187] J. F. Stanton, Chem. Phys. Lett. **281**, 130 (1997).

[188] X. Zhang et al., J. Chem. Phys. **126**, 044312 (2007).

[189] A. D. Becke, J. Chem. Phys. **98**, 1372 (1993).

[190] J.-D. Chai and M. Head-Gordon, J. Chem. Phys. **128**, 084106 (2008).

[191] J.-D. Chai and M. Head-Gordon, Phys. Chem. Chem. Phys. **10**, 6615 (2008).

[192] J.-D. Chai and M. Head-Gordon, Chem. Phys. Lett. **467**, 176 (2008).

[193] Y. Zhao and D. G. Truhlar, Accounts Chem. Res. **41**, 157 (2008).

[194] J. A. Pople, M. Head-Gordon, and K. Raghavachari, J. Chem. Phys. **87**, 5968 (1987).

[195] C. Møller and M. S. Plesset, Phys. Rev. **46**, 618 (1934).

[196] D. E. Woon and T. H. Dunning, J. Chem. Phys. **103**, 4572 (1995).

[197] C. C. J. Roothaan, Rev. Mod. Phys. **32**, 179 (1960).

[198] T. J. Lee and D. Jayatilaka, Chem. Phys. Lett. **201**, 1 (1993).

[199] M. Rittby and R. J. Bartlett, J. Phys. Chem. **92**, 3033 (1988).

[200] J. F. Stanton, J. Gauss, J. D. Watts, and R. J. Bartlett, J. Chem. Phys. **94**, 4334 (1991).

[201] C. Hampel, K. A. Peterson, and H.-J. Werner, Chem. Phys. Lett. **190**, 1 (1992).

[202] J. D. Watts, J. Gauss, and R. J. Bartlett, Chem. Phys. Lett. **200**, 1 (1992).

[203] D. Feller, J. Chem. Phys. **98**, 7059 (1993).

[204] T. Helgaker, W. Klopper, H. Koch, and J. Noga, J. Chem. Phys. **106**, 9639 (1997).

[205] Y. Shao et al., Phys. Chem. Chem. Phys. **8**, 3172 (2006).

[206] H.-J. Werner et al., Molpro, version 2009.1, a package of ab initio programs, 2009, see http://www.molpro.net.

[207] C. Janssen, E. Seidl, and M. Colvin, Object-oriented implementation of parallel ab initio programs, in *ACS Symposium Series, Parallel Computing in Computational Chemistry*, volume 592, pages 47–61, 1995.

[208] M. Kabelac, H. Valdes, E. C. Sherer, C. J. Cramer, and P. Hobza, Phys. Chem. Chem. Phys. **9**, 5000 (2007).

[209] K. P. Huber and G. Herzberg, *Molecular Spectra and Molecular Structure. IV. Constants of Diatomic Molecules*, Van Nostrand Reinhold Co., 1979.

[210] A. R. Hoy and P. R. Bunker, J. Mol. Spec. **74**, 1 (1979).

[211] G. Herzberg, *Electronic Spectra and Electronic Structure of Polyatomic Molecules*, Van Nostrand, 1966.

[212] P. R. Schreiner et al., Nature **453**, 906 (2008).

[213] J. A. Coxon, Can. J. Phys. **58**, 933 (1980).

[214] P. Soloveichik, B. A. O'Donnell, M. I. Lester, J. S. Francisco, and A. B. McCoy, J. Phys. Chem. A **114**, 1529 (2010).

[215] A. Engdahl and B. Nelander, J. Chem. Phys. **122**, 126101 (2005).

[216] A. Landera, A. M. Mebel, and R. I. Kaiser, Chem. Phys. Lett. **459**, 54 (2008).

[217] I. V. Tokmakov and M. C. Lin, Inorg. Chem. **33**, 633 (2001).

[218] G. Dixon-Lewis and A. Williams, Nature **196**, 1309 (1962).

[219] R. N. Dixon and B. F. Mason, Nature **197**, 1198 (1963).

[220] D. H. Liskow, H. F. Schaefer, and C. F. Bender, J. Am. Chem. Soc. **93**, 6734 (1971).

[221] W. A. Traub, D. G. Johnson, and K. V. Chance, Science **247**, 446 (1990).

[222] K. Suma, Y. Sumiyoshi, and Y. Endo, Science **308**, 1885 (2005).

[223] K. Suma, Y. Sumiyoshi, and Y. Endo, Science **311**, 1278 (2006).

[224] Z. Sun et al., J. Am. Chem. Soc. **130**, 14962 (2008).

[225] A. Hofzumahaus et al., Science **324**, 1702 (2009).

[226] E. Ohara, J. Chem. Soc. Jpn. **61**, 569 (1940).

[227] J. M. Anglada, S. Olivella, and A. Solé, J. Phys. Chem. A **111**, 1695 (2007).

[228] S. W. Benson, J. Chem. Phys. **33**, 306 (1960).

[229] J. L. Arnau and P. A. Giguère, J. Chem. Phys. **60**, 270 (1974).

[230] M. Diem, T.-L. Tso, and E. K. C. Lee, J. Chem. Phys. **76**, 6452 (1982).

[231] D. I. Mendeleev, (1895).

[232] A. Engdahl and B. Nelander, Science **295**, 482 (2002).

[233] B. Plesničar, Acta Chim. Slov. **52**, 1 (2005).

[234] K. Suma, Y. Sumiyoshi, and Y. Endo, J. Am. Chem. Soc. **127**, 14998 (2005).

[235] P. A. Denis and F. R. Ornellas, J. Phys. Chem. A **113**, 499 (2009).

[236] E. L. Derro, C. Murray, T. D. Sechler, and M. I. Lester, J. Phys. Chem. A **111**, 11592 (2007).

[237] C. Murray, E. L. Derro, T. D. Sechler, and M. I. Lester, J. Phys. Chem. A **111**, 4727 (2007).

[238] C. Murray, E. L. Derro, T. D. Sechler, and M. I. Lester, Accounts Chem. Res. **42**, 419 (2009).

[239] T. M. Lesko, A. J. Colussi, and M. R. Hoffmann, J. Am. Chem. Soc. **126**, 4432 (2004).

[240] J. Lind, G. Merényi, E. Johansson, and T. Brinck, J. Phys. Chem. A **107**, 676 (2003).

[241] D. J. Mckay and J. S. Wright, J. Am. Chem. Soc. **120**, 1003 (1998).

[242] B. M. Gimarc and M. Zhao, J. Phys. Chem. **98**, 1596 (1994).

[243] M. Zhao and B. M. Gimarc, J. Phys. Chem. **97**, 4023 (1993).

[244] M. Martins-Costa, J. M. Anglada, and M. F. Ruiz-López, Int. J. Quantum Chem. **111**, 1543 (2011).

[245] J. M. Anglada and S. Olivella, J. Chem. Theory Comput. **6**, 2743 (2010).

[246] J. M. Beames, M. I. Lester, C. Murray, M. E. Varner, and J. F. Stanton, J. Chem. Phys. **134**, 044304 (2011).

[247] A. J. C. Varandas, Phys. Chem. Chem. Phys. **13**, 9796 (2011).

[248] A. J. C. Varandas, Phys. Chem. Chem. Phys. **13**, 15619 (2011).

[249] A. E. Aust and J. F. Eveleigh, Proc. Soc. Exp. Biol. Med. **222**, 246 (1999).

[250] K. Sehested, H. Corfitzen, J. Holcman, and E. J. Hart, J. Phys. Chem. A **102**, 2667 (1998).

[251] G. Fitzgerald and H. F. Schaefer, J. Chem. Phys. **81**, 362 (1984).

[252] G. Fitzgerald, T. J. Lee, H. F. Schaefer, and R. J. Bartlett, J. Chem. Phys. **83**, 6275 (1985).

[253] J. T. Fermann, B. C. Hoffman, G. S. Tschumper, and H. F. Schaefer, J. Chem. Phys. **106**, 5102 (1997).

[254] A. V. Levanov, D. V. Sakharov, A. V. Dashkova, E. E. Antipenko, and V. V. Lunin, Eur. J. Inorg. Chem. , 5144 (2011).

[255] P. Meier, M. Neff, and G. Rauhut, J. Chem. Theory Comput. **7**, 148 (2011).

[256] X. Huang, E. F. Valeev, and T. J. Lee, J. Chem. Phys. **133**, 244108 (2010).

[257] D. Feller, K. A. Peterson, and J. G. Hill, J. Chem. Phys. **133**, 184102 (2010).

[258] K. A. Peterson, T. B. Adler, and H.-J. Werner, J. Chem. Phys. **128**, 084102 (2008).

[259] K. E. Yousaf and K. A. Peterson, J. Chem. Phys. **129**, 184108 (2008).

[260] H. H. Nielsen, Phys. Rev. **60**, 794 (1941).

[261] H. H. Nielsen, Phys. Rev. **68**, 181 (1945).

[262] H. H. Nielsen, Rev. Mod. Phys. **23**, 90 (1951).

[263] D. A. Clabo, W. D. Allen, R. B. Remington, Y. Yamaguchi, and H. F. Schaefer, Chem. Phys. **123**, 187 (1988).

[264] J. J. Wilke, D. S. Hollman, and H. F. Schaefer, GRENDEL++ (General energy derivatives for electronic structure) is a C++ code for the computation of high-order energy derivatives from finite difference formulae for use in anharmonic vibrational analysis. `http://www.ccc.uga.edu/~jjwilke/grendel`.

[265] A. R. Hoy, I. M. Mills, and G. Strey, Mol. Phys. **24**, 1265 (1972).

[266] T. A. Ruden, T. Helgaker, P. Jorgensen, and J. Olsen, J. Chem. Phys. **121**, 5874 (2004).

[267] O. Bain and P. A. Giguère, Can. J. Chem. **33**, 527 (1955).

[268] R. L. Redington, W. B. Olson, and P. C. Cross, J. Chem. Phys. **36**, 1311 (1962).

[269] T. K. K. Srinivasan and P. A. Giguère, J. Raman Spec. **2**, 125 (1974).

[270] W. B. Olson, R. H. Hunt, B. W. Young, A. G. Maki, and J. W. Brault, J. Mol. Spec. **127**, 12 (1988).

[271] R. H. Hunt, R. A. Leacock, C. W. Peters, and K. T. Hecht, J. Chem. Phys. **42**, 1931 (1965).

[272] J. A. Lannon, F. D. Verderame, and R. W. Anderson, J. Chem. Phys. **54**, 2212 (1971).

[273] D. T. Petkie, T. M. Goyette, J. J. Holton, F. C. de Lucia, and P. Helminger, J. Mol. Spec. **171**, 145 (1995).

[274] D. T. Petkie et al., J. Mol. Spec. **192**, 25 (1998).

[275] P. L. Raston, C. J. Knapp, and W. Jaeger, Phys. Chem. Chem. Phys. **13**, 18789 (2011).

[276] S. Y. Lin and H. Guo, J. Chem. Phys. **119**, 5867 (2003).

[277] G. Pelz, K. M. T. Yamada, and G. Winnewisser, J. Mol. Spec. **159**, 507 (1993).

[278] W. D. Allen et al., Chem. Phys. **145**, 427 (1990).

[279] F. A. Evangelista, A. C. Simmonett, H. F. Schaefer, D. Mukherjee, and W. D. Allen, Phys. Chem. Chem. Phys. **11**, 4728 (2009).

[280] M. S. Newman, J. Chem. Educ. **32**, 344 (1955).

[281] M. Martins-Costa, J. M. Anglada, and M. F. Ruiz-López, Chem. Phys. Lett. **481**, 180 (2009).

[282] D. Wales, *Energy Landscapes: Applications to Clusters, Biomolecules and Glasses*, Cambridge University Press, 2003.

[283] P. G. Mezey, *Potential Energy Hypersurfaces*, volume 53 of *Studies in Physical and Theoretical Chemistry*, Elsevier, 1987.

[284] D. J. Wales, Science **293**, 2067 (2001).

[285] C. F. Bender, S. V. O'Neil, P. K. Pearson, and H. F. Schaefer, Science **176**, 1412 (1972).

[286] M. D. Barnes, P. R. Brooks, R. F. Curl, and B. R. Johnson, Science **261**, 1434 (1993).

[287] L. Sun, K. Song, and W. L. Hase, Science **296**, 875 (2002).

[288] P. A. M. van Koppen, M. T. Bowers, E. R. Fisher, and P. B. Armentrout, J. Am. Chem. Soc. **116**, 3780 (1994).

[289] D. S. Hollman, A. C. Simmonett, and H. F. Schaefer, Phys. Chem. Chem. Phys. **13**, 2214 (2011).

[290] D. J. Wales, Science **271**, 925 (1996).

[291] K. D. Ball et al., Science **271**, 963 (1996).

[292] M. Ternes, C. P. Lutz, C. F. Hirjibehedin, F. J. Giessibl, and A. J. Heinrich, Science **319**, 1066 (2008).

[293] G. Czakó and J. M. Bowman, Science **334**, 343 (2011).

[294] O. L. Polyansky et al., Science **299**, 539 (2003).

[295] N. Tasinato, G. Regini, P. Stoppa, A. Pietropolli Charmet, and A. Gambi, J. Chem. Phys. **136**, 214302 (2012).

[296] W. Łodyga and J. Makarewicz, J. Chem. Phys. **136**, 174301 (2012).

[297] U. Bozkaya, J. M. Turney, Y. Yamaguchi, and H. F. Schaefer, J. Chem. Phys. **136**, 164303 (2012).

[298] E. Kamarchik, Y. Wang, and J. M. Bowman, J. Chem. Phys. **134**, 114311 (2011).

[299] B. C. Dian, J. R. Clarkson, and T. S. Zwier, Science **303**, 1169 (2004).

[300] A. P. Jardine et al., Science **304**, 1790 (2004).

[301] A. M. Lindenberg et al., Science **308**, 392 (2005).

[302] A. G. Császár and N. C. Handy, J. Chem. Phys. **102**, 3962 (1995).

[303] H. Meyer, Annu. Rev. Phys. Chem. **53**, 141 (2002).

[304] E. Matyus, G. Czakó, B. T. Sutcliffe, and A. G. Császár, J. Chem. Phys. **127**, 084102 (2007).

[305] A. G. Császár, WIREs Comput. Mol. Sci. **2**, 273 (2011).

[306] W. D. Allen and A. G. Császár, J. Chem. Phys. **98**, 2983 (1993).

[307] W. D. Allen, A. G. Császár, V. Szalay, and I. M. Mills, Mol. Phys. **89**, 1213 (1996).

[308] G. Czakó, T. Furtenbacher, A. G. Császár, and V. Szalay, Mol. Phys. **102**, 2411 (2004).

[309] W. D. Allen, A. Bodi, V. Szalay, and A. G. Császár, J. Chem. Phys. **124**, 224310 (2006).

[310] M. A. El'yashevich and M. V. Wolkenshtein, Zh. Eksp. Teor. Fiz. **9**, 101 (1945).

[311] M. V. Wolkenshtein, L. A. Gribov, M. A. El'yashevich, and Y. Y. Stepanov, *Kolébanya Molekul*, Yzhdatelstvo "Nauka", Moskow, 1972.

[312] E. B. Wilson, J. C. Decius, and P. C. Cross, *Molecular Vibrations: The Theory of Infrared and Raman Vibrational Spectra*, McGraw–Hill, New York, 1955.

[313] N. Neto, Chem. Phys. **87**, 43 (1984).

[314] N. Neto, Chem. Phys. **91**, 89 (1984).

[315] N. Neto, Chem. Phys. **91**, 101 (1984).

[316] N. Neto, Chem. Phys. **108**, 27 (1986).

[317] Wolfram Research, Inc., 2012, *Mathematica v8.0.4.0*.

[318] I. J. Schwatt, *An Introduction to the Operations with Series*, Chelsea, New York, 1924.

[319] Y. A. Brychkov, *Handbook of Special Functions: Derivatives, Integrals, Series and Other Formulas*, CRC Press, Boca Raton, Florida, 2008.

[320] The On-Line Encyclopedia of Integer Sequences, A008971. `http://oeis.org/A008971`.

[321] (a) The Wolfram Functions Site, Inverse sine: Differentiation (formula 01.12.20.005.01). `http://functions.wolfram.com/01.12.20.0005.01` (b) The Wolfram Functions Site, Inverse sine: Differentiation (formula 01.12.20.003.02). `http://functions.wolfram.com/01.12.20.0003.02` (c) The Wolfram Functions Site, Inverse sine: Differentiation (formula 01.12.20.006.01). `http://functions.wolfram.com/01.12.20.0006.01` (d) The Wolfram Functions Site, Inverse sine: Differentiation (formula 01.12.20.007.01). `http://functions.wolfram.com/01.12.20.0007.01`.

[322] R. Bonneau and D. Baker, Annu. Rev. Biophys. Biomol. Struct. **30**, 173 (2001).

[323] Y. Zhang, H. Liu, and W. Yang, J. Chem. Phys. **112**, 3483 (2000).

[324] R. V. Stanton, M. Peräkylä, D. Bakowies, and P. A. Kollman, J. Am. Chem. Soc. **120**, 3448 (1998).

[325] H. Hu and W. Yang, Annu. Rev. Phys. Chem. **59**, 573 (2008).

[326] R. A. Friesner and V. Guallar, Annu. Rev. Phys. Chem. **56**, 389 (2005).

[327] M. Häser and J. Almlöf, J. Chem. Phys. **96**, 489 (1992).

[328] S. Saebo and P. Pulay, Annu. Rev. Phys. Chem. **44**, 213 (1993).

[329] M. Head-Gordon, P. Maslen, and C. A. White, J. Chem. Phys. **108**, 616 (1998).

[330] P. Y. Ayala and G. E. Scuseria, J. Chem. Phys. **110**, 3660 (1999).

[331] G. E. Scuseria and P. Y. Ayala, J. Chem. Phys. **111**, 8330 (1999).

[332] P. Y. Ayala and G. E. Scuseria, J. Comput. Chem. **21**, 1524 (2000).

[333] J. Finley and K. Hirao, Chem. Phys. Lett. **328**, 51 (2000).

[334] P. Y. Ayala, K. N. Kudin, and G. E. Scuseria, J. Chem. Phys. **115**, 9698 (2001).

[335] Y. Nakao and K. Hirao, J. Chem. Phys. **120**, 6375 (2004).

[336] O. Christiansen, P. Manninen, P. Jørgensen, and J. Olsen, J. Chem. Phys. **124**, 084103 (2006).

[337] A. Sodt, J. E. Subotnik, and M. Head-Gordon, J. Chem. Phys. **125**, 194109 (2006).

[338] M. Beer and C. Ochsenfeld, J. Chem. Phys. **128**, 221102 (2008).

[339] P. M. W. Gill, B. G. Johnson, and J. A. Pople, Chem. Phys. Lett. **217**, 65 (1994).

[340] B. Doser, D. S. Lambrecht, and C. Ochsenfeld, Phys. Chem. Chem. Phys. **10**, 3335 (2008).

[341] J. Zienau, J. Kussmann, F. Koziol, and C. Ochsenfeld, Phys. Chem. Chem. Phys. **9**, 4552 (2007).

[342] M. Beer, J. Kussmann, and C. Ochsenfeld, J. Chem. Phys. **134**, 074102 (2011).

[343] C. Ochsenfeld, J. Kussmann, and F. Koziol, Angew. Chem. Int. Ed. Engl. **43**, 4485 (2004).

[344] D. P. Tew and W. Klopper, Mol. Phys. **108**, 315 (2010).

[345] L. Kong, F. A. Bischoff, and E. F. Valeev, Chem. Rev. **112**, 75 (2012).

[346] S. Ten-No, Theor. Chim. Acta **131**, 1070 (2012).

[347] T. Shiozaki, E. F. Valeev, and S. Hirata, J. Chem. Phys. **131**, 044118 (2009).

[348] E. F. Valeev, Chem. Phys. Lett. **395**, 190 (2004).

[349] D. P. Tew, W. Klopper, C. Neiss, and C. Hättig, Phys. Chem. Chem. Phys. **9**, 1921 (2007).

[350] C. Ochsenfeld and M. Head-Gordon, Chem. Phys. Lett. **270**, 399 (1997).

[351] M. Challacombe, J. Chem. Phys. **110**, 2332 (1999).

[352] M. Kuemin, S. Schweizer, C. Ochsenfeld, and H. Wennemers, J. Am. Chem. Soc. **131**, 15474 (2009).

[353] C. V. Sumowski and C. Ochsenfeld, J. Phys. Chem. A **113**, 11734 (2009).

[354] I. Mayer, Simple theorems, proofs, and derivations in quantum chemistry, 2003.

[355] H. Fliegl, C. Hättig, and W. Klopper, J. Chem. Phys. **124**, 044112 (2006).

[356] C. Neiss, C. Hättig, and W. Klopper, J. Chem. Phys. **125**, 064111 (2006).

[357] M. Hanauer and A. Köhn, J. Chem. Phys. **131**, 124118 (2009).

[358] J. Almlöf, Chem. Phys. Lett. **181**, 319 (1991).

[359] M. Häser, Theor. Chim. Acta **87**, 147 (1993).

[360] P. R. Surján, Chem. Phys. Lett. **406**, 318 (2005).

[361] S. Schweizer, B. Doser, and C. Ochsenfeld, J. Chem. Phys. **128**, 154101 (2008).

[362] P. Pulay, Chem. Phys. Lett. **73**, 393 (1980).

[363] J. M. Turney et al., WIREs Comput. Mol. Sci. **2**, 556 (2011).

[364] G. van Rossum and F.L. Drake (eds.), Python Reference Manual, PythonLabs, Virginia, USA, 2001. Available at `http://www.python.org`.

[365] D. Ascher, P.F. Dubois, K. Hinsen, J. Hugunin and T. Oliphant, Numerical Python, Lawrence Livermore National Laboratory, Livermore, California, USA, 2001. Available at `http://www.numpy.org`.

[366] B. J. Persson and P. R. Taylor, J. Chem. Phys. **105**, 5915 (1996).

[367] C. Ochsenfeld, C. A. White, and M. Head-Gordon, J. Chem. Phys. **109**, 1663 (1998).

[368] C. Ochsenfeld, Chem. Phys. Lett. **327**, 216 (2000).

[369] P. Wind, T. Helgaker, and W. Klopper, Theor. Chim. Acta **106**, 280 (2001).

[370] F. A. Bischoff, S. Wolfsegger, D. P. Tew, and W. Klopper, Mol. Phys. **107**, 963 (2009).

Epilogue

Over the past half century, *ab initio* quantum chemistry has matured from a specialized, exotic research area to a ubiquitous, essential tool for research in all areas of chemistry. In the course of this maturation process, numerous methods for handling electron correlation have been invented and developed. By around the turn of the century, most of the methods necessary for general, everyday chemical problems had reached a level of maturity beyond which little qualitative improvement could be seen from further theoretical study. Much of the methodological development of the past decade has been principally useful for specialized problems, poorly behaved systems, and highly quantitative applications. The development of linear scaling *ab initio* methods has been particularly interesting in this regard. As methods able to handle progressively larger molecules at a reasonable computational cost have developed, the range of problems that can be handled quantitatively has expanded beyond the scope of problems for which highly quantitative data is valuable. In this regard, error cancellation is the *ab initio* theoretician's ally and foe. For the purpose of gaining a qualitative understanding of chemistry and the world around us, error cancellation makes a number of chemical problems accessible that would otherwise be insurmountable. From the perspective of those who wish to develop new, mathematically elegant approaches to *ab initio* computation, however, error cancellation can be a frustrating force that propels less elegant methods to prominence above more rigorous and thorough approaches. In a fight for relevance, mathematically minded theoreticians are forced to scrounge together odd problems

for which the error cancellation is not substantial enough with less rigorous methods to gain a correct qualitative understanding. Theoretical chemists are stuck in a difficult no-man's land between the world of mathematicians and physicists, where elegant mathematical or fundamental research is justified on the grounds of pure human curiosity, and the world of biology and social sciences, where research is more easily motivated by its direct impact on the lives of humans and other living things. Compounding the problem is the fact that the field of chemistry is split between these two worlds, and people in the former world often have to convince those in the latter world that their research is worth funding. The future of *ab initio* methodological development will likely be characterized by increasingly divergent lines of study by members of these two worlds. In this regard, perhaps it is unwise for researchers to put substantial effort into spanning these divergent ideologies.

The preceding discussion is, of course, overflowing with sweeping generalizations. There is no one solution to the divergence of research motivations. In fact, it is not entirely self-evident that there needs to be a solution. It *is* important, however, for those who practice science to be aware of the tension and to know where they stand on the spectrum.